Анализ результатов эксперимента Нейтрино-4 по поиску стерильного нейтрино и сравнение с результатами других экспериментов

А.П. Серебров, Р.М. Самойлов

Neutrino-4 collaboration

1. НИЦ «КИ» Петербургский институт ядерной физики, Гатчина, Россия
2. ОАО "ГНЦ НИИАР", 433510 Димитровград, Россия,
3. ДИТИ МИФИ, 433511 Димитровград, Россия

А.П. Серебров1, Р.М. Самойлов1, В.Г. Ивочкин1, А.К. Фомин1, А.О.Полюшкин1, В.Г. Зиновьев1, П.В. Неустроев1, В.Л. Головцов1, А.В. Чёрный1, О.М. Жеребцов1, М.Е. Чайковский1, А.Л. Петелин2, А.Л. Ижутов2, А.А. Тузов2, С.А. Сазонтов2, М.О. Громов2, В.В. Афанасьев2, М.Е. Зайцев3, А.А. Герасимов1, В. В.Федоров1

Семинар ПИЯФ 17 сентября 2020

Reactor antineutrino anomaly

T. Mueller, D. Lhuillier, M. Fallot et al., Phys. Rev. C 83, 054615 (2011).

- Observed/predicted averaged event ratio: R=0.927±0.023 (3.0 σ)

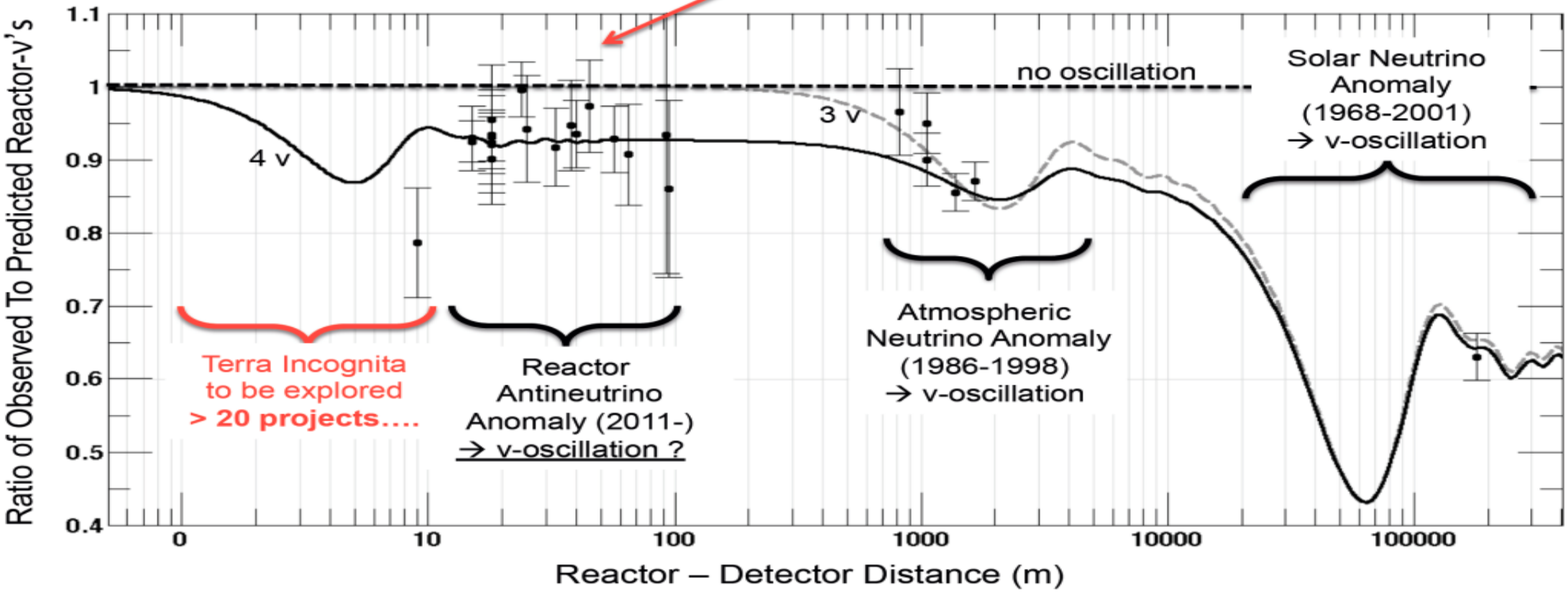

$$P(\tilde{\nu}_e \rightarrow \tilde{\nu}_e) = 1 - \sin^2 2\theta_{14} \ \sin^2\left(1.27 \frac{\Delta m^2_{14}[eV^2]L[m]}{E_{\tilde{\nu}}[MeV]}\right)$$

The first observation of effect of oscillation in Neutrino-4 experiment on search for sterile neutrino

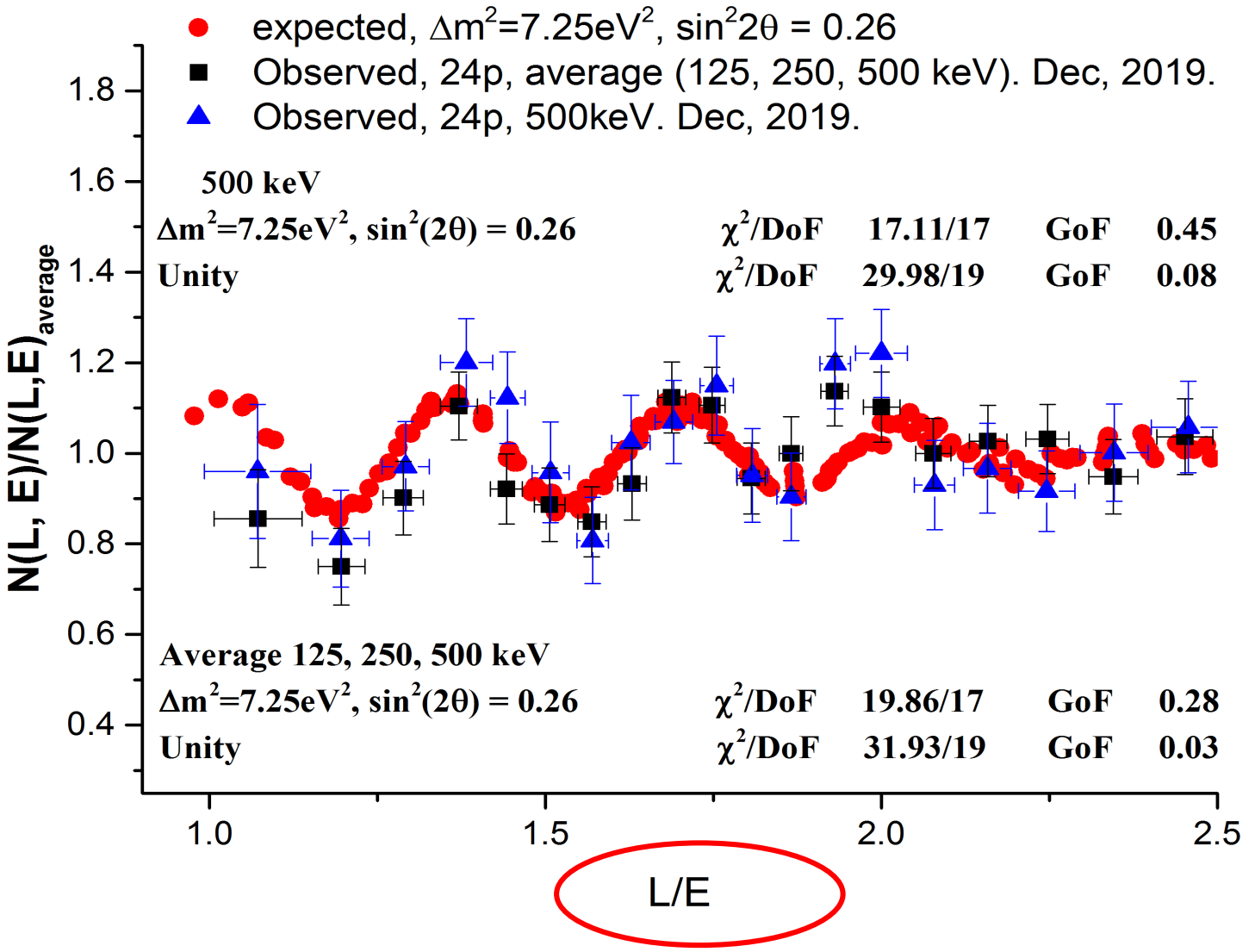

The period of oscillation for neutrino energy 4 MeV is 1.4 m

A.P.Serebrov, et al.
JETP Letters,
Volume 109, 2019
Issue 4, pp 213–221.

JETP Letters,
Volume 112, 2020
Issue 4, pp 211–225.

arxiv:2003.03199
arxiv:2005.05301

NEUTRINO 2020

Reactor antineutrino anomaly with oscillation curve obtained in experiment Neutrino-4

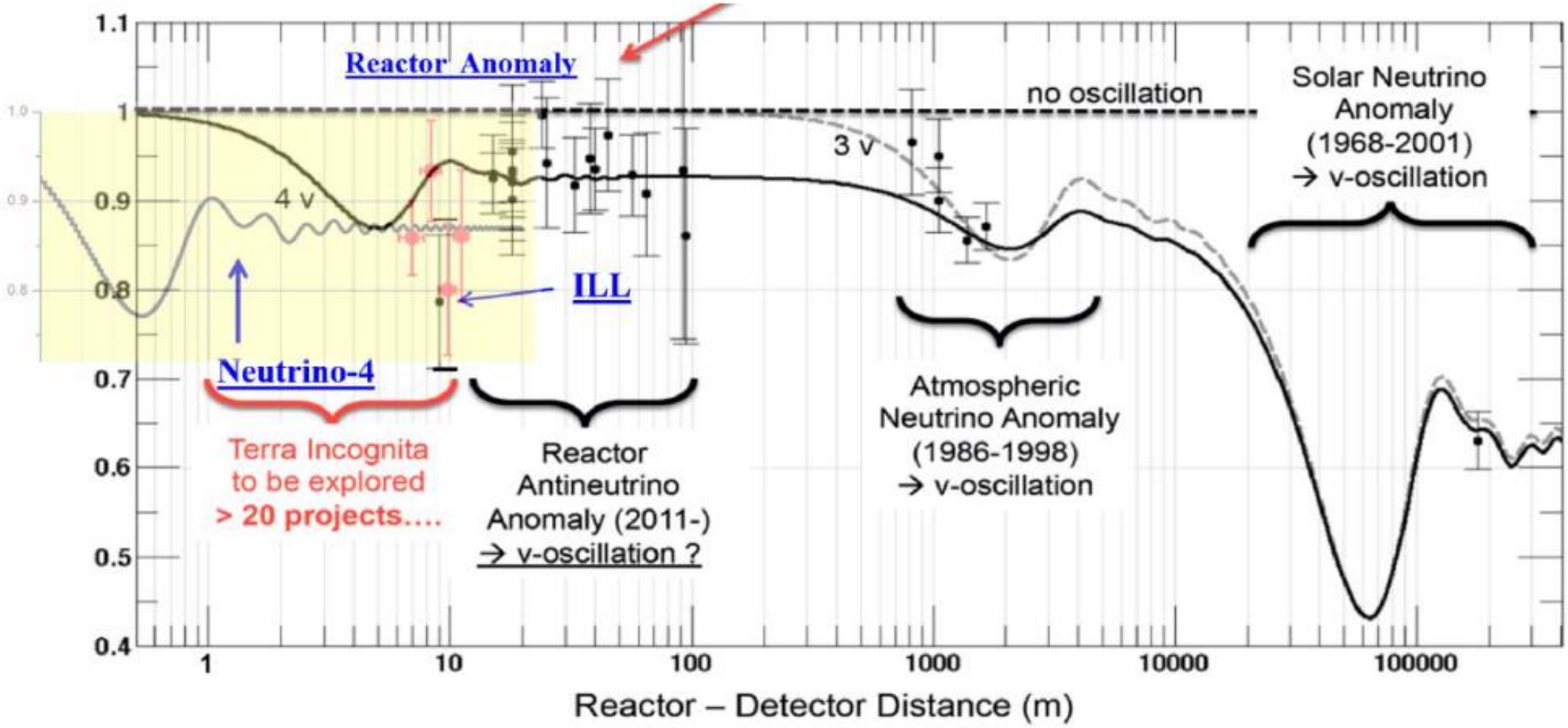

Fig.13. Reactor antineutrino anomaly [28] with oscillation curve obtained in experiment Neutrino-4.

Reactor SM-3

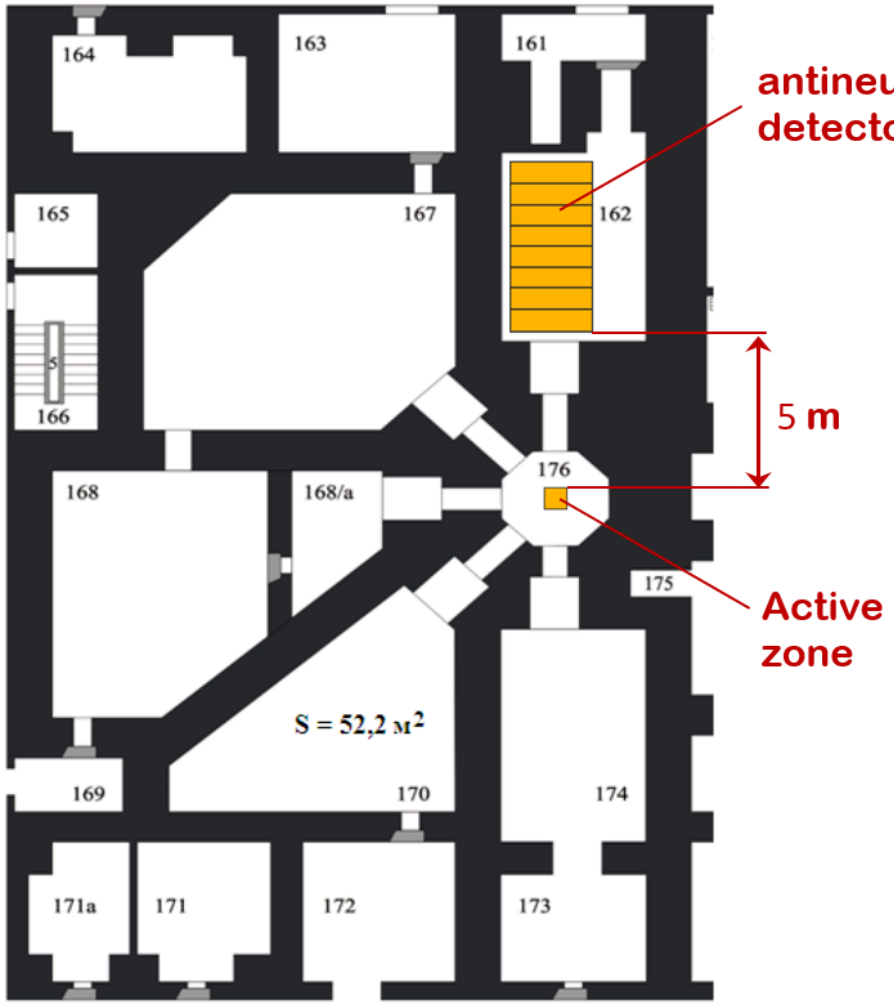

100 MW thermal power
Compact core 42x42x35cm
Highly enriched ^{235}U fuel

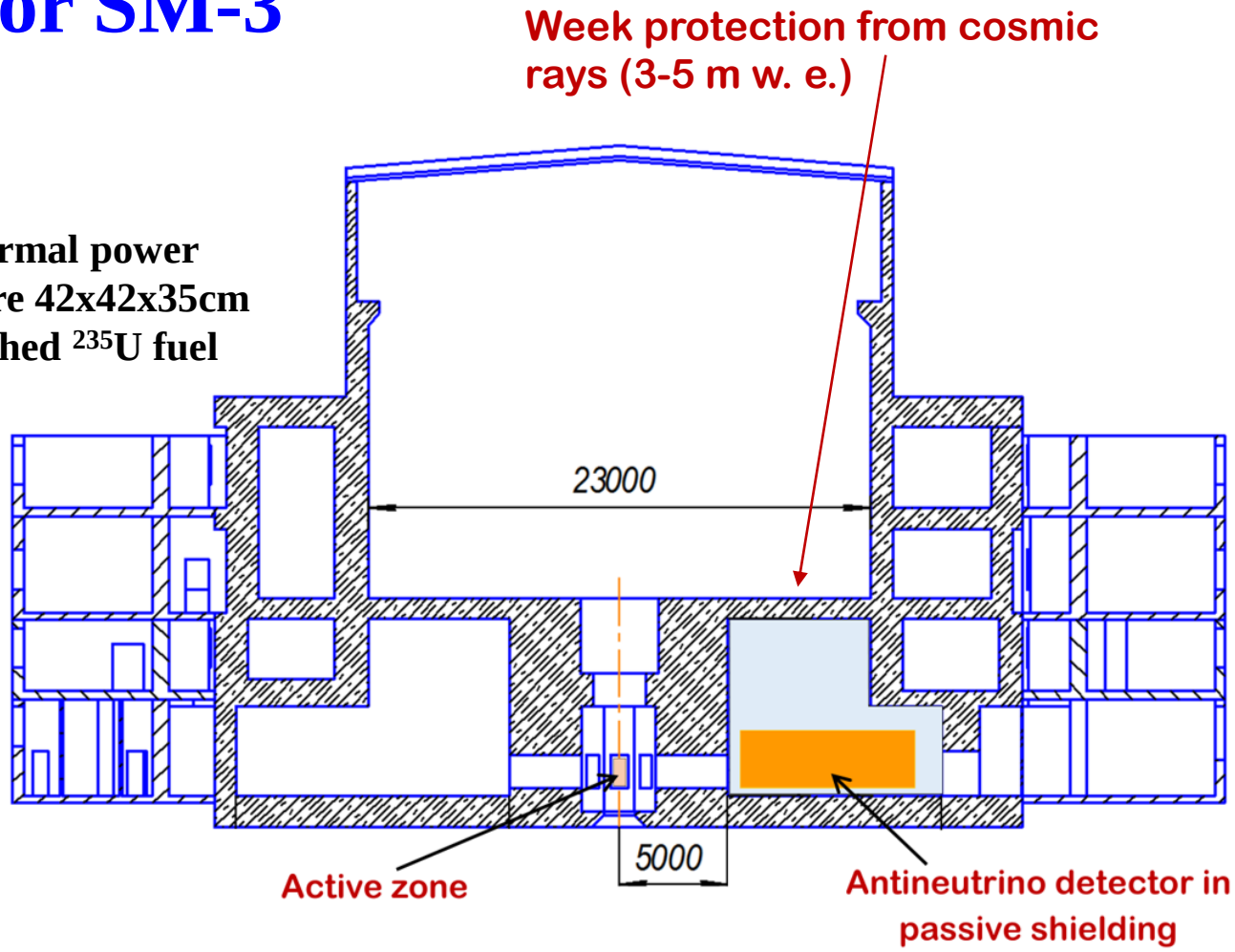

Due to some peculiar characteristics of its construction, reactor SM-3 provides the most favorable conditions to search for neutrino oscillations at short distances. However, SM-3 reactor, as well as other research reactors, is located on the Earth's surface, hence, cosmic background is the major difficulty in considered experiment.

Movable and spectrum sensitive antineutrino detector at SM-3 reactor

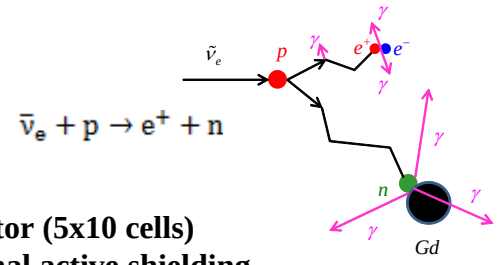

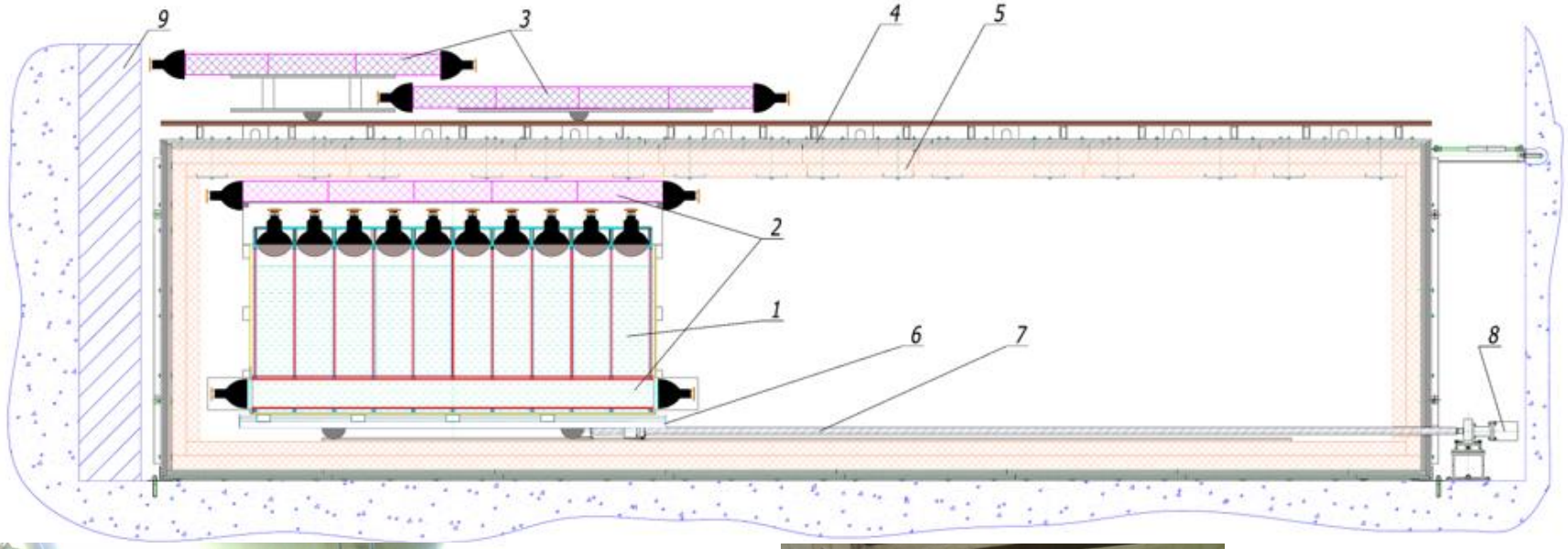

1. detector (5x10 cells)
2. internal active shielding
3. external active shielding
4. steel and lead
5. borated polyethylene
6. moveable platform
7. feed screw
8. step motor
9. shielding

Passive shielding - 60 tons

Neutrino channel outside and inside →

Range of measurements is 6 – 12 meters

Detector prototype ←

Full-scale detector →

Liquid scintillator detector 50 sections 0.235x0.235x0.85м³

Gamma background in passive shielding does not depend neither on the power of the reactor nor on distance from the reactor

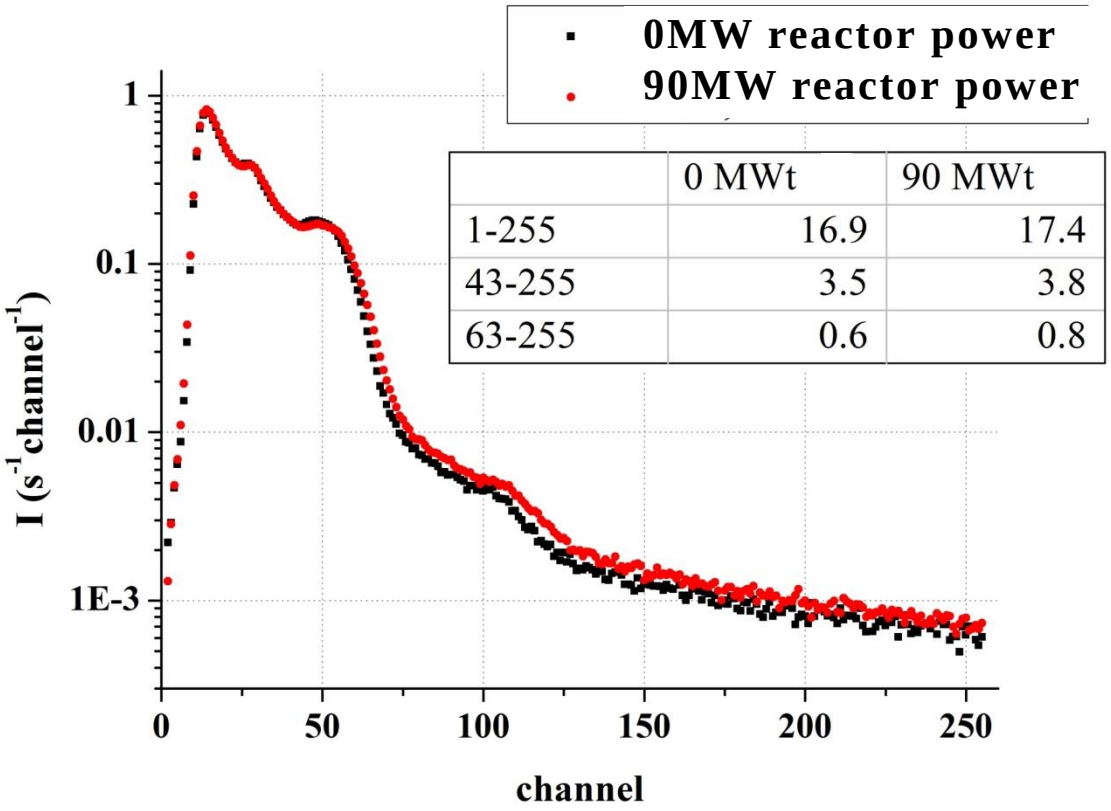

	0 MWt	90 MWt
1-255	16.9	17.4
43-255	3.5	3.8
63-255	0.6	0.8

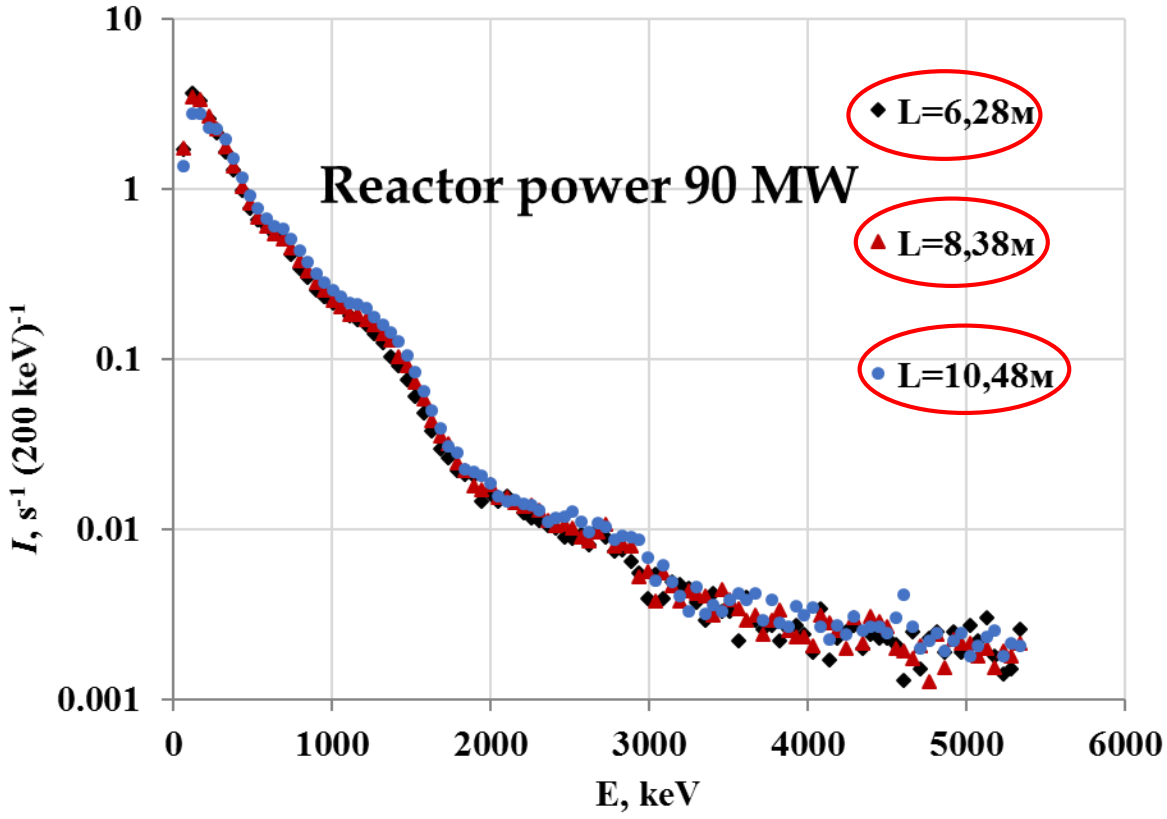

The background of fast neutrons in passive shielding does not depend neither on the power of the reactor nor on distance from the reactor

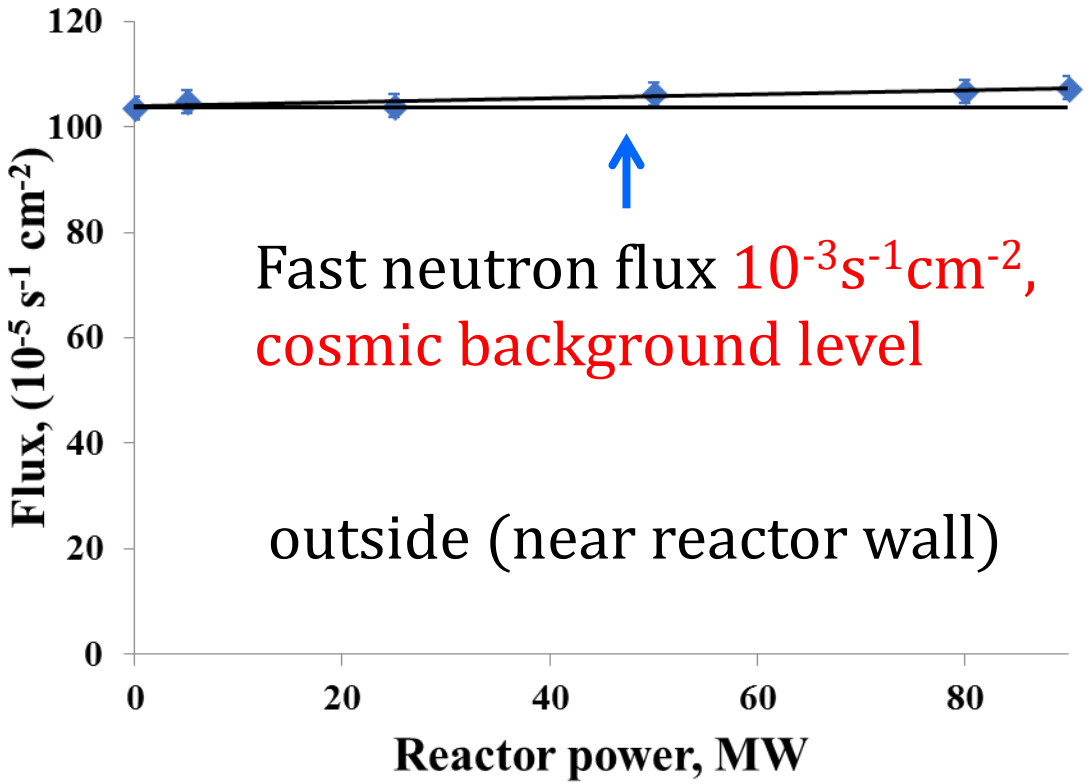

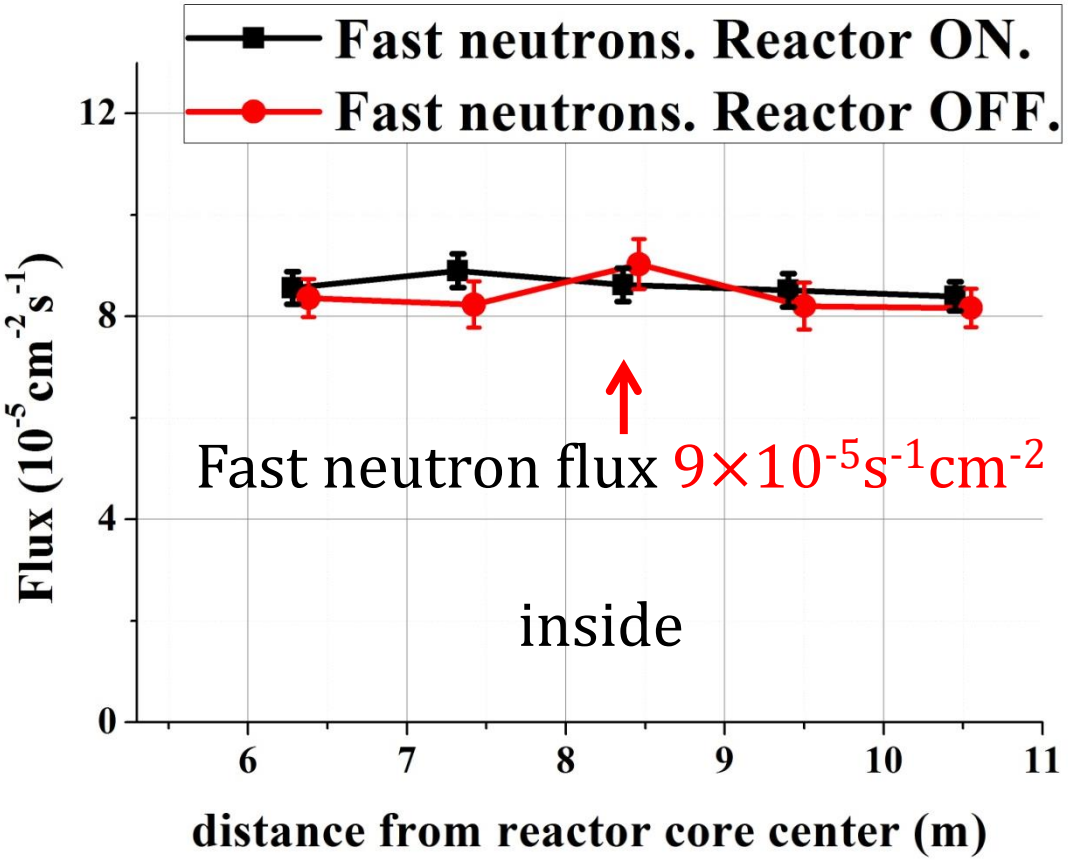

The background of fast neutrons in passive shielding is 10 times less than outside.
The background of fast neutrons outside of passive shielding is defined by cosmic rays and practically does not depend on reactor power.

Absence of noticeable dependence of the background on both distance and reactor power was observed. As a result, we consider that difference in reactor ON/OFF signals appears mostly (>95%) due to antineutrino flux from operating reactor.

INVESTIGATION OF BACKGROUND CONDITIONS WITH ANTINEUTRINO DETECTOR MODEL

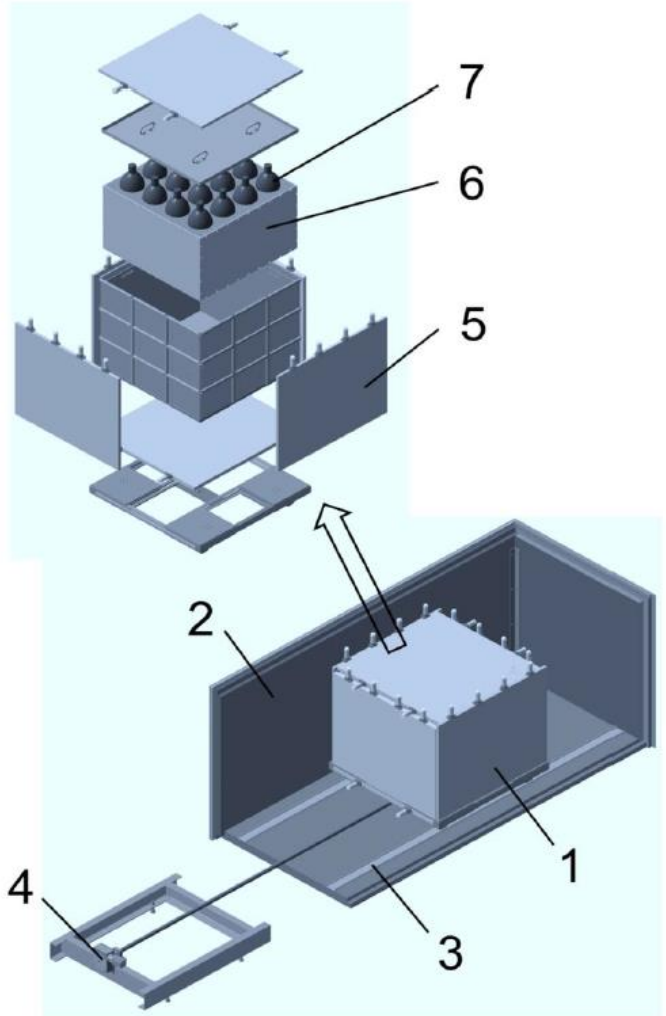

FIG. 6. Model of the neutrino detector installed in passive shielding [24,25]. 1 – detector of reactor antineutrino, 2 – passive shielding, 3 – rails,4 – engine for detector movement, 5 – active shielding with PMT,6 – volume with liquid scintillator with Gd,7 – detector's PMT.

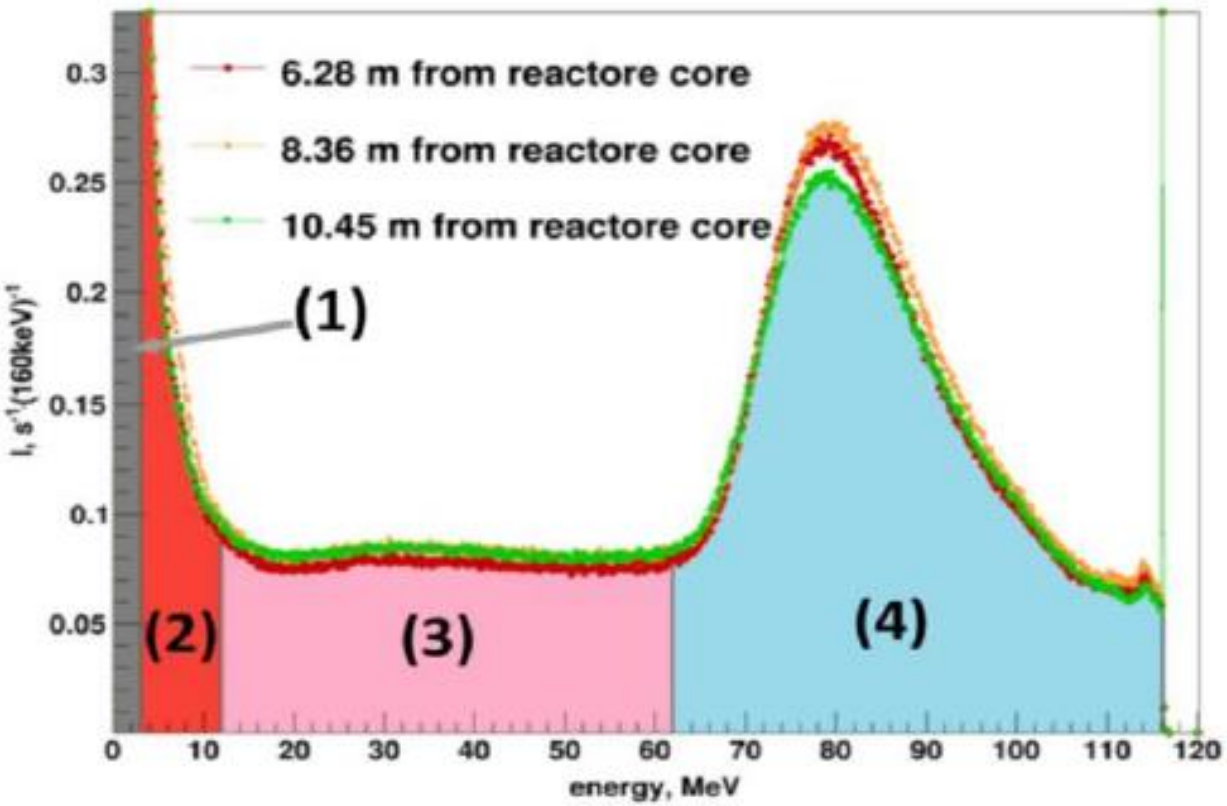

FIG. 7. Detector energy spectrum at different distances from the reactor core and a division of spectrum into zones: 1 – radioactive contamination background, 2 - neutrons, 3 –soft component of cosmic rays, 4 -muons.

COSMIC BACKGROUND, ACTIVE SHIELDING.
ENERGY AND TIME SPECTRA OF CORRELATED SIGNALS

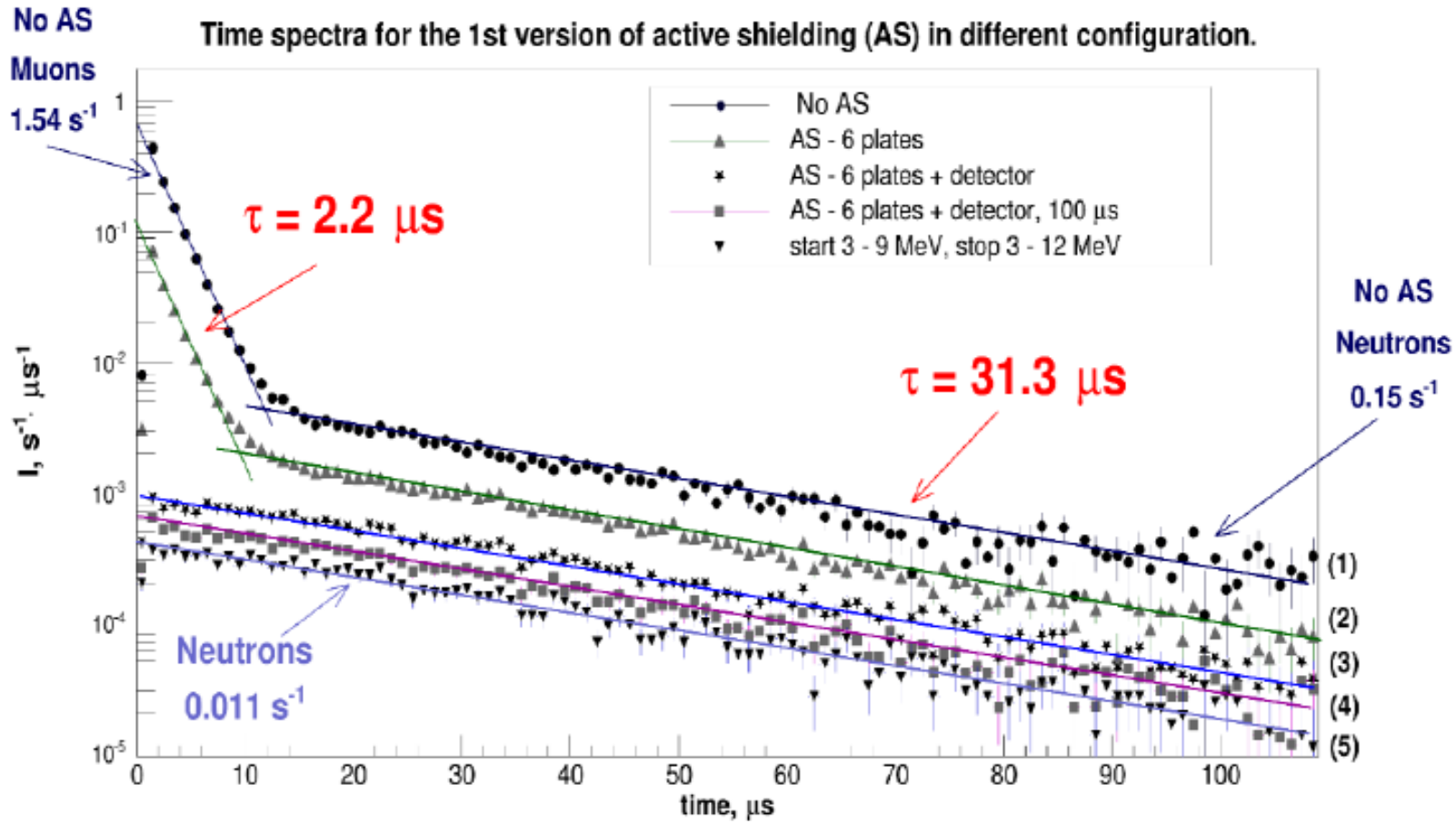

FIG. 10. Time spectra at different configurations of active shielding: 1 - no active shielding, 2 – plates of active shielding are on, 3 – the same + ban from the detector at signals higher than 12 MeV, 4 – the same + ban on 100 μs after the detector signal, at energy higher than 12 MeV, or after the signal in active shielding, 5 – the same + limit on start and stop signals in ranges 3 – 9 MeV and 3 – 12 MeV respectively.

INVESTIGATION OF BACKGROUND CONDITIONS WITH ANTINEUTRINO DETECTOR MODEL

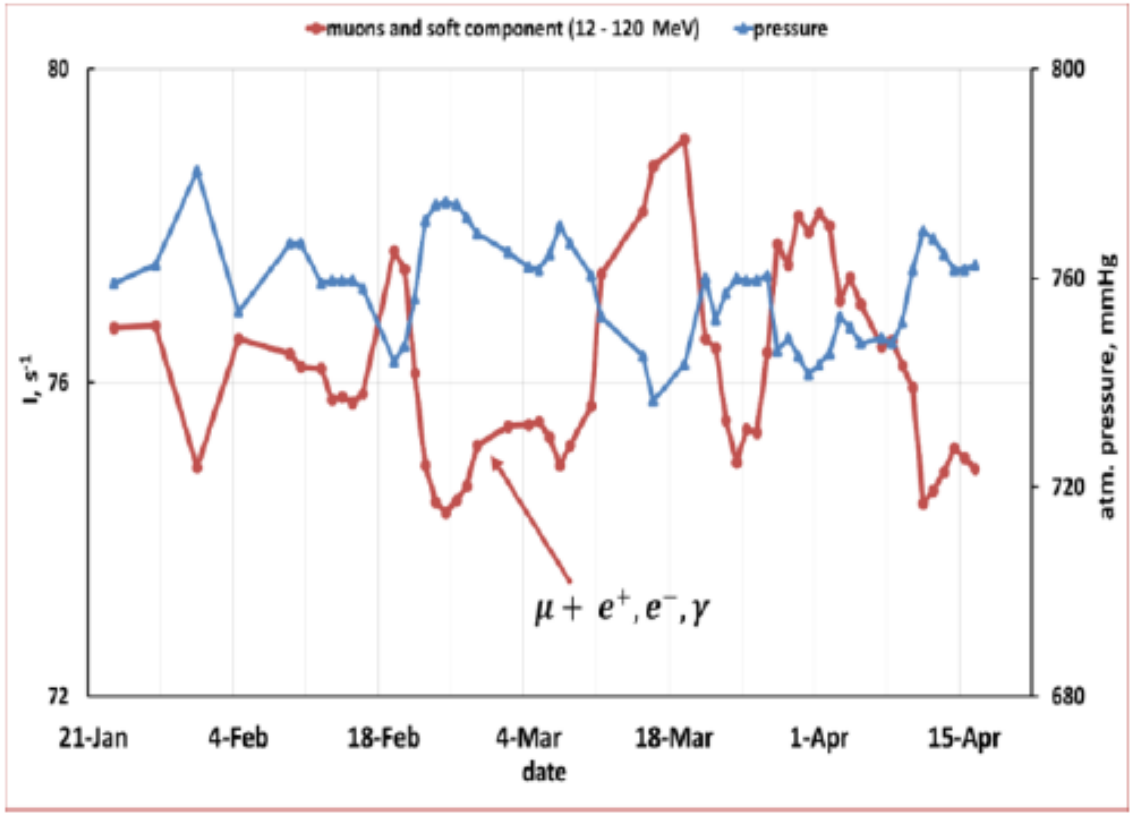

FIG. 8. Barometric effect of cosmic rays: the left axis illustrates a summary detector count rate in the energy areas 3 and 4, the right axis shows atmospheric pressure, the horizontal axis gives the measurement time since 23 of January till 15 of April of 2014.

The fluctuations in the cosmic background are determined by the fluctuations in atmospheric pressure that is **±1.1%.**

Broadening in the statistical distribution of the neutrino signal due to fluctuations in the cosmic background will be **5%** with respect to statistic error.

ON
90 MW

Measurements with the detector have started in June 2016. Measurements with the reactor ON were carried out for 720 days, and with the reactor OFF- for 417 days. In total, the reactor was switched on and off 87 times.

(ON – OFF)/ OFF = 50%

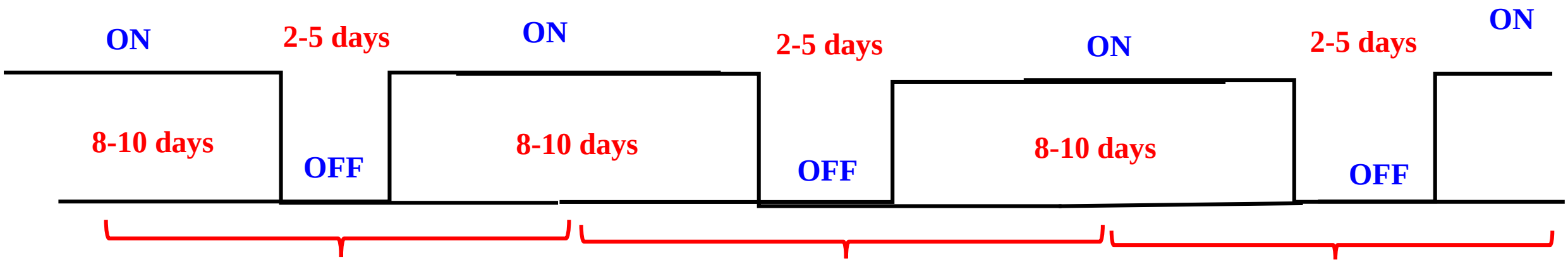

Additional dispersion of measurement result which appears due to fluctuations of cosmic background

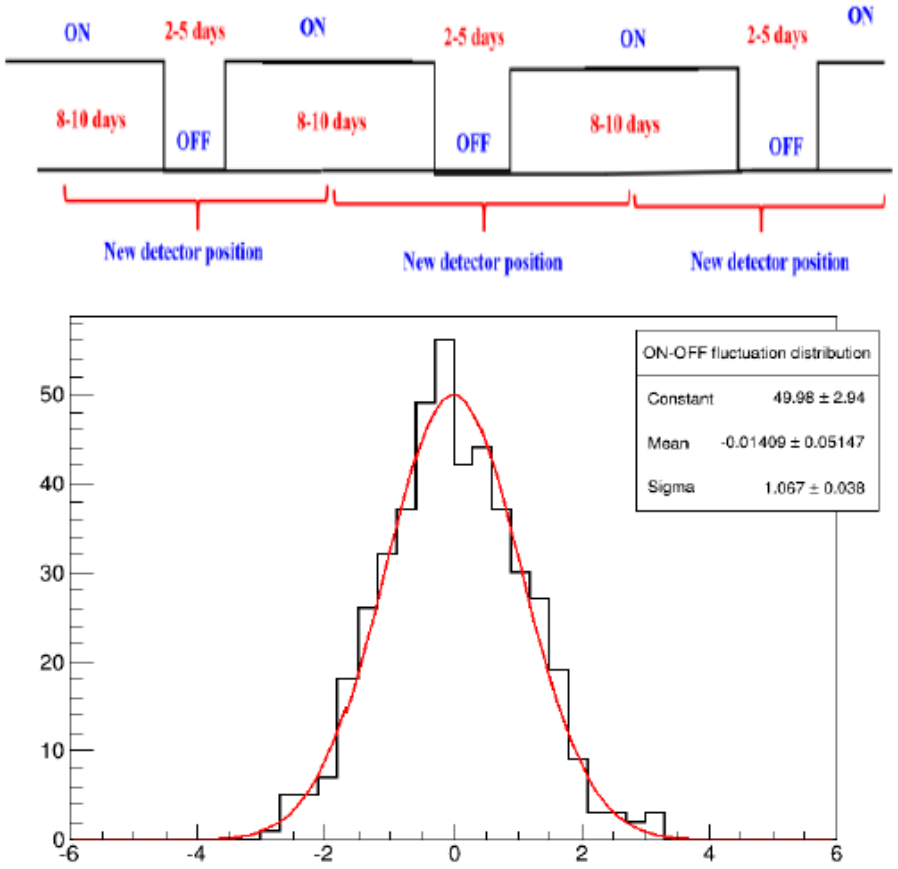

FIG. 36. Top - scheme of detector operation and detector movements; bottom - the distribution of deviations from average value of correlated events rates differences (ON-OFF) normalized on their statistical uncertainties.

$$\sigma = 1.070 \pm 0.045$$

That distribution has the form of normal distribution, but its width exceeds unit by **7.0 ± 4.5 %.**

Broadening in the statistical distribution of the neutrino signal due to fluctuations in the cosmic background will be **5%.**

Energy calibration of the full-scale detector

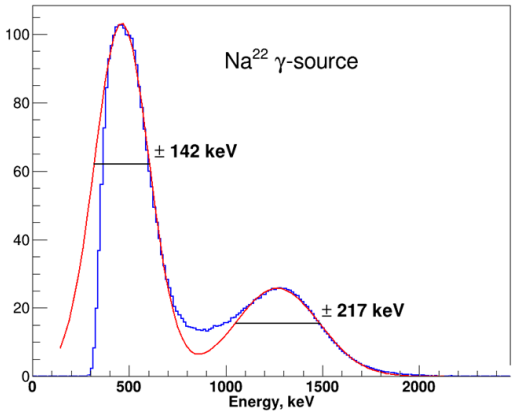

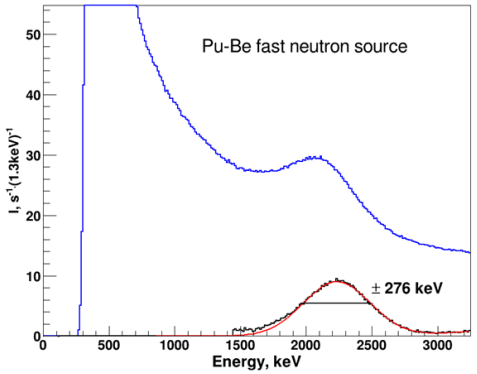

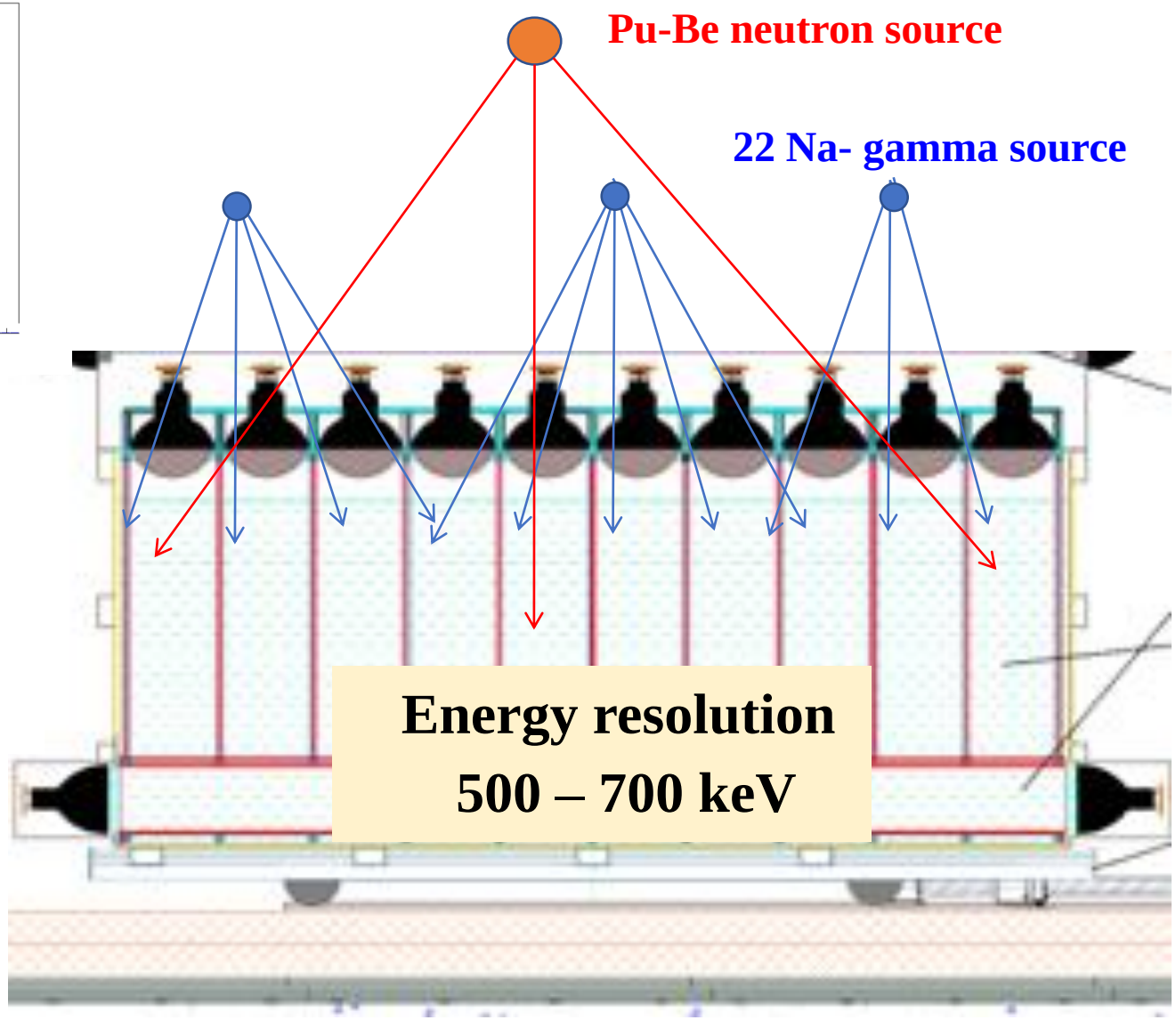

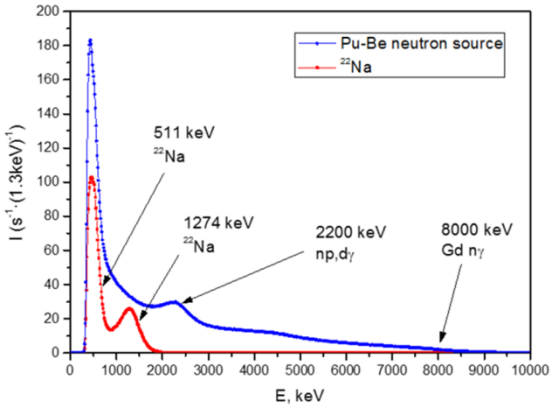

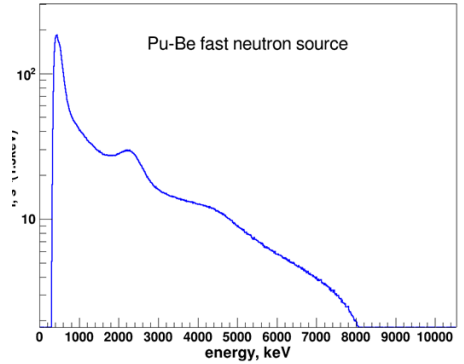

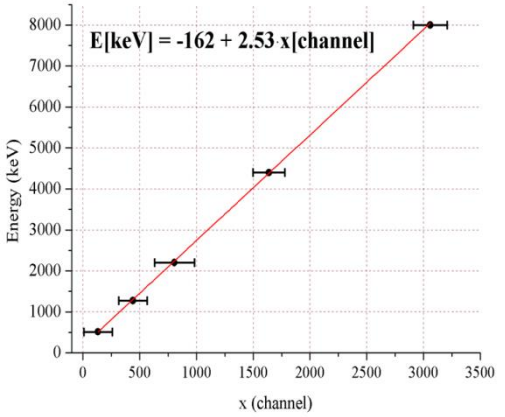

The effect of total internal reflection at the border of scintillator and air at low angles

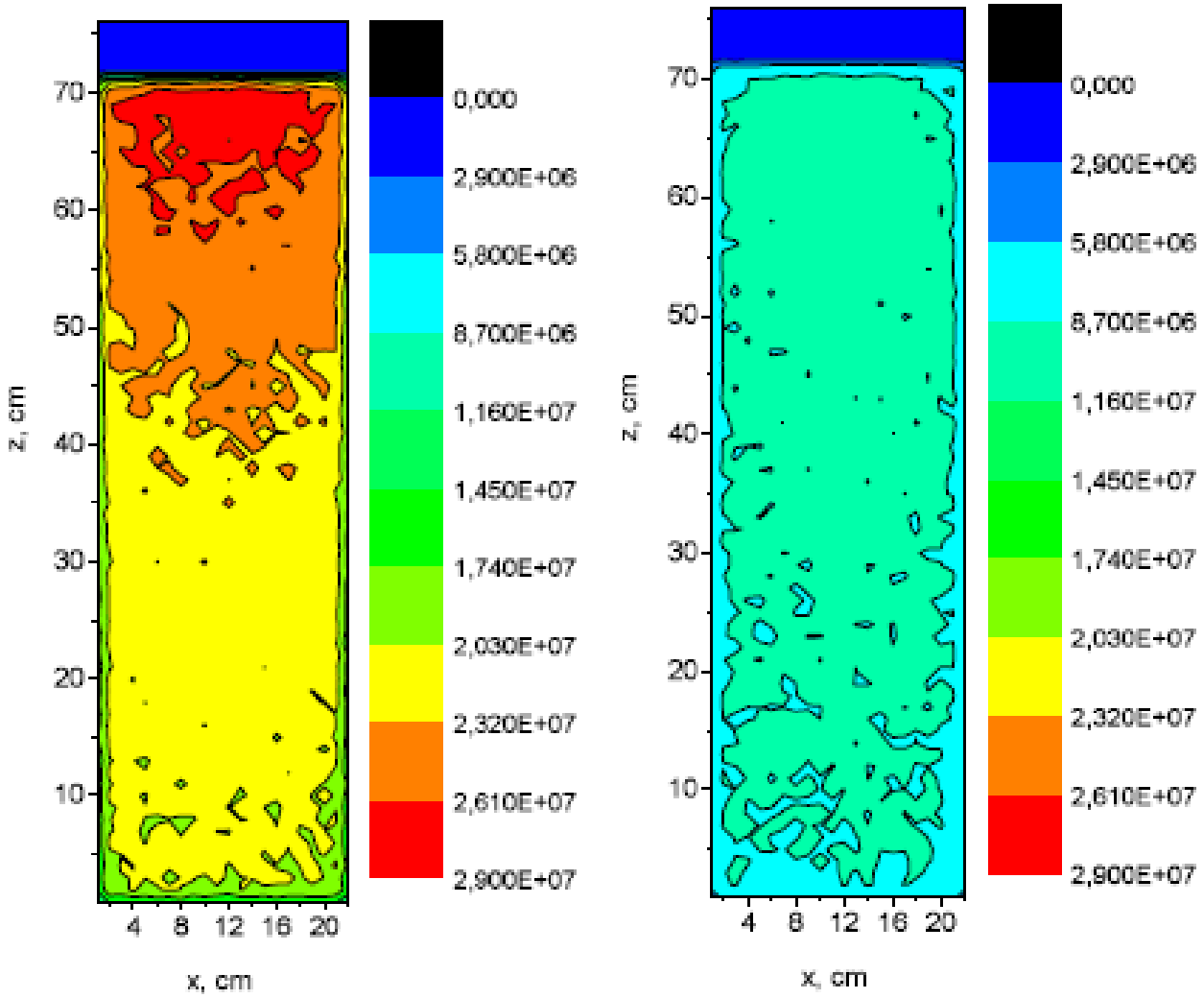

The effect of total internal reflection at the border of scintillator and air at low angles of descent evens the transportation conditions for light coming from various distances. Finally, a mirror at the bottom of the light guide also helps to even light collection conditions for various positions in the detector section.

The scheme of the experiment with single section

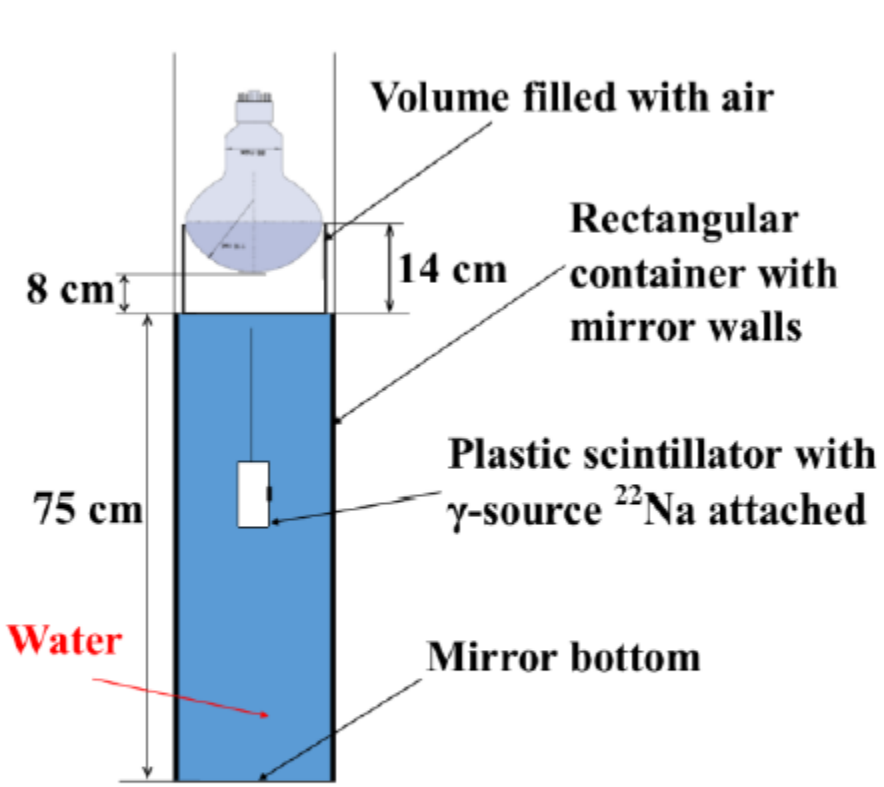

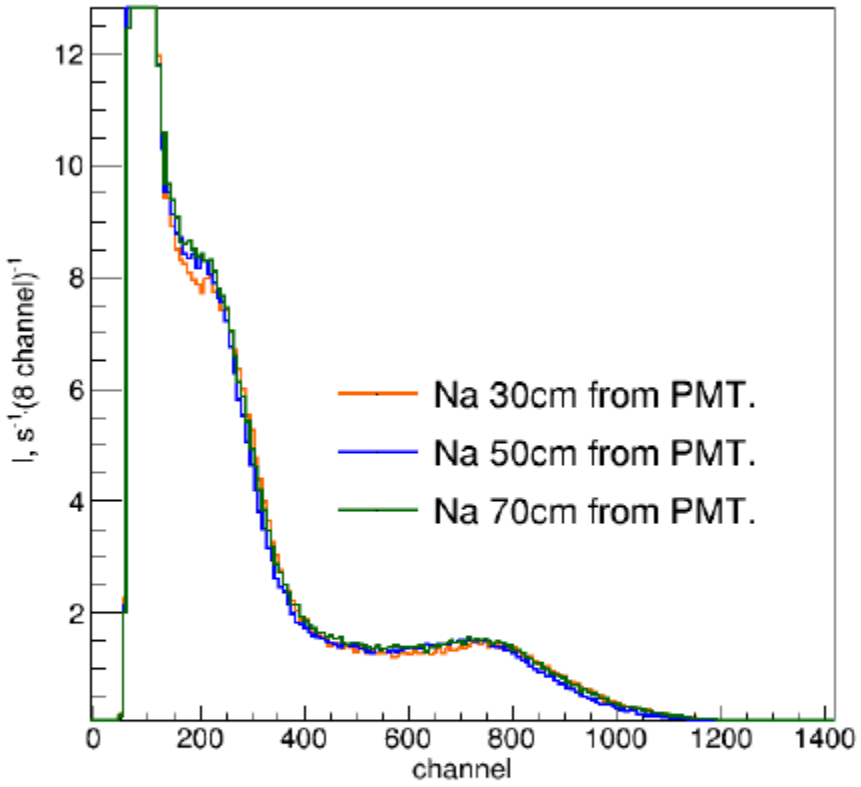

FIG. 17. Top – results of MC simulation for model of single section in case with optical contact (on the left) and without optical contact (on the right). Bottom – scheme of model to measure with full-scale detector section analogue (on the left); ^{22}Na source spectrum with different scintillator position for model of full-scale detector section with air gap (on the right).

COMPARISON OF EXPERIMENTAL ANTINEUTRINO SPECTRUM WITH CALCULATED REACTOR SPECTRUM
(Problems with energy spectrum)

a) The ratio of an experimental spectrum of prompt signals to the spectrum, expected from MC calculations for 3 ranges (~2m) with centers 7.3m, 9.3m and 11.1m

b) polynomial fit of results averaged by distance (red curve)

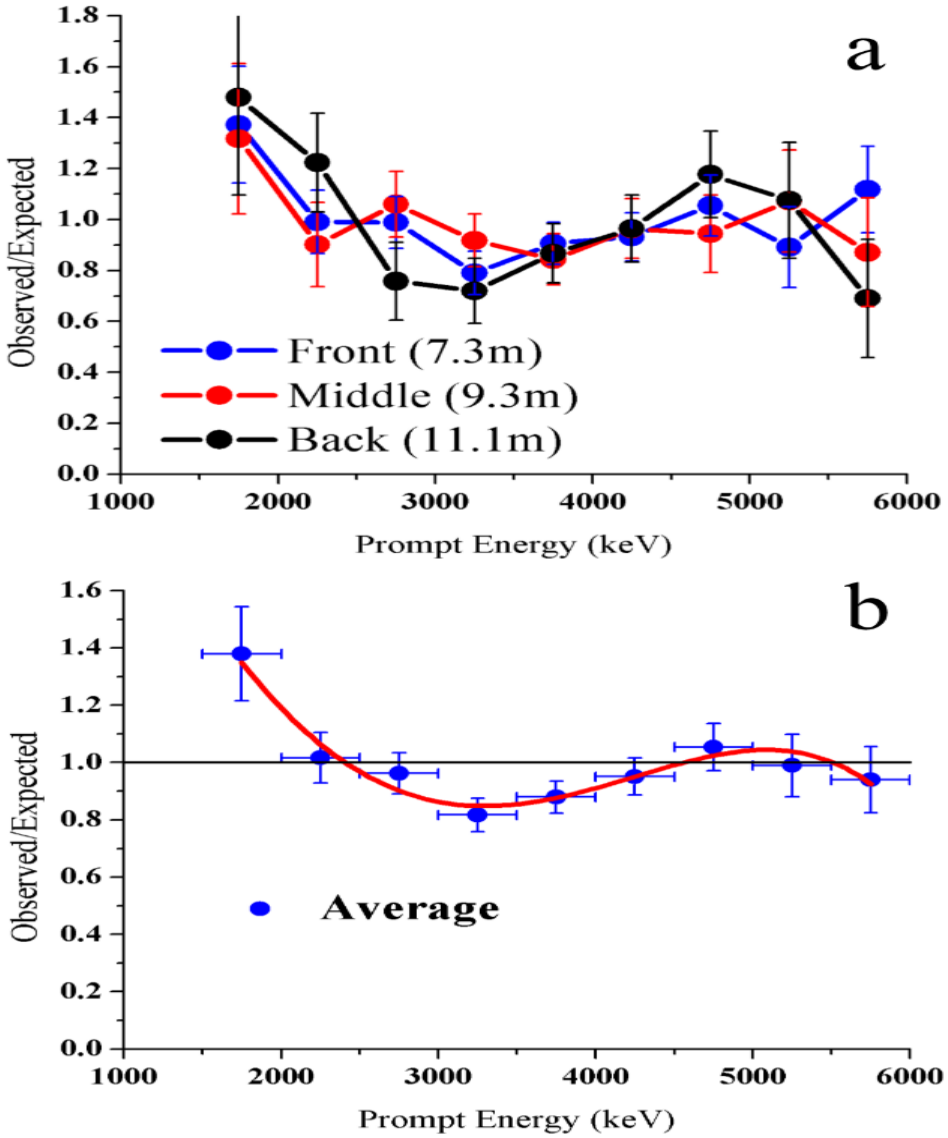

Problems with energy spectrum

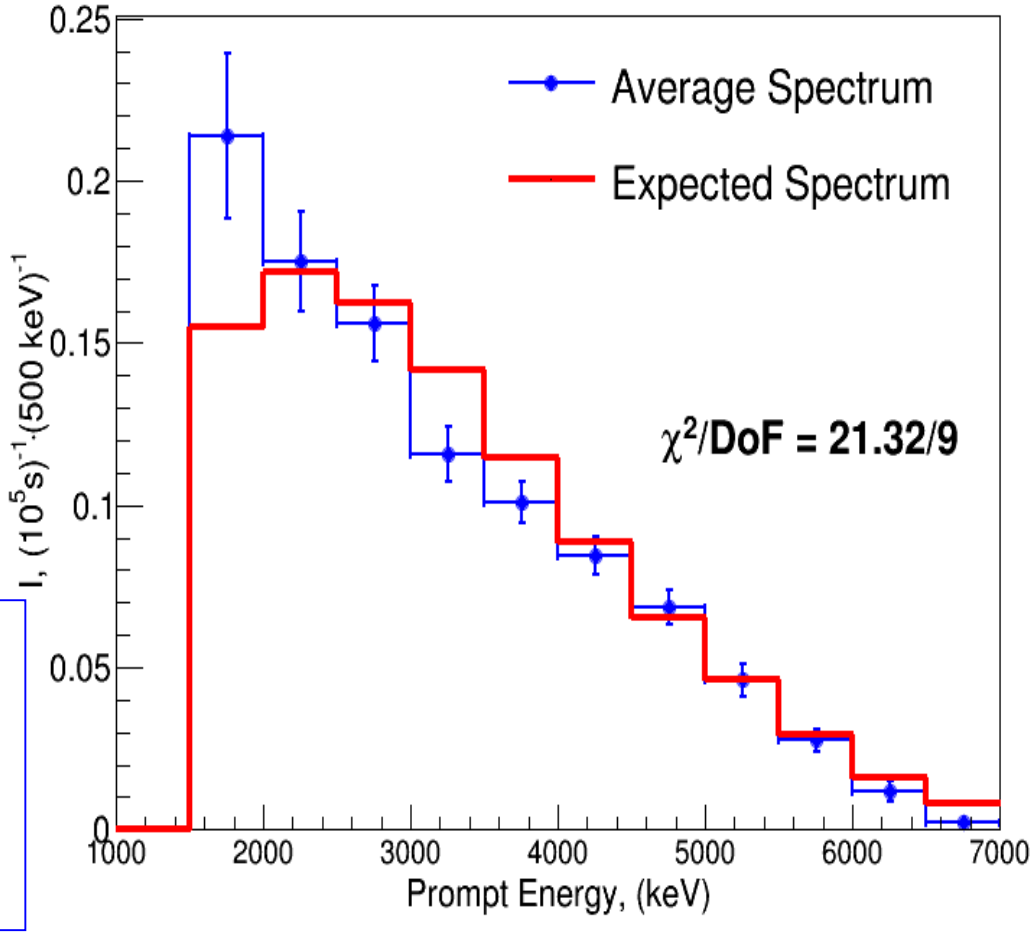

Spectrum of prompt signals in the detector for a total cycle of measurements summed over all distances (average distance — 8.6 meters). The red line shows Monte -Carlo simulation with neutrino spectrum of ^{235}U, as the SM-3 reactor works on highly enriched uranium.

There is problems with energy spectrum therefore we proposed the spectrum independent method of the experimental data analysis

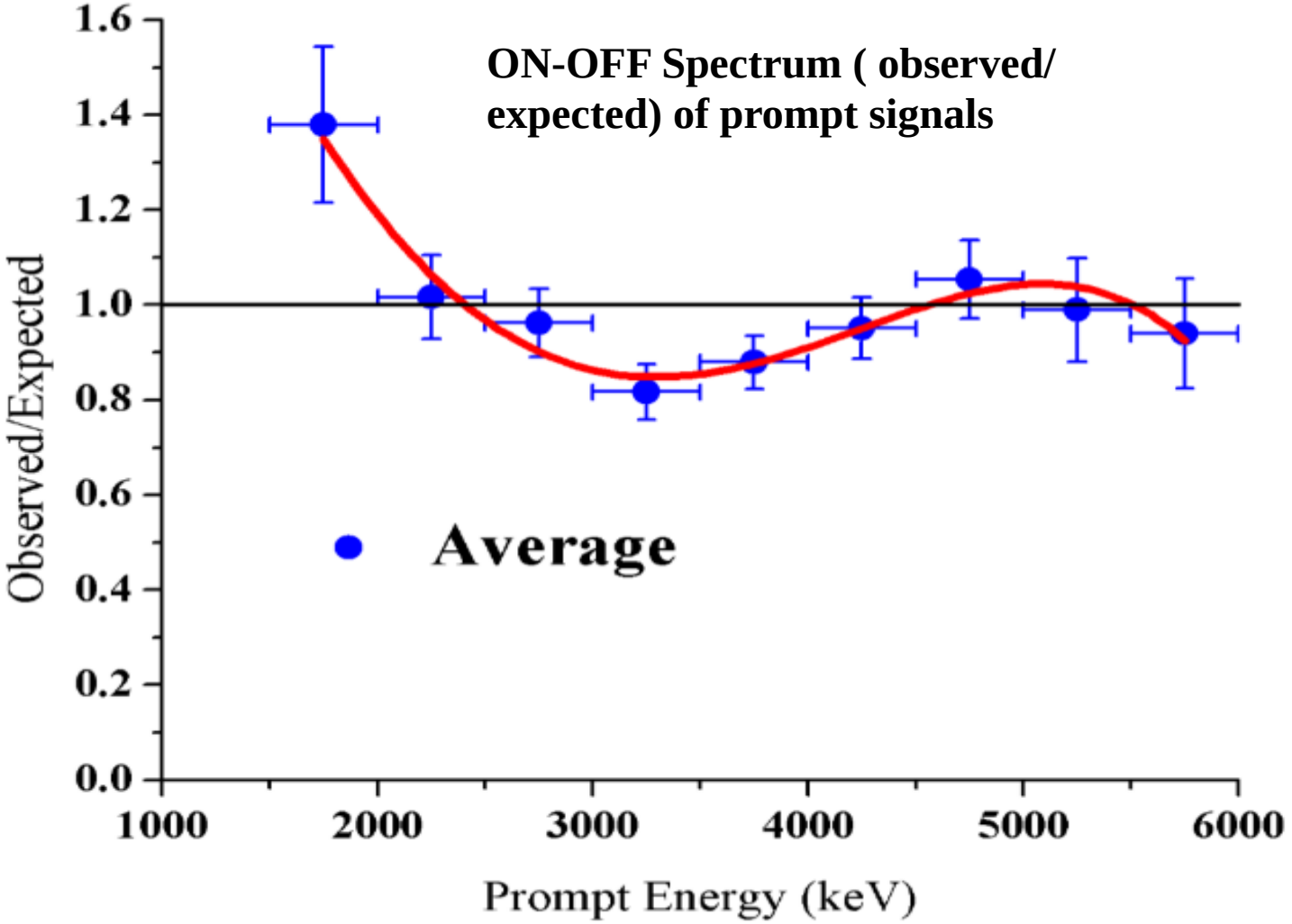

Spectrum (observed/ expected) of prompt signals in the detector for a total cycle of measurements summed over all distances (average distance — 8.6 meters).
Expected - Monte -Carlo simulation with neutrino spectrum of ^{235}U, as the SM-3 reactor works on highly enriched uranium.

SPECTRAL INDEPENDENT METHOD OF DATA TREATMENT AND ANALYSIS OF THE RUSULT

$N(E_i, L_k)$

Number of antineutrino events

Probability of antineutrino disappearance

$$P(\tilde{\nu}_e \to \tilde{\nu}_e) = 1 - \sin^2 2\theta_{14} \sin^2\left(1.27 \frac{\Delta m^2_{14}[eV^2]L[m]}{E_{\tilde{\nu}}[MeV]}\right) \quad (1)$$

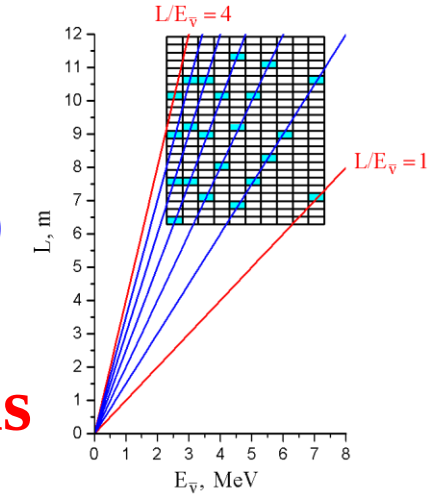

The spectrum independent method of experimental data analysis

$$R^{exp}_{i,k} = \frac{N(E_i, L_k)L_k^2}{K^{-1}\sum_k^K N(E_i, L_k)L_k^2} = \frac{[1 - \sin^2 2\theta_{14} \sin^2(1.27\Delta m^2_{14} L_k / E_i)]}{K^{-1}\sum_k^K [1 - \sin^2 2\theta_{14} \sin^2(1.27\Delta m^2_{14} L_k / E_i)]} = R^{th}_{i,k} \quad (2)$$

The denominator is significantly simplified with a range of measurement distances significantly greater than the characteristic oscillation period:

$$R^{th}_{ik} \approx \frac{1 - \sin^2 2\theta_{14} \sin^2(1.27\Delta m^2_{14} L_k / E_i)}{1 - 1/2 \sin^2 2\theta_{14}} \xrightarrow[\theta_{14}=0]{} 1$$

The method of the analysis of experimental data should not rely on precise knowledge of spectrum. One can carry out model independent analysis using equation (2), where numerator is the rate of antineutrino events with correction to geometric factor $1/L^2$ and denominator is its value averaged over all distances.

MONTE CARLO SIMULATION OF EXPECTED RESULTS WITH EMPLOYING OF SPECTRAL INDEPENDENT METHOD OF DATA ANALYSIS

The source of antineutrino with geometrical dimensions of the reactor core 42x42x35cm3 was simulated, as well as a detector of antineutrino taking into account its geometrical dimensions (50 sections of 22.5x22.5x75cm3).

The expected effect for the different energy resolution from MC calculation

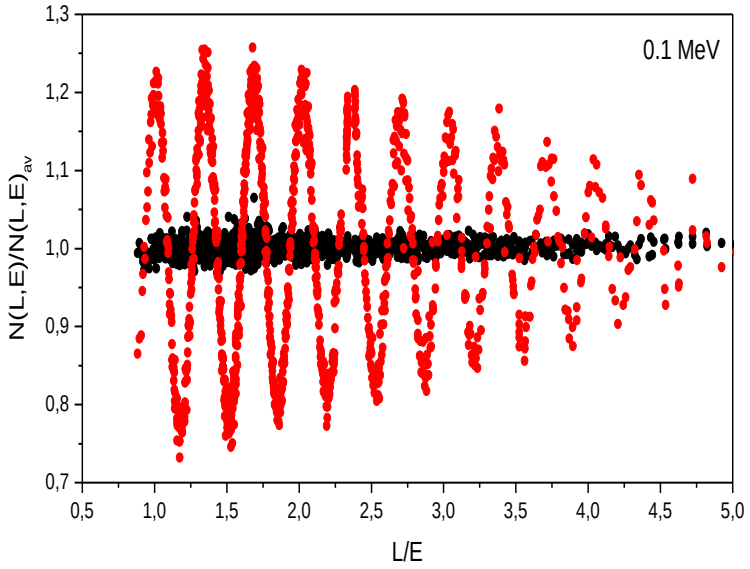

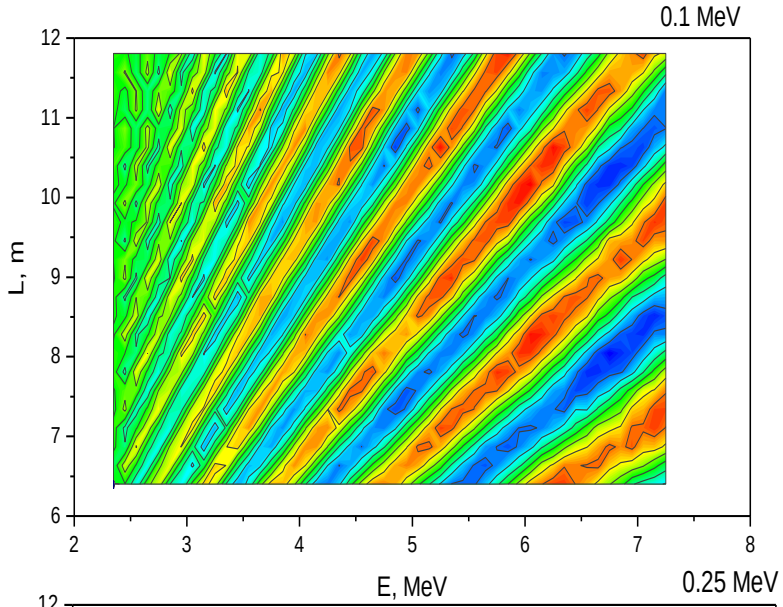

energy resolution 0.1 MeV

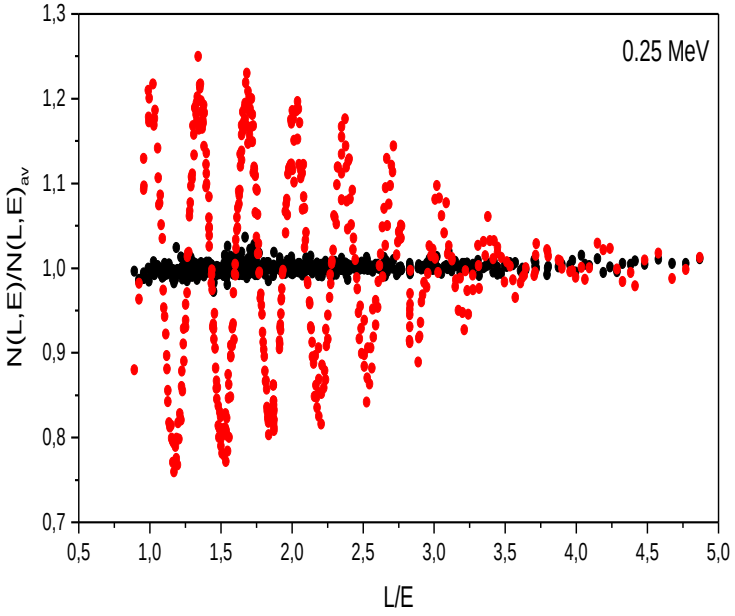

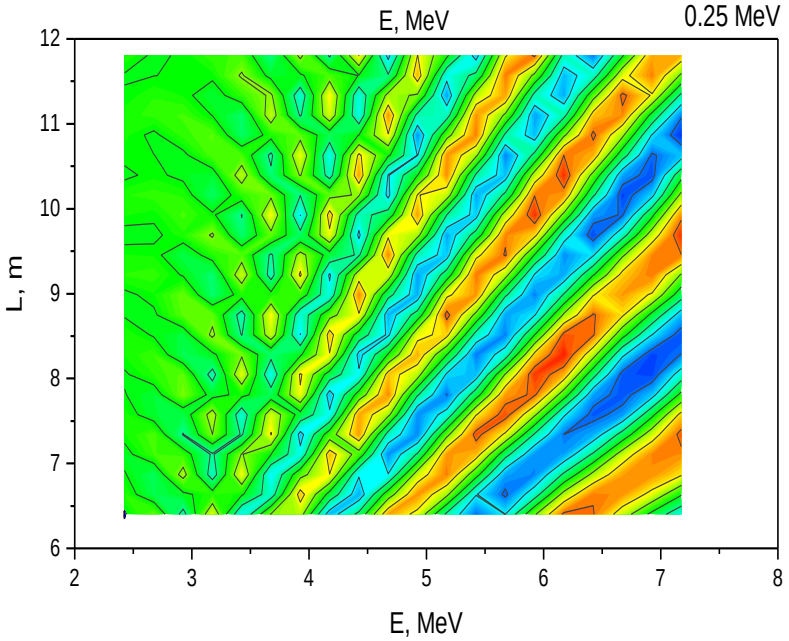

energy resolution 0.25 MeV

The expected effect for the different energy resolution from MC calculation

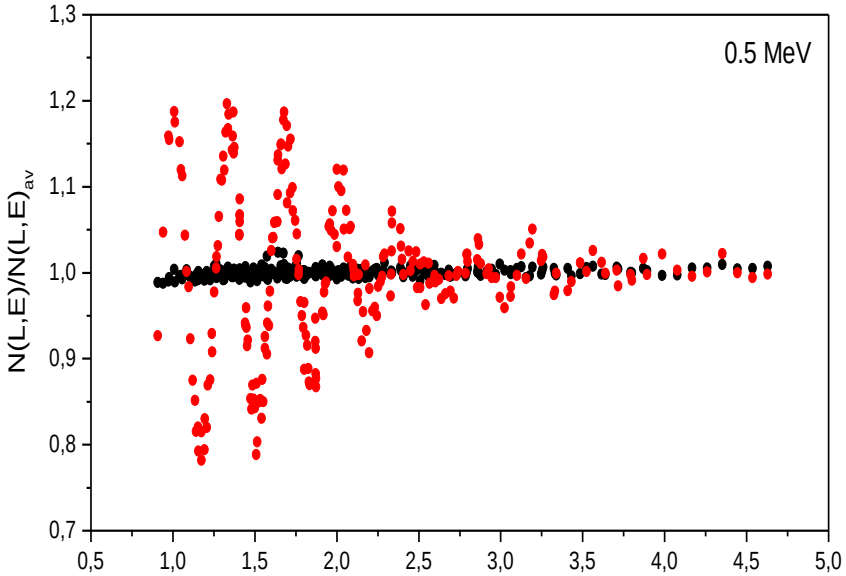

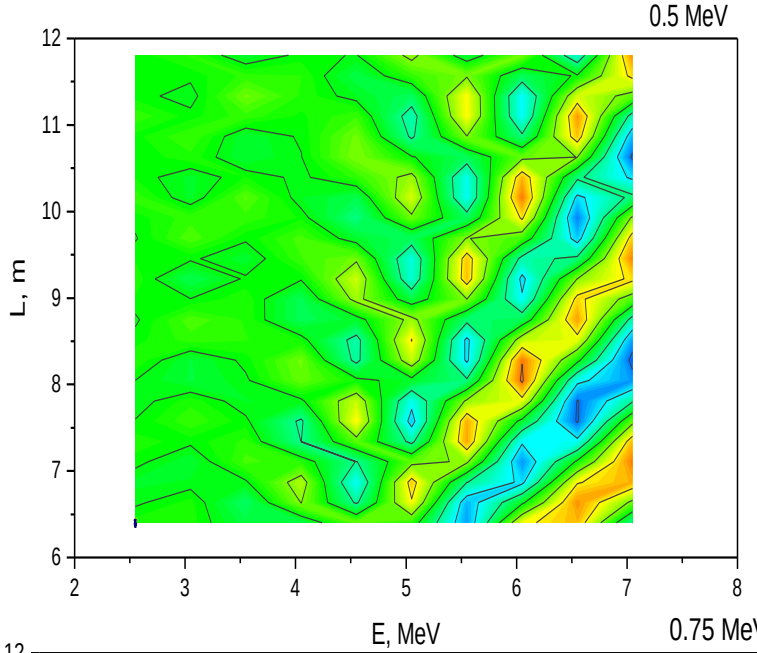

energy resolution 0.5 MeV (our case)

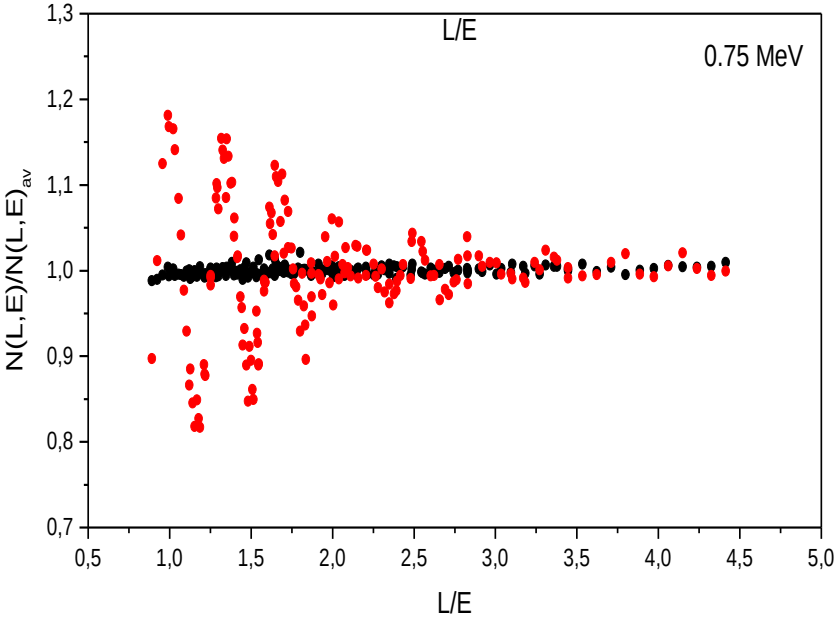

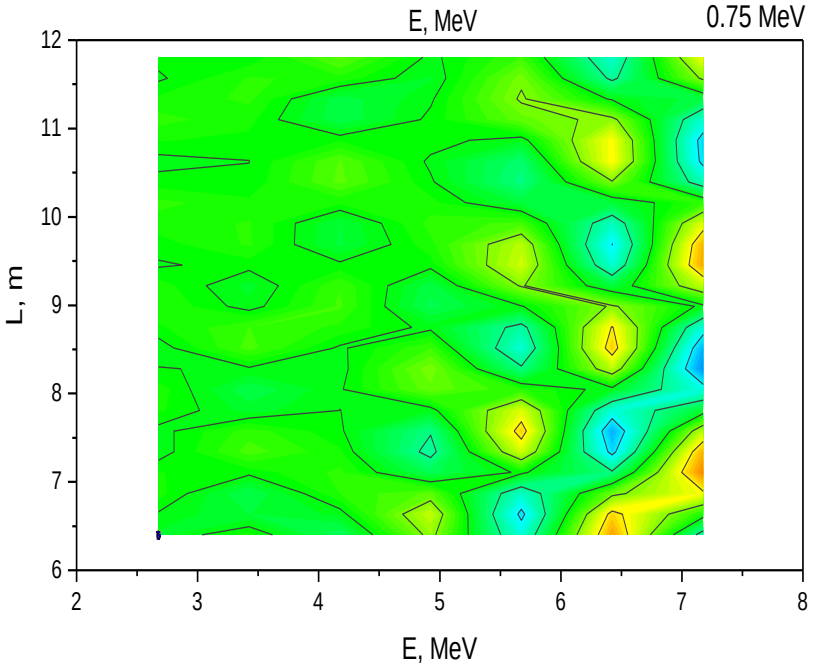

energy resolution 0.75 MeV

METHOD OF COHERENT DATA SUMMATION TO OBTAIN DEPENDENCE FROM RATIO L/E

METHOD OF COHERENT DATA SUMMATION TO OBTAIN DEPENDENCE FROM RATIO L/E

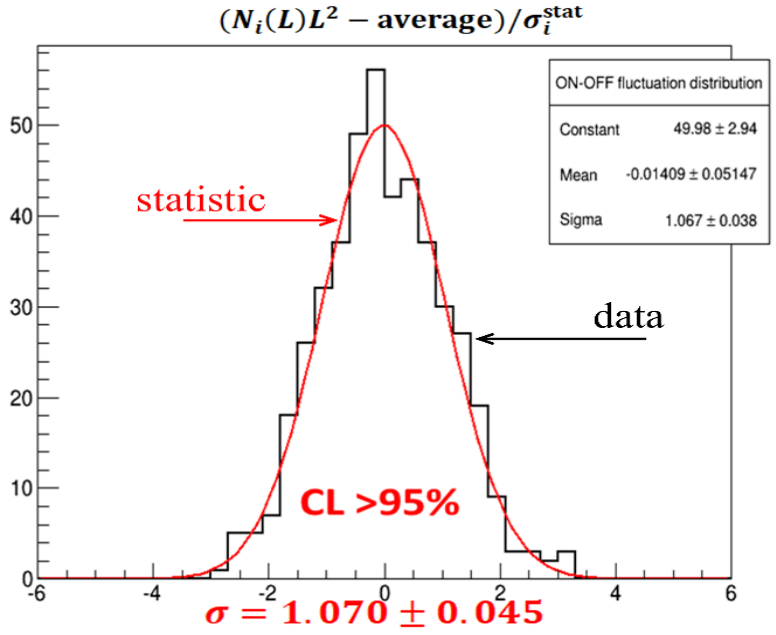

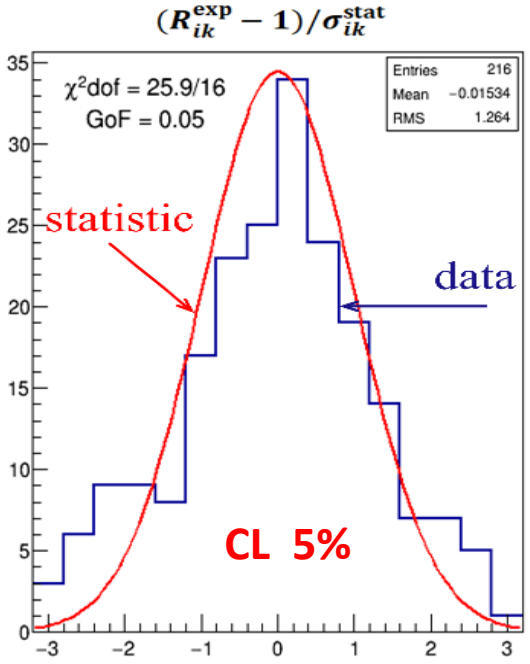

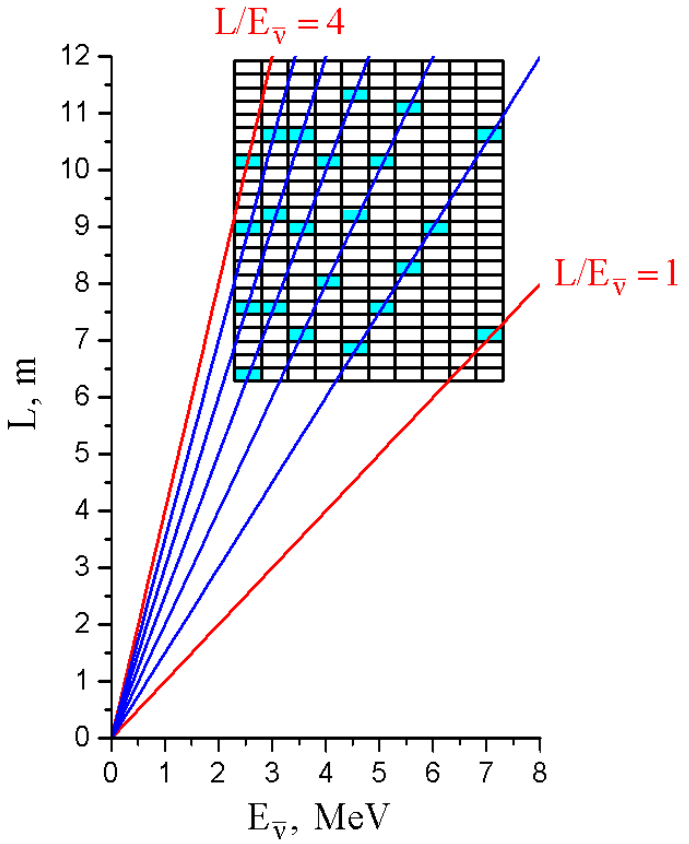

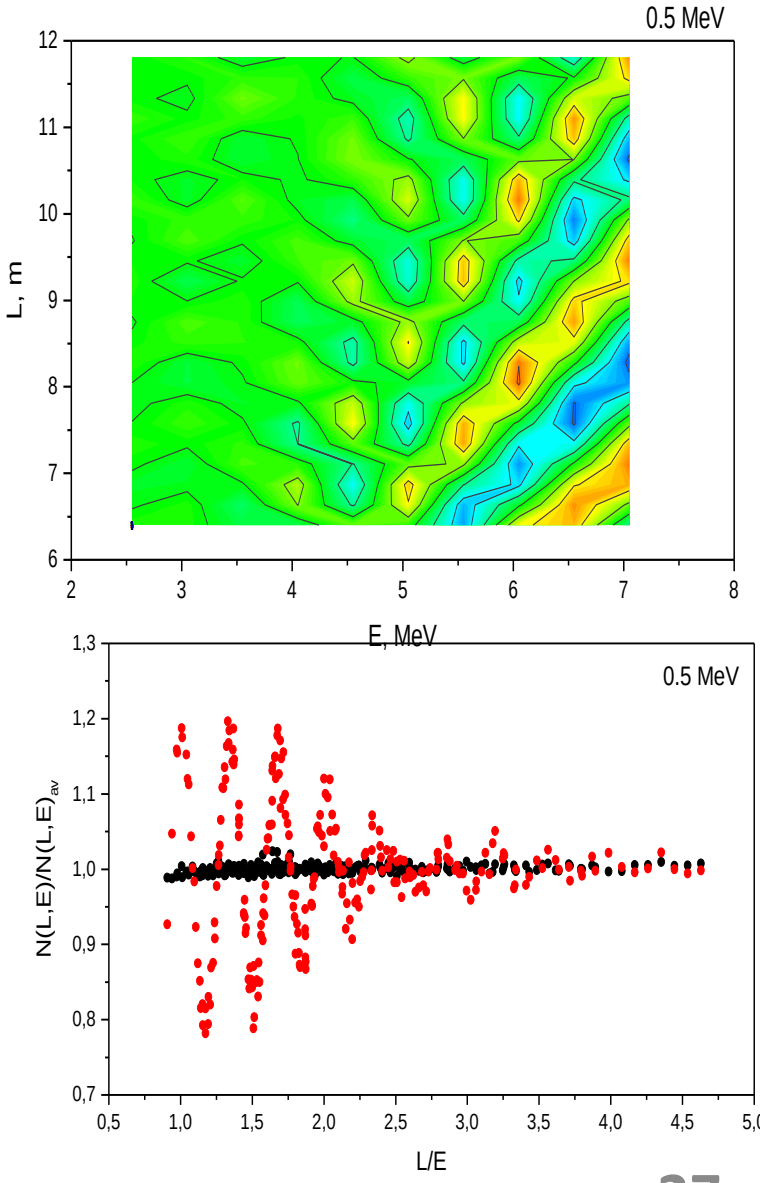

$N(E_i, L_k)$

Number of antineutrino events

Probability of antineutrino disappearance

$$P(\tilde{\nu}_e \to \tilde{\nu}_e) = 1 - \sin^2 2\theta_{14} \sin^2\left(1.27 \frac{\Delta m^2_{14}[eV^2]L[m]}{E_{\tilde{\nu}}[MeV]}\right) \quad (1)$$

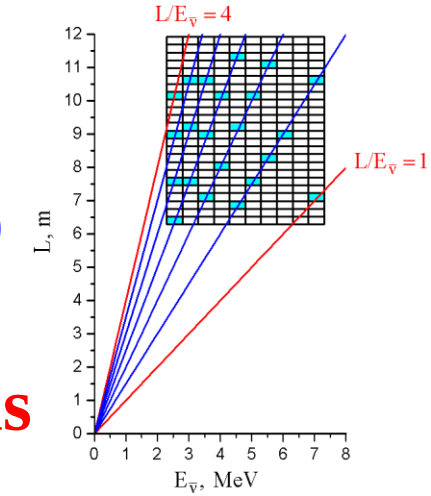

The spectrum independent method of experimental data analysis

$$R^{\exp}_{i,k} = \frac{N(E_i, L_k)L_k^2}{K^{-1}\sum_k^K N(E_i, L_k)L_k^2} = \frac{[1 - \sin^2 2\theta_{14} \sin^2(1.27\Delta m^2_{14} L_k / E_i)]}{K^{-1}\sum_k^K [1 - \sin^2 2\theta_{14} \sin^2(1.27\Delta m^2_{14} L_k / E_i)]} = R^{th}_{i,k} \quad (2)$$

The results of the analysis of optimal parameters Δm^2_{14} and $\sin^2 2\theta_{14}$ using χ^2 method

$$\sum_{i,k} [(R^{\exp}_{i,k} - R^{th}_{i,k})^2 / (\Delta R^{\exp}_{i,k})^2] = \chi^2(\sin^2 2\theta_{14}, \Delta m^2_{14})$$

The results of the analysis of optimal parameters Δm^2_{14} and $\sin^2 2\theta_{14}$ using χ^2 method

We observed the oscillation effect at C.L. 99.7% (3.5σ) in vicinity of :

$$\Delta m^2_{14} \approx 7 eV^2$$

$$\sin^2 2\theta_{14} \approx 0.4$$

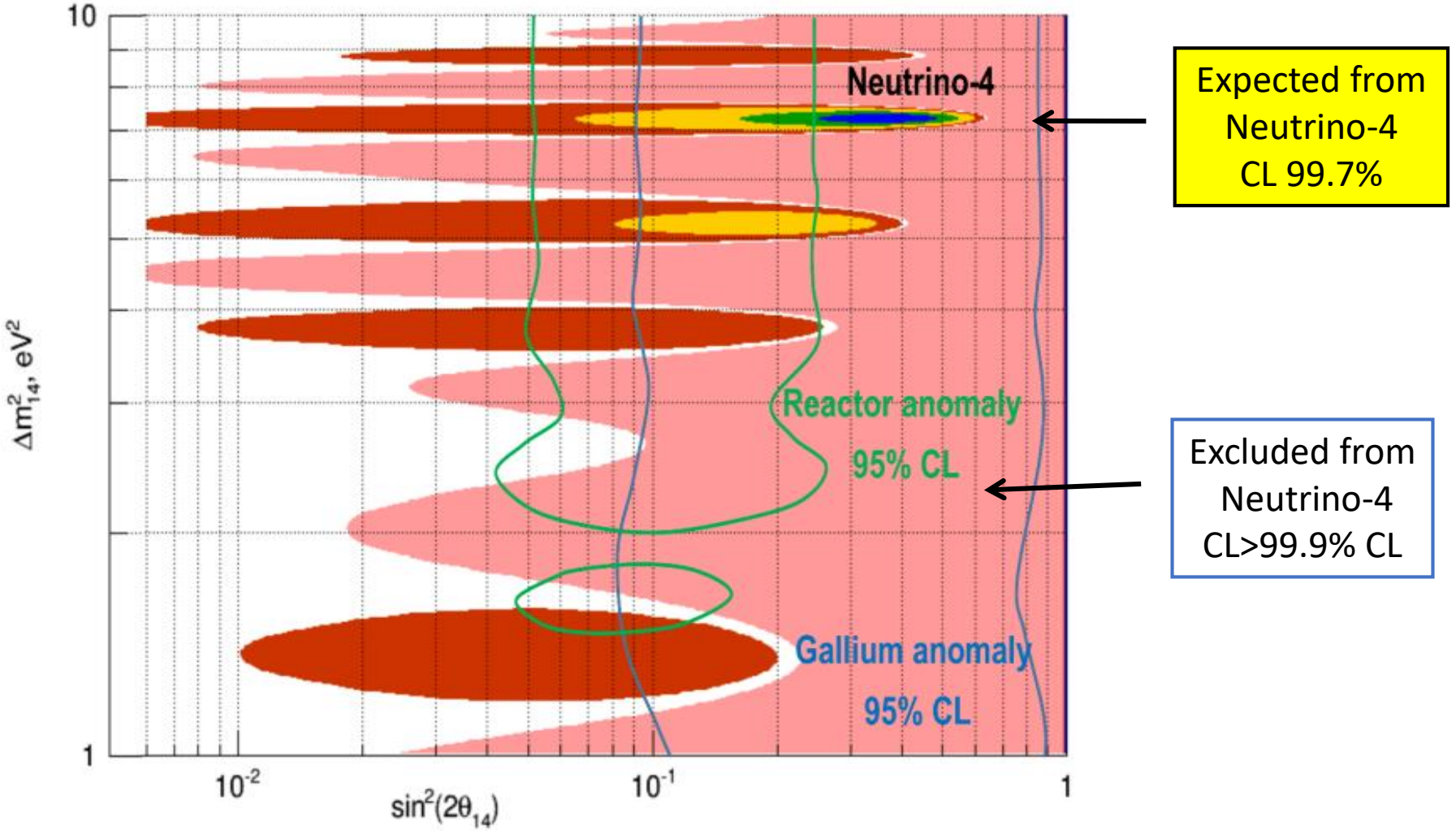

Analysis of the confidence level of the result

We observed the oscillation effect at C.L. 99.7% (3.5 σ) in vicinity of :

$$\Delta m_{14}^2 \approx 7 eV^2 \qquad \sin^2 2\theta_{14} \approx 0.4$$

It is often discussed that stricter limitations on the confidence level of the result can be obtained using the Feldman-Cousins method. In compliance Wilks theorem $\Delta\chi^2$method is possible to apply successfully if effect is observed at the level of reliability 3σ more. The result of processing without taking into account systematic errors with an energy interval of 500 keV is $\sin^2 2\theta_{14} = 0.38 \pm 0.11(3.5\sigma)$, and when averaging data over 125keV, 250keV and 500keV is $\sin^2 2\theta_{14} \approx 0.26 \pm 0.08(3.2\sigma)$. Since the reliability of the effect we observe exceeds 3σ, we do not consider it mandatory to use the Feldman-Cousins method and propose to do another additional analysis of our data.

3.2 σ ⟶ **3.0 σ**

Results of analysis of data with energy interval 500keV

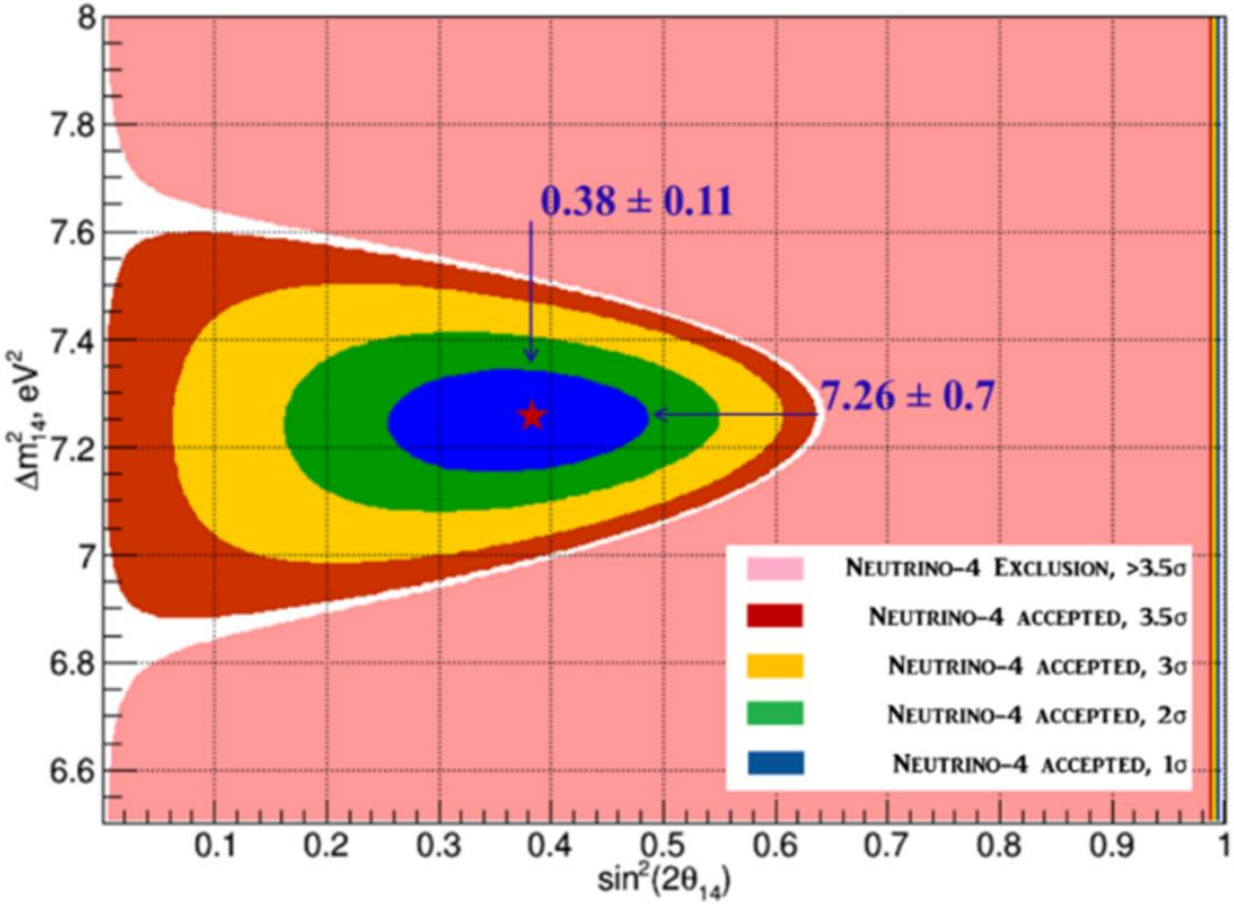

Results of data analysis with average by energy intervals 125keV, 250keV и 500keV

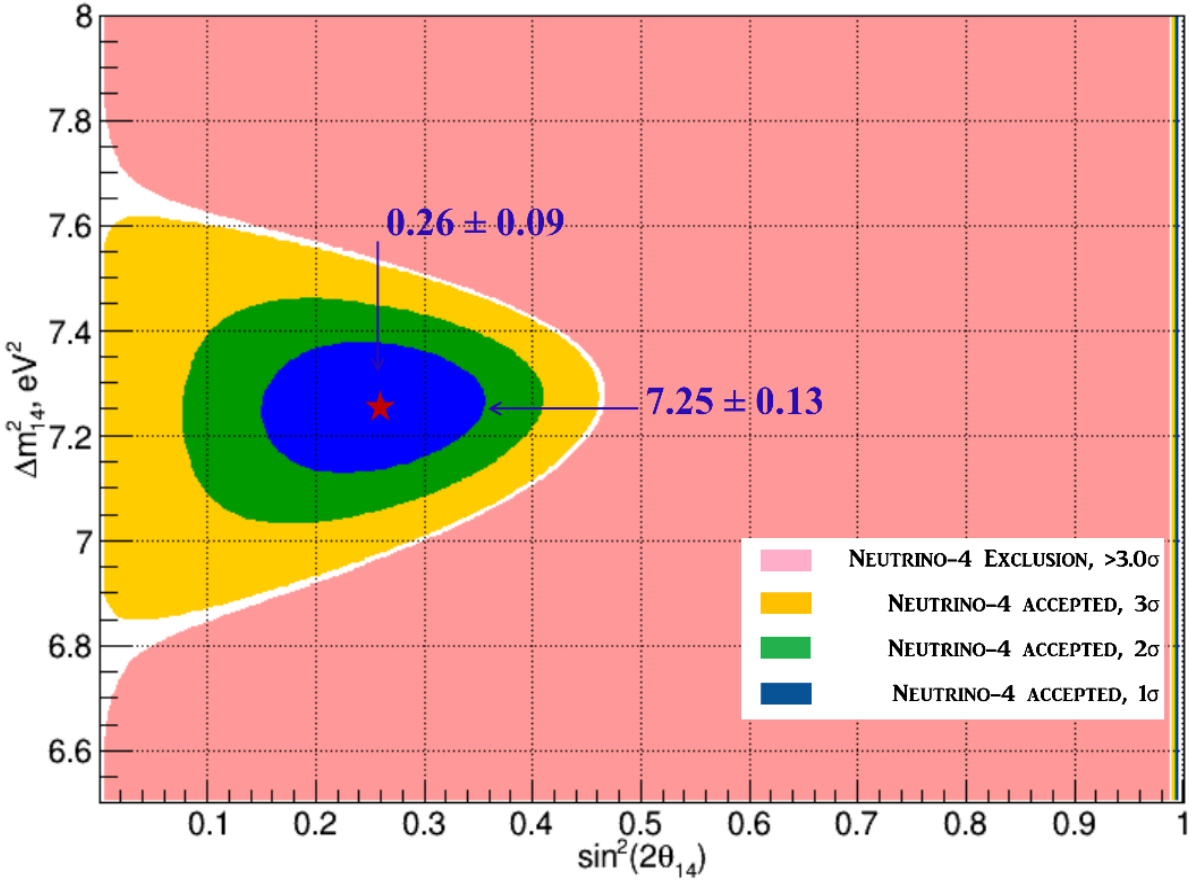

For reasons of reliability of the final result we choose the case of data processing with averaging

$$\Delta m^2_{14} \approx 7.25 \text{eV}^2$$

$$\sin^2 2\theta_{14} \approx 0.26 \pm 0.08(3.0)\sigma$$

All data 2016 -2019 + background 20119

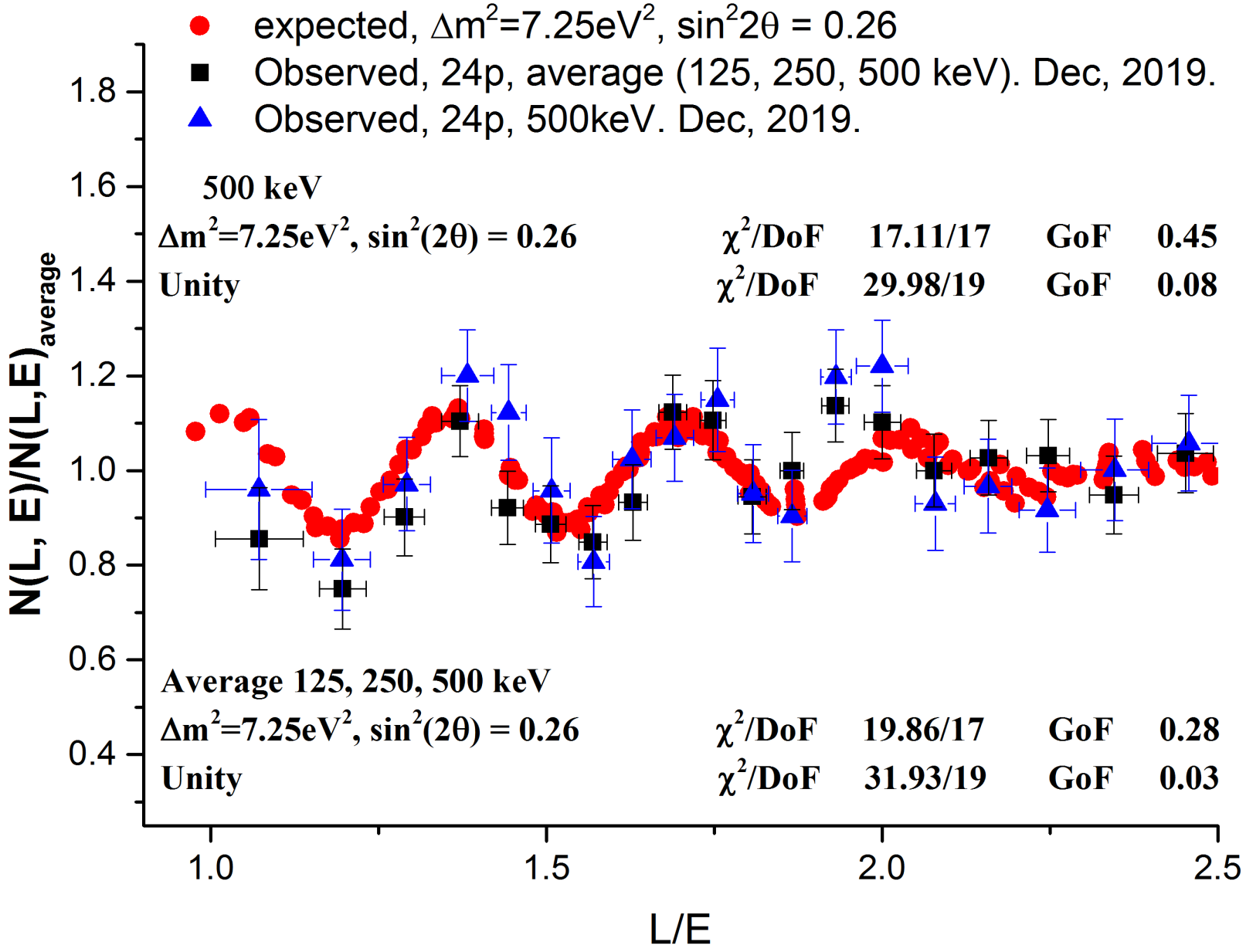

The period of oscillation for neutrino energy 4 MeV is 1.4 m

A.P.Serebrov, et al.
JETP Letters,
Volume 109, 2019
Issue 4, pp 213–221.

JETP Letters,
Volume 112, 2020
Issue 4, pp 211–225.

arxiv:2003.03199
arxiv:2005.05301

NEUTRINO 2020

Dependence of antineutrino flux on the distance to the reactor core. a - direct experimental dependence, b – normalized experimental dependence, c - oscillation curve with the experimental results in range 6-12 m.

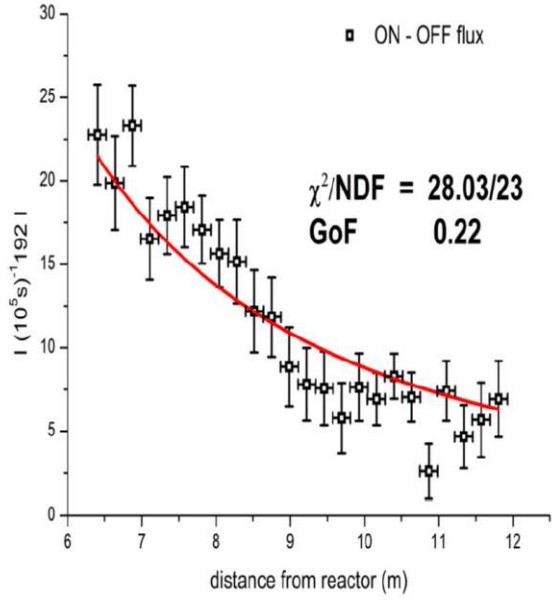

Fig. 10. Dependence of antineutrino flux on the distance to the reactor core – direct measurements.

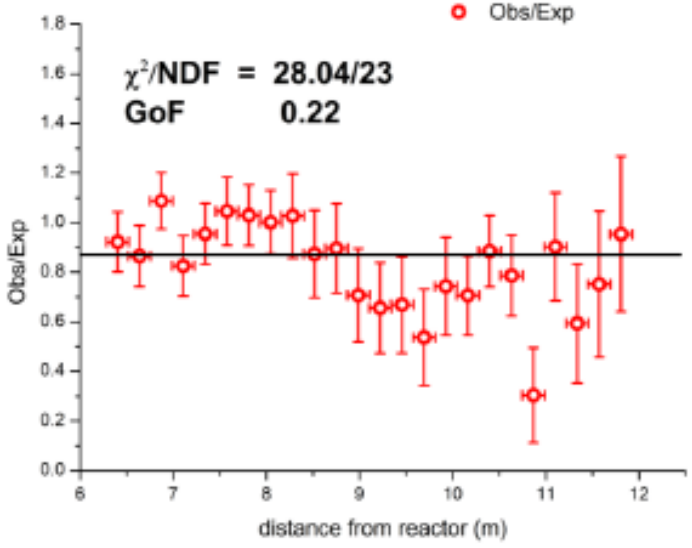

FIG. 58. Representation of experimental results in form of dependence of antineutrino flux on the distance to the reactor core normalized with the law A/L^2.

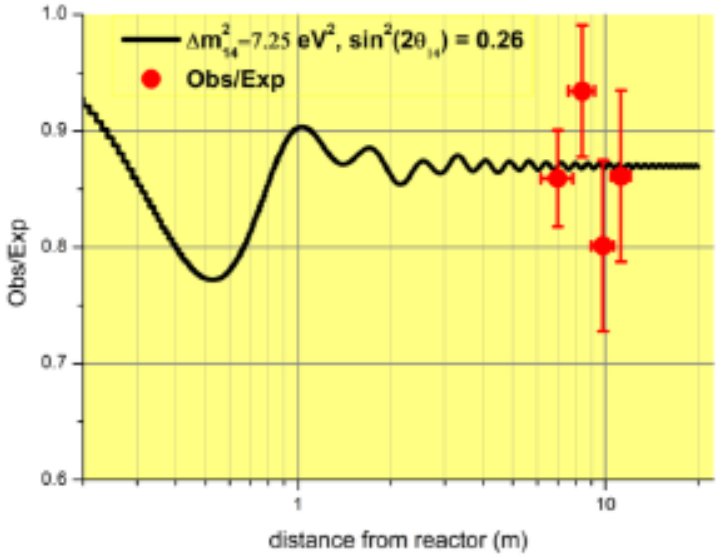

FIG. 59. Oscillation curve and experimental results in range 6-12 m.

a **b** **c**

Analysis of possible systematic effects

To carry out analysis of possible systematic effects one should turn off antineutrino flux (reactor) and perform the same analysis of background data

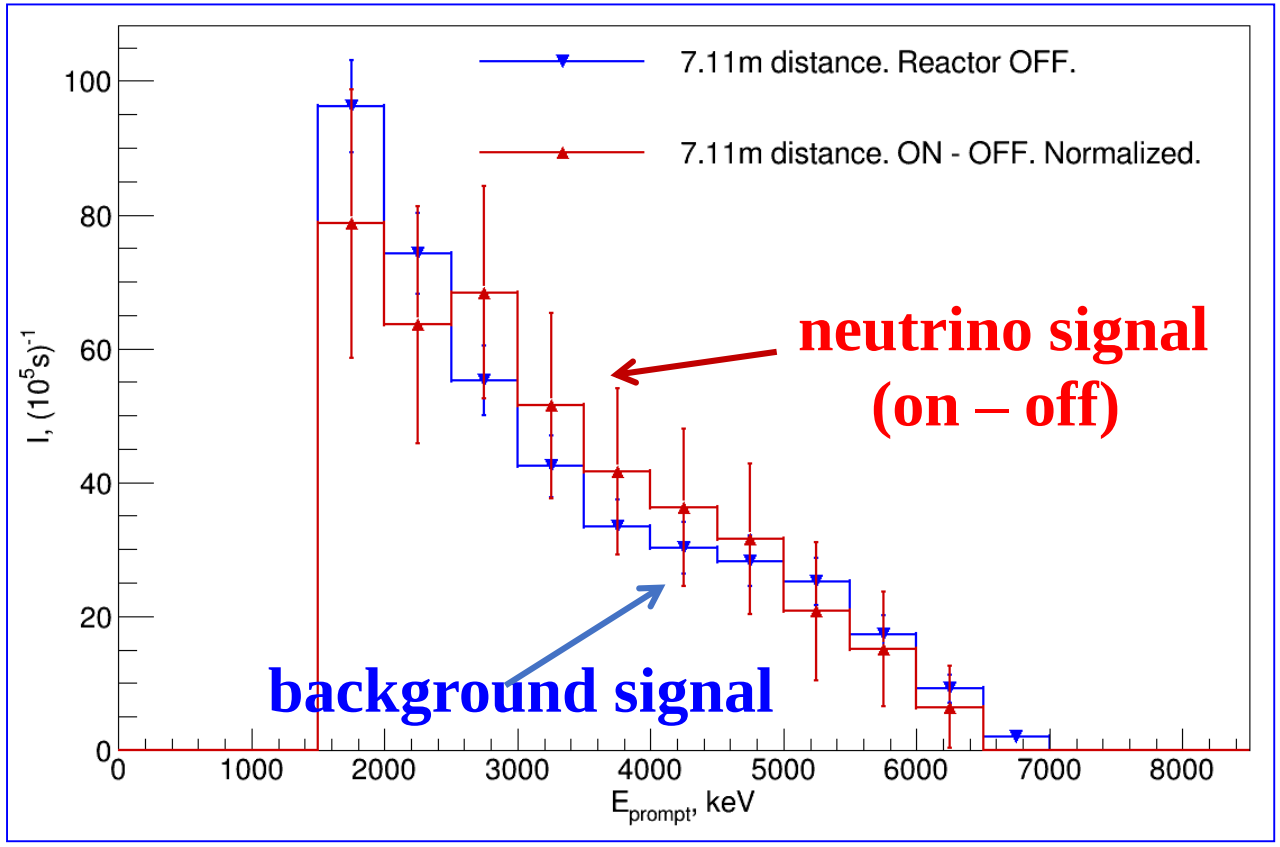

The spectrum for neutrino signal and background signal are similar therefore test for systematic effect have to be adequate .

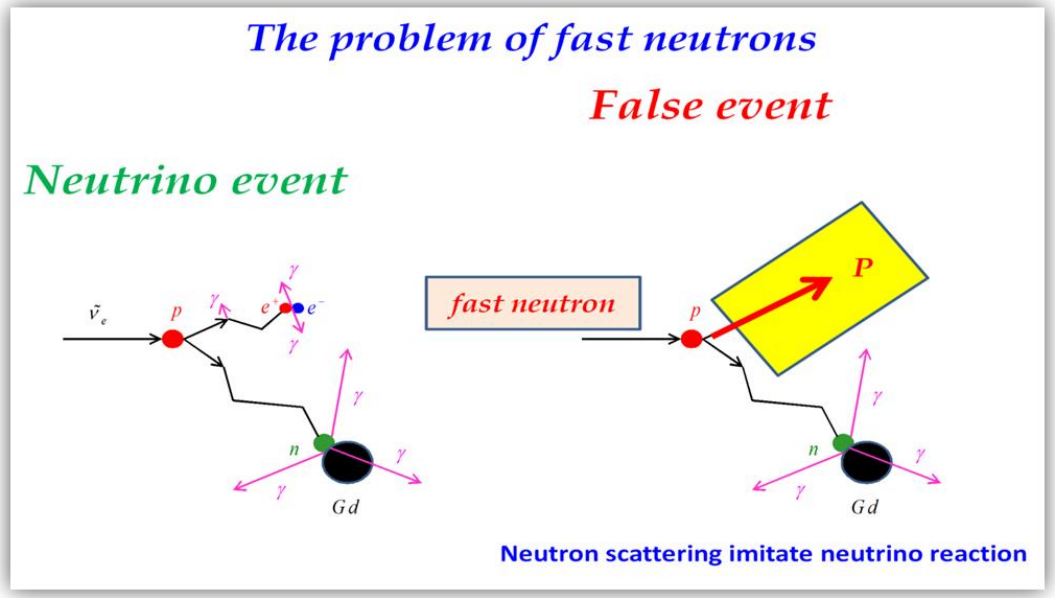

Test of systematic effects

To carry out analysis of possible systematic effects one should turn off antineutrino flux (reactor) and perform the same analysis of obtained data

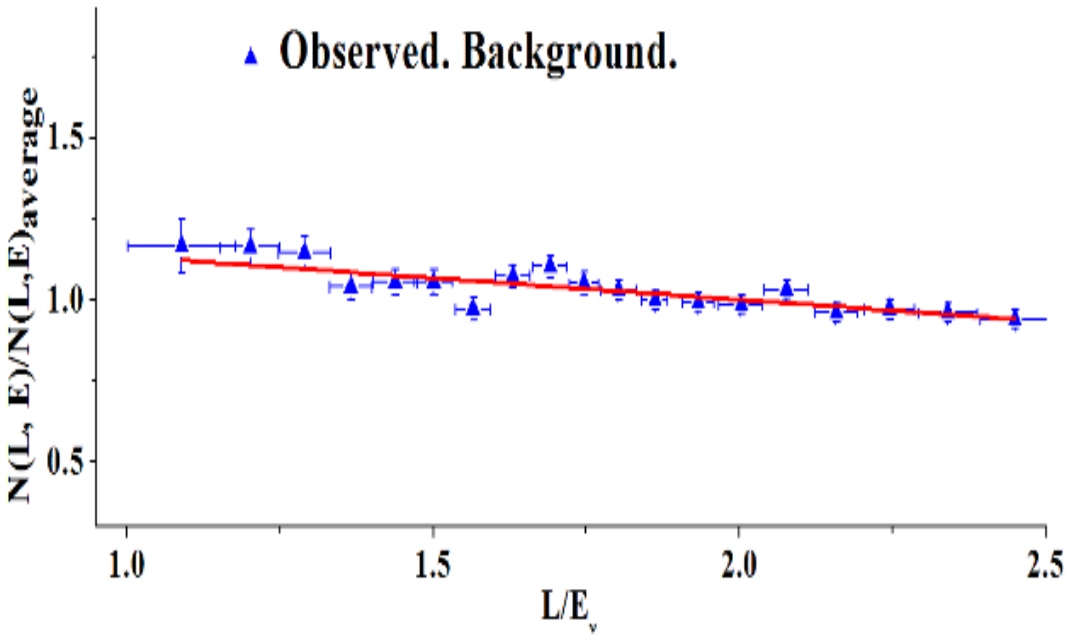

data analysis using coherent summation method

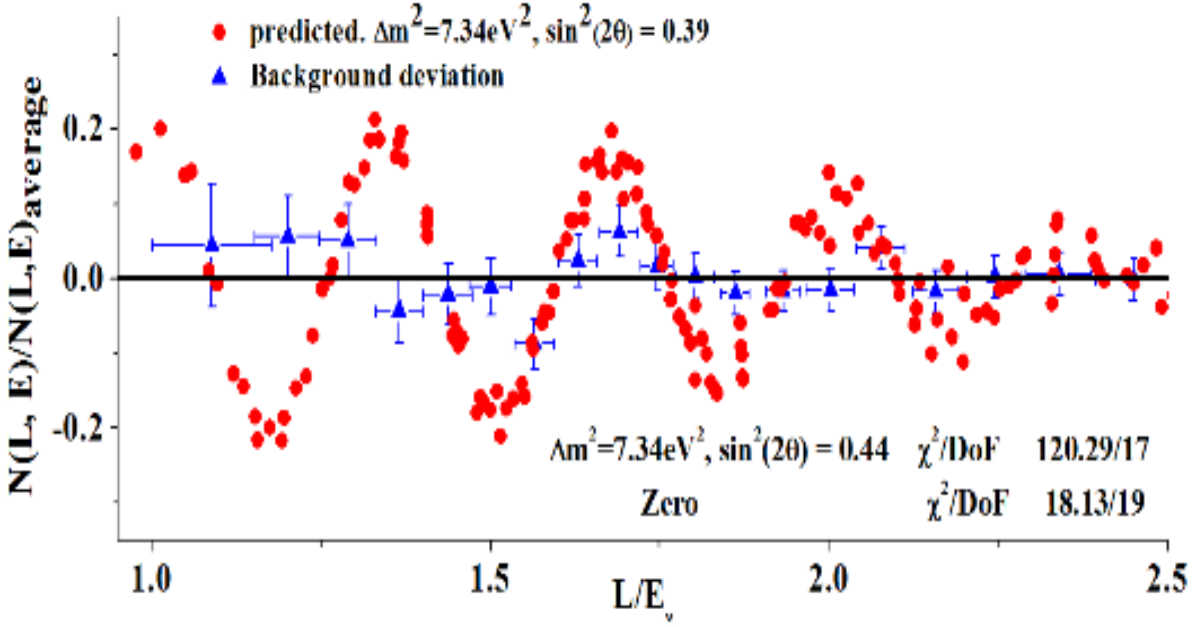

analysis of the results on oscillation parameters plane

Thus no instrumental systematic errors were observed.

Influence of unequal efficiency of different detector rows.

The next question is an influence of unequal efficiency of neutrino events registration in different detector rows.

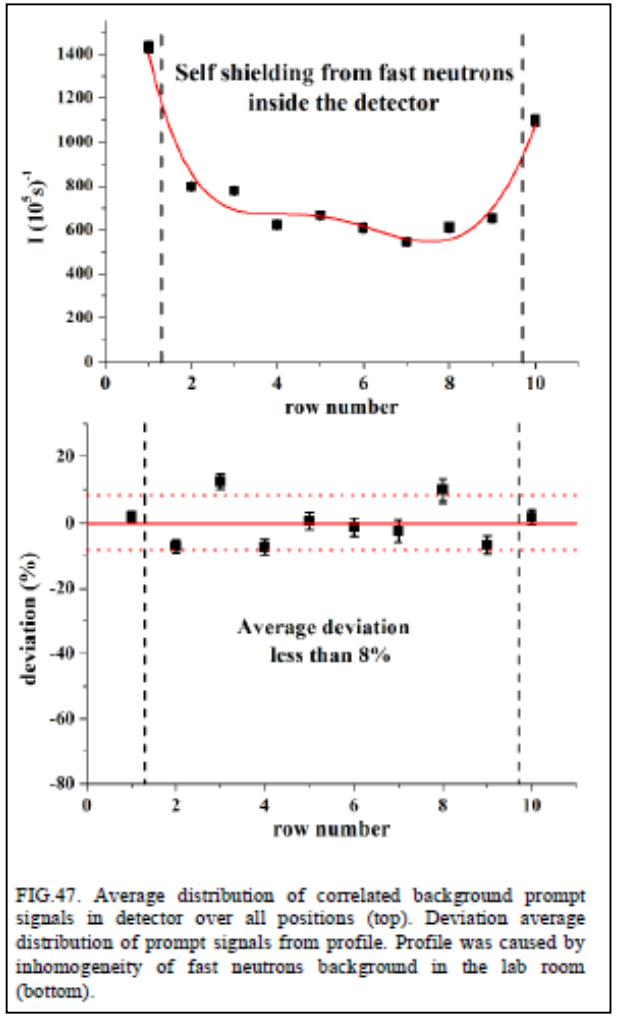

FIG.47. Average distribution of correlated background prompt signals in detector over all positions (top). Deviation average distribution of prompt signals from profile. Profile was caused by inhomogeneity of fast neutrons background in the lab room (bottom).

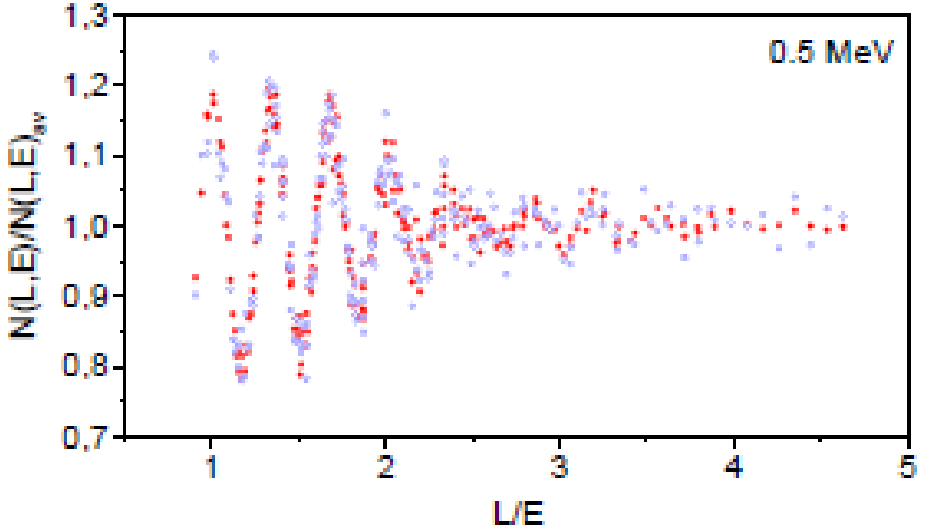

It can be seen, that deviations in the efficiency of detecting correlated events at different distances did not affect the effect of oscillations .

This situation can be explained since the effect of oscillations is resonant and successfully survives in the presence of noise.

Efficiencies affect the final results, one must take into account that averaging of spectra obtained with various rows at the same distance.

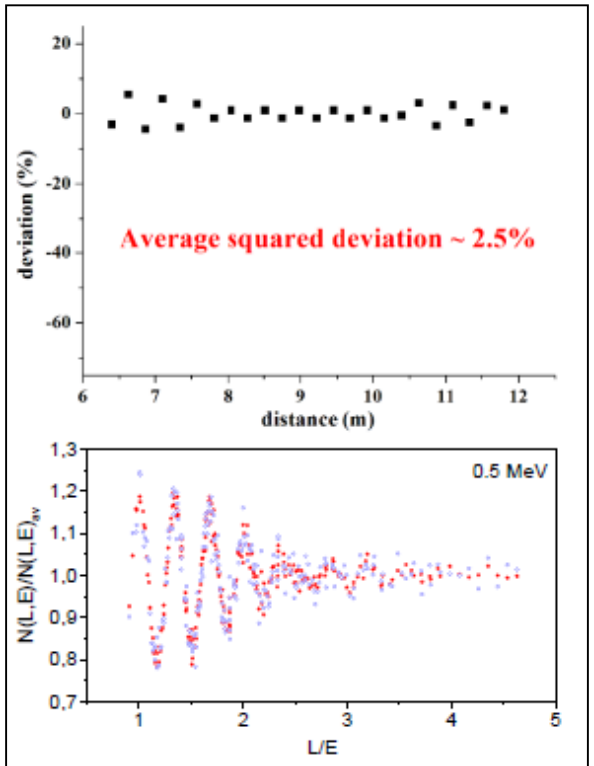

FIG. 48. Top – deviation of counts of correlated background of each distance from the reactor after averaging over rows from the mean value. MC modeling of the oscillation effect considering deviations of the detection efficiencies for correlated events at different distances. Red dots – oscillation effect ignoring the influence of deviations of the correlated events registration efficiencies at different distances; blue dots – oscillation effect considering this influence.

There is no influence of unequal efficiency of different detector rows

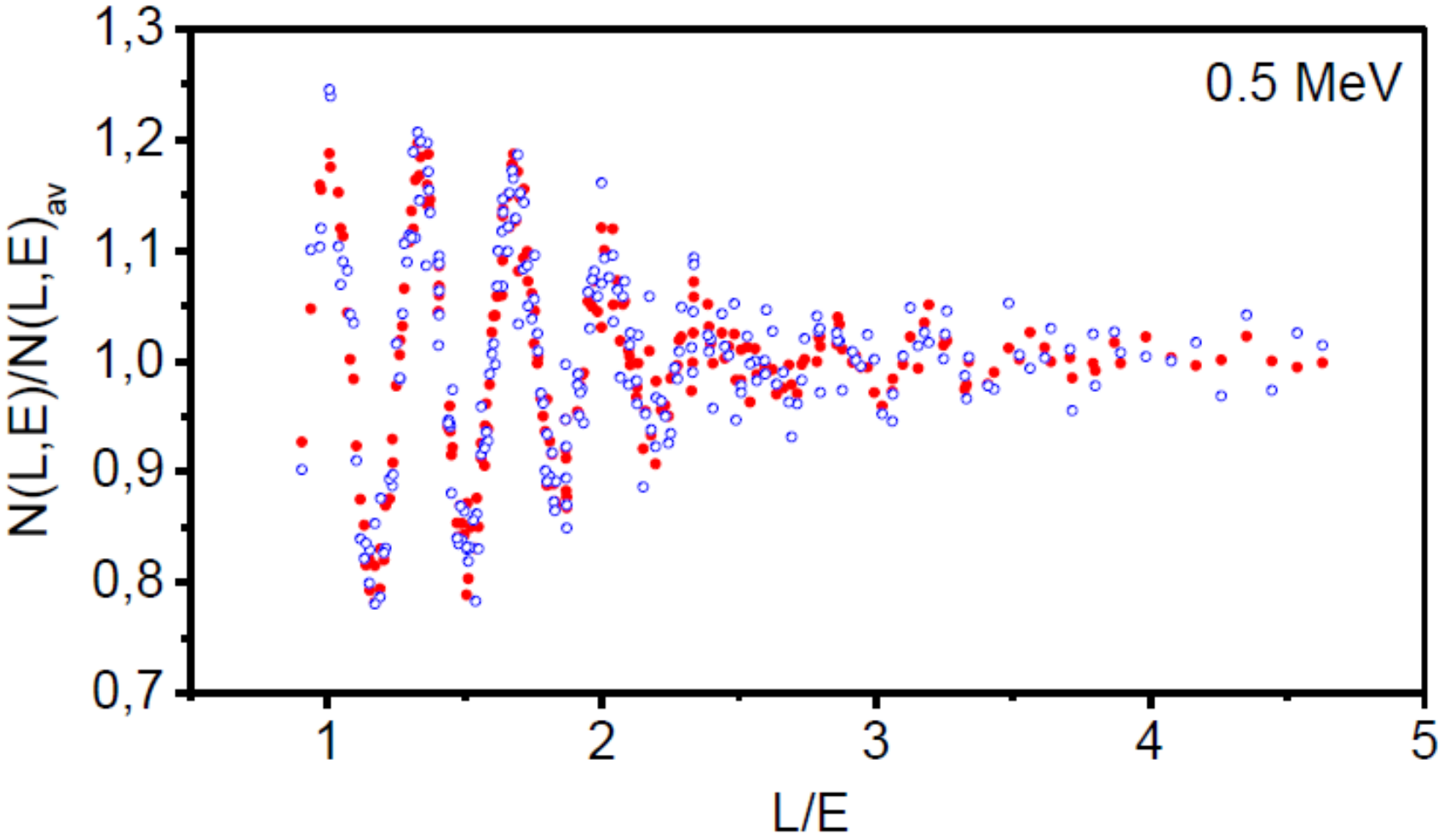

Deviation of counts of correlated background of each distance from the reactor after averaging over rows from the mean value. MC modeling of the oscillation effect considering deviations of the detection efficiencies for correlated events at different distances. Red dots – oscillation effect ignoring the influence of deviations of the correlated events registration efficiencies at different distances; blue dots – oscillation effect considering this influence.

Stability of the oscillation effect

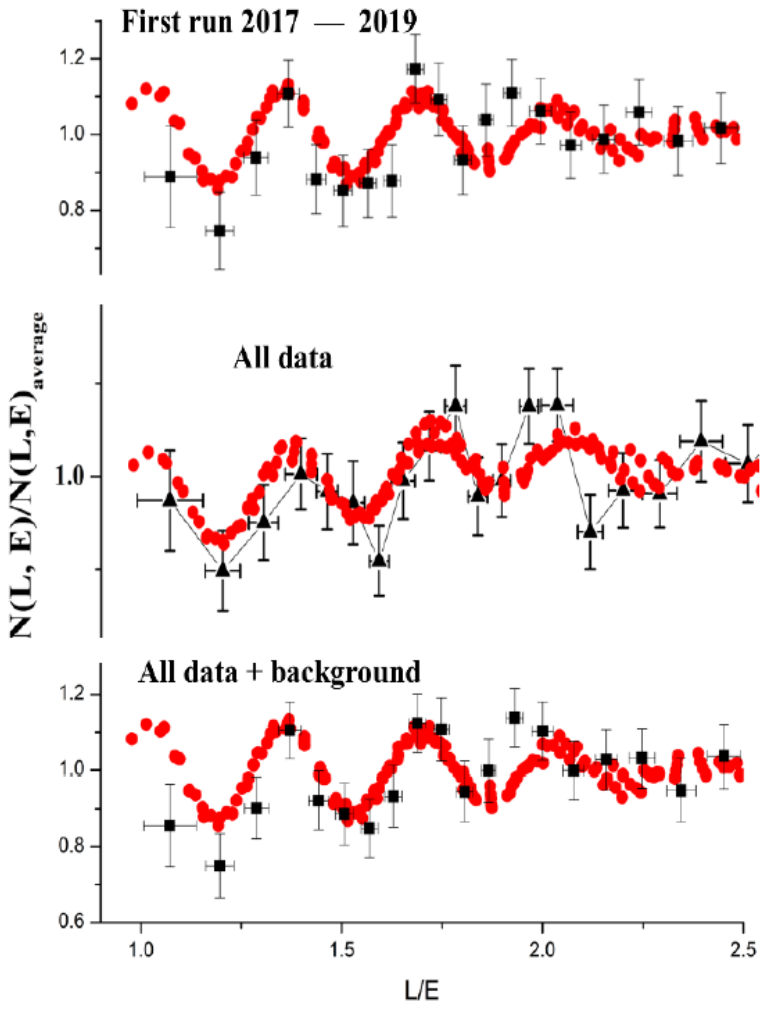

FIG. 54. Stability of the oscillation effect. Black figures are experimental points, red circles expected dependence.

Stability of the correlated background

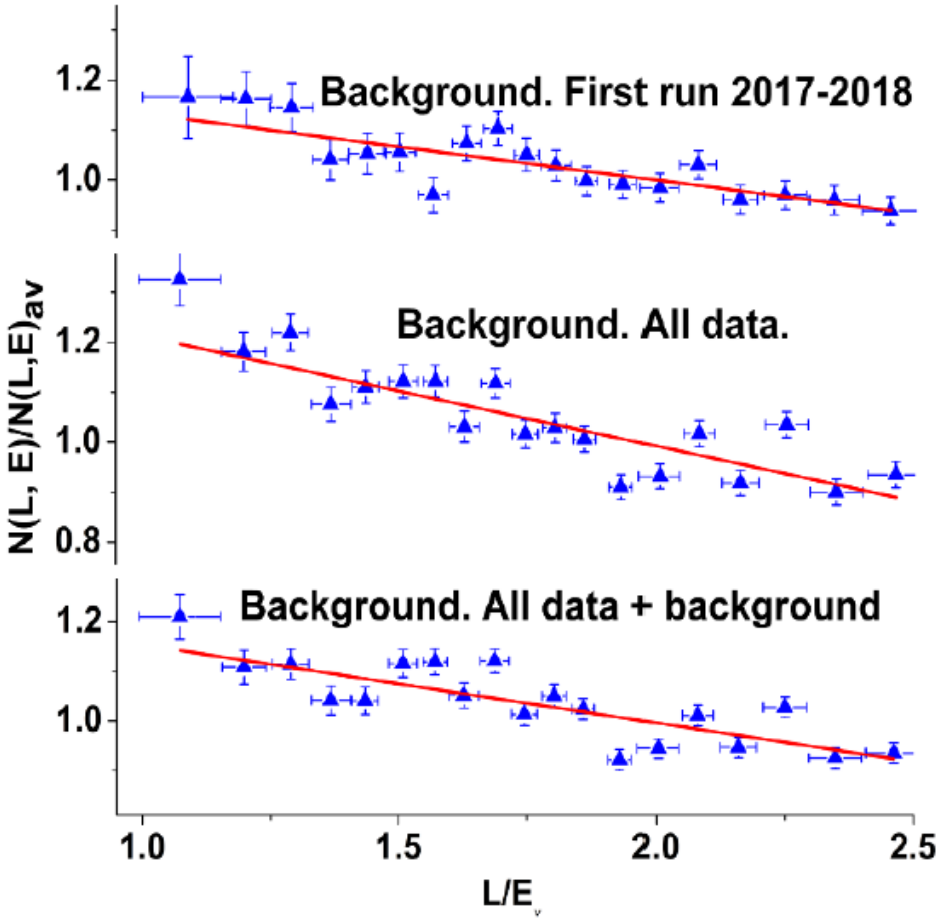

FIG. 55. Stability of the correlated background (blue dots). Red line is linear approximation.

SYSTEMATIC ERRORS OF THE EXPERIMENT

$$\Delta m_{14}^2 = 7.25 \pm 0.13_{st} \pm 1.08_{syst} = 7.25 \pm 1.09.$$

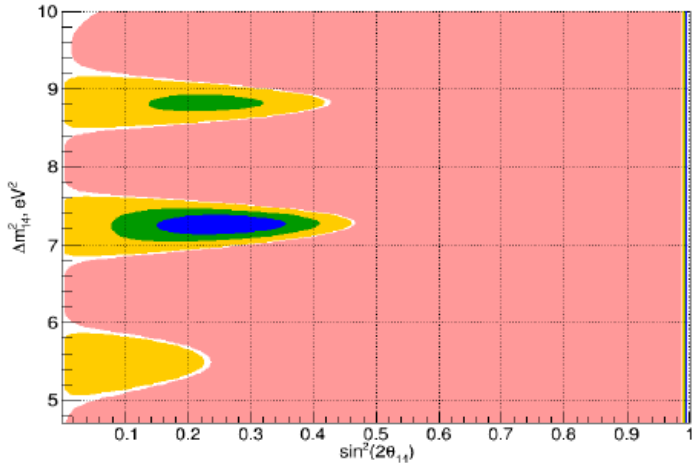

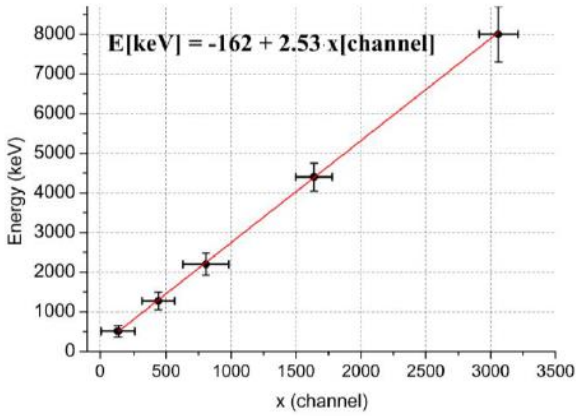

$$\sin^2 2\theta = 0.26 \pm 0.08_{stat} \pm 0.05_{syst} = 0.26 \pm 0.09(2.9\sigma)$$

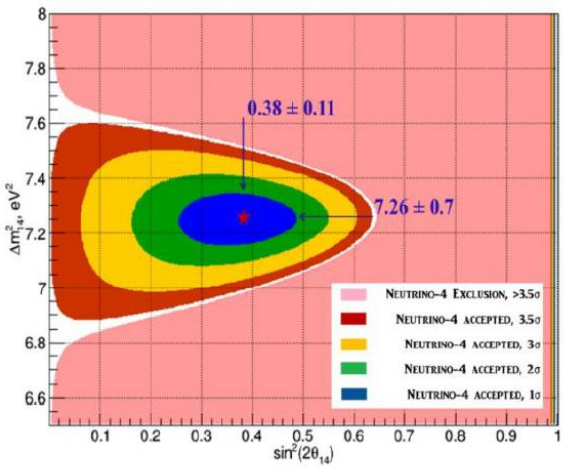

Fig. 5. The significantly magnified central area if prompt spectrum has 500 keV bin width.

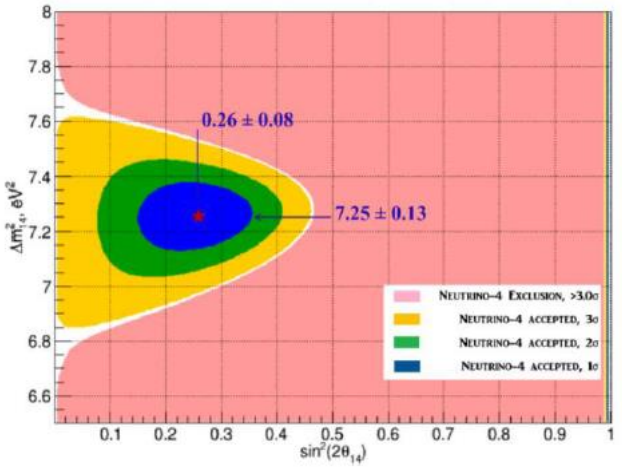

FIG. 53. Confidence levels of the area around oscillation parameters obtained as the best fit in case of averaging over three data sets.

SYSTEMATIC ERRORS OF THE EXPERIMENT

$$\boldsymbol{\Delta m^2_{14} = 7.25 \pm 0.13_{st} \pm 1.08_{syst} = 7.25 \pm 1.09 eV^2}$$

$$\sin^2 2\theta = 0.26 \pm 0.08_{stat} \pm 0.05_{syst} = 0.26 \pm 0.09 (2.9\sigma)$$

COMPARISON OF THE RESULT OF EXPERIMENT NEUTRINO-4 WITH REACTOR AND GALLIUM ANOMALIES

Reactor antineutrino anomaly with oscillation curve obtained in experiment Neutrino-4

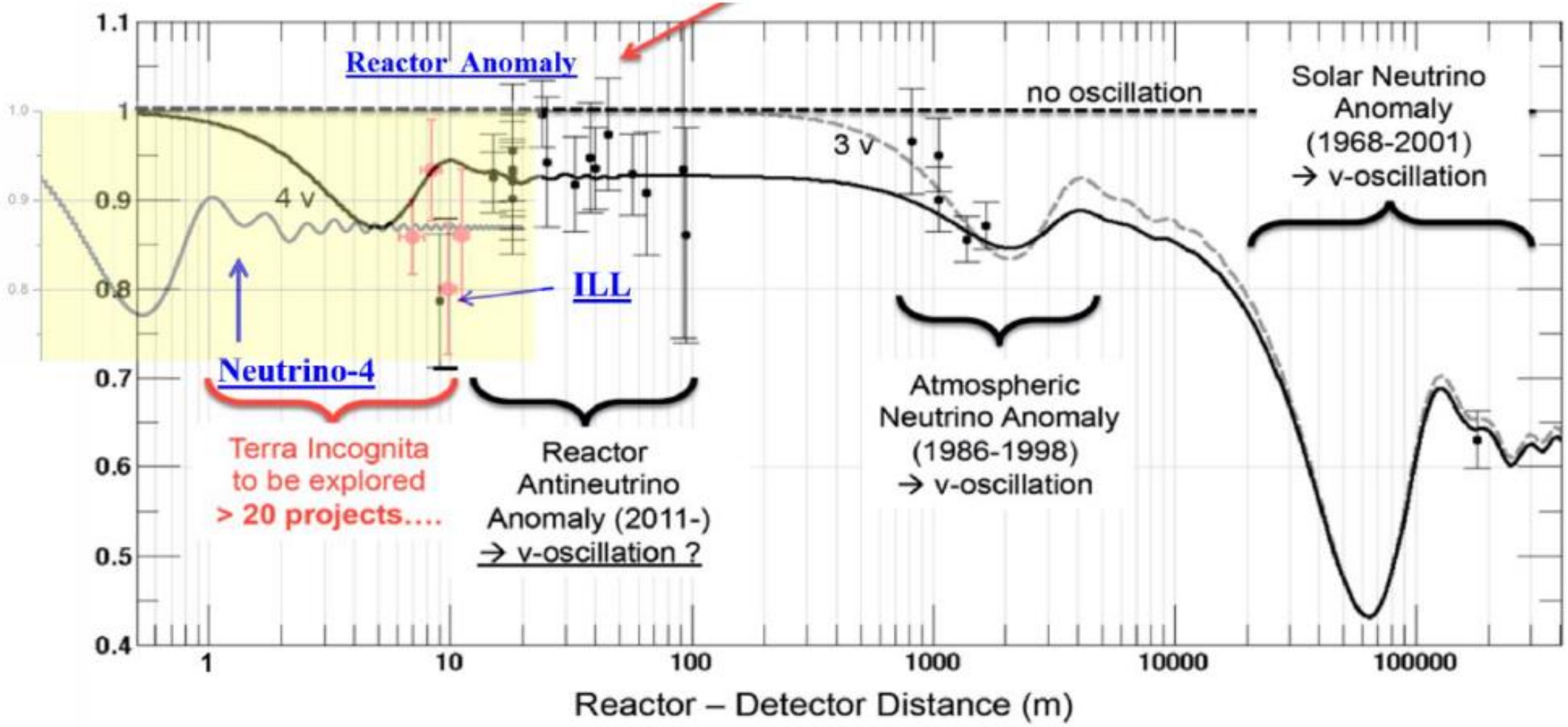

Fig.13. Reactor antineutrino anomaly [28] with oscillation curve obtained in experiment Neutrino-4.

COMPARISON OF THE RESULT OF EXPERIMENT NEUTRINO-4 WITH REACTOR AND GALLIUM ANOMALIES

$$sin^2 2\theta_{14} \approx 0.26 \pm 0.09\ (2.9\sigma)$$

Neutrino-4 experiment

$$sin^2 2\theta_{14} \approx 0.32 \pm 0.10\ (3.2\sigma)$$

gallium anomaly

$$sin^2 2\theta_{14} \approx 0.13 \pm 0.05\ (2.6\sigma)$$

reactor antineutrino anomaly

Combination of these results gives an estimation for mixing angle

$$sin^2 2\theta_{14} \approx 0.19 \pm 0.04\ (4.6\sigma)$$

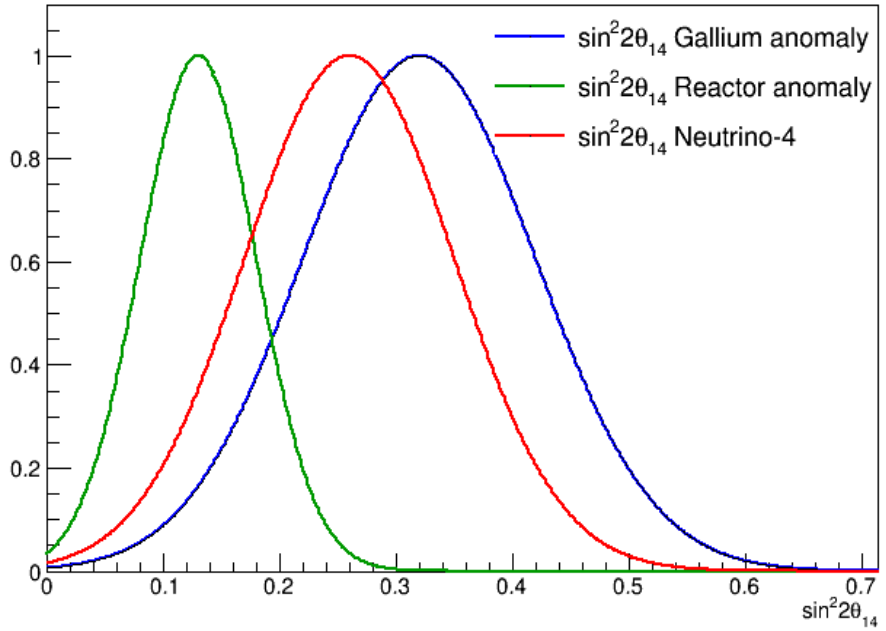

COMPARISON WITH OTHER RESULTS OF EXPERIMENTS AT RESEARCH REACTORS AND NUCLEAR POWER PLANTS

COMPARISON WITH OTHER RESULTS OF EXPERIMENTS AT RESEARCH REACTORS AND NUCLEAR POWER PLANTS

The period of oscillation for neutrino energy 4 MeV is 1.4 m

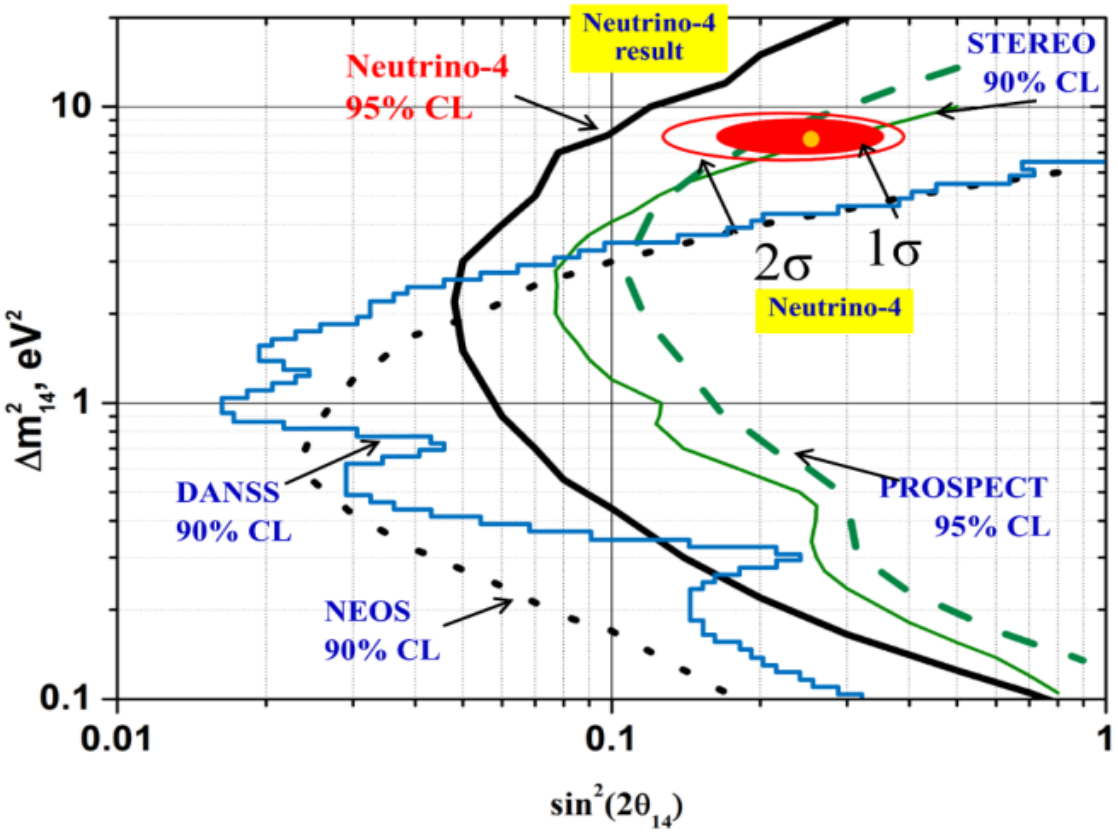

Comparison of results of the Neutrino-4 experiment with results of other experiments – sensitivities of the experiments

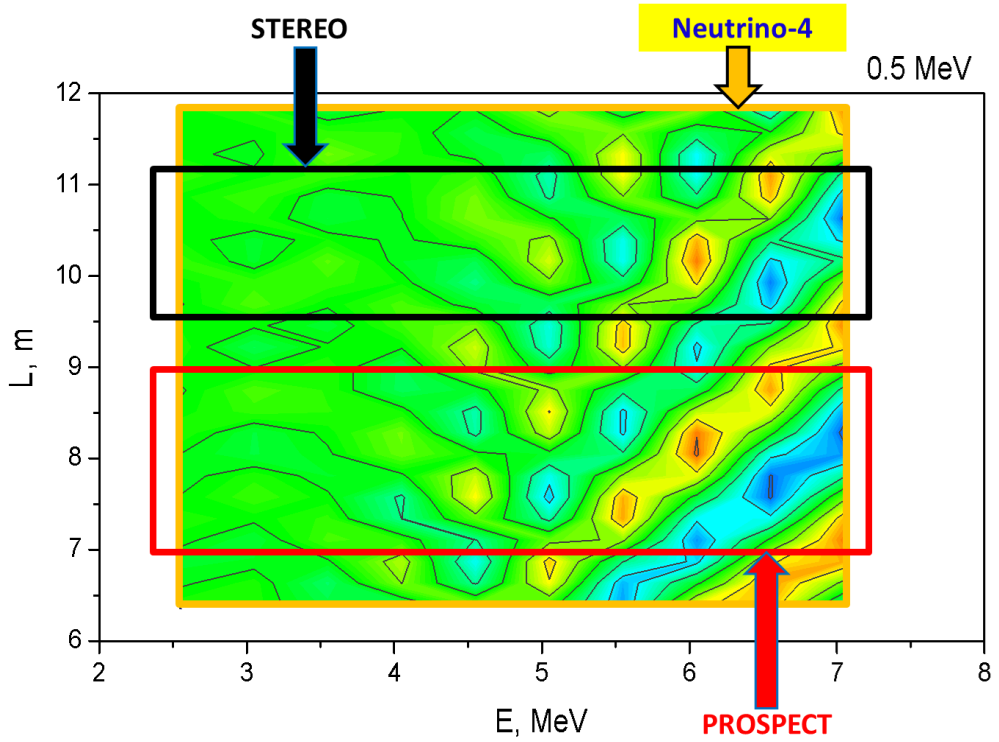

Comparison of planes of parameters (E,L) in experiments Neutrino-4, STEREO and PROSPECT.

In experiments on nuclear power plants sensitivity to identification of effect of oscillations with large Δm^2_{14} is considerably suppressed because of the big sizes of an active zone (3.7 m). Experiment Neutrino-4 has some advantages in sensitivity to large values of Δm^2_{14} owing to a compact reactor core, close minimal detector distance from the reactor and wide range of detector movements.

COMPARISON WITH OTHER RESULTS OF EXPERIMENTS AT RESEARCH REACTORS

Experiment	Days with reactor ON	Days with reactor OFF	S/B ratio	Number of events, d^{-1}
Neutrino-4	720 (90 MW)	417	0.5	223 (6-9 m)
PROSPECT	33 (85 MW)	28	1.3	771 (7-9 m)
STEREO	179 (58 MW)	235	1.1	366 (9 – 11m)

NEUTRINO MODEL 3+1

THE STRUCTURE OF 3+1 NEUTRINO MODEL AND REPRESENTATION OF PROBABILITIES OF VARIOUS OSCILLATIONS

$$\begin{bmatrix}\nu_e\\ \nu_\mu\\ \nu_\tau\\ \nu_s\end{bmatrix} = \begin{bmatrix}U_{e1} & U_{e2} & U_{e3} & U_{e4}\\ U_{\mu1} & U_{\mu2} & U_{\mu3} & U_{\mu4}\\ U_{\tau1} & U_{\tau2} & U_{\tau3} & U_{\tau4}\\ U_{s1} & U_{s2} & U_{s3} & U_{s4}\end{bmatrix}\begin{bmatrix}\nu_1\\ \nu_2\\ \nu_3\\ \nu_4\end{bmatrix}$$

$$|U_{e4}|^2 = \sin^2(\theta_{14})$$
$$|U_{\mu4}|^2 = \sin^2(\theta_{24})\cdot\cos^2(\theta_{14})$$
$$|U_{\tau4}|^2 = \sin^2(\theta_{34})\cdot\cos^2(\theta_{24})\cdot\cos^2(\theta_{14})$$

$$\boldsymbol{P_{\nu_e\nu_e} = 1 - 4|U_{e4}|^2\left(1-|U_{e4}|^2\right)\sin^2\left(\frac{\Delta m^2_{14}L}{4E_{\nu_e}}\right) = 1 - \sin^2 2\theta_{ee}\sin^2\left(\frac{\Delta m^2_{14}L}{4E_{\nu_e}}\right)}$$

$$\boldsymbol{P_{\nu_\mu\nu_\mu} = 1 - 4\left|U_{\mu4}\right|^2\left(1-\left|U_{\mu4}\right|^2\right)\sin^2\left(\frac{\Delta m^2_{14}L}{4E_{\nu_\mu}}\right) = 1 - \sin^2 2\theta_{\mu\mu}\sin^2\left(\frac{\Delta m^2_{14}L}{4E_{\nu_\mu}}\right)}$$

$$\boldsymbol{P_{\nu_\mu\nu_e} = 4|U_{e4}|^2\left|U_{\mu4}\right|^2\sin^2\left(\frac{\Delta m^2_{14}L}{4E_{\nu_e}}\right) = \sin^2 2\theta_{\mu e}\sin^2\left(\frac{\Delta m^2_{14}L}{4E_{\nu_e}}\right)}$$

The relations of oscillations parameters required for comparative analysis of experimental results are:

$$\sin^2 2\theta_{ee} \equiv \sin^2 2\theta_{14}$$

$$\sin^2 2\theta_{\mu\mu} = 4\sin^2\theta_{24}\cos^2\theta_{14}(1-\sin^2\theta_{24}\cos^2\theta_{14}) \approx \sin^2 2\theta_{24}$$

$$\sin^2 2\theta_{\mu e} = 4\sin^2\theta_{14}\sin^2\theta_{24}\cos^2\theta_{14} \approx \frac{1}{4}\sin^2 2\theta_{14}\sin^2 2\theta_{24}$$

It is an important relation which can be used for experimental verification of 3+1 neutrino model.

It is important that amplitudes of electron and muon oscillations with disappearance determines the amplitude $\sin^2 2\theta_{\mu e}$ in process with appearance of electron neutrinos in muon neutrino beam.

COMPARISON OF EXPERIMENT NEUTRINO-4 RESULTS WITH RESULTS OF THE ICECUBE EXPERIMENT

•Spencer Axani, arXiv:2003.02796

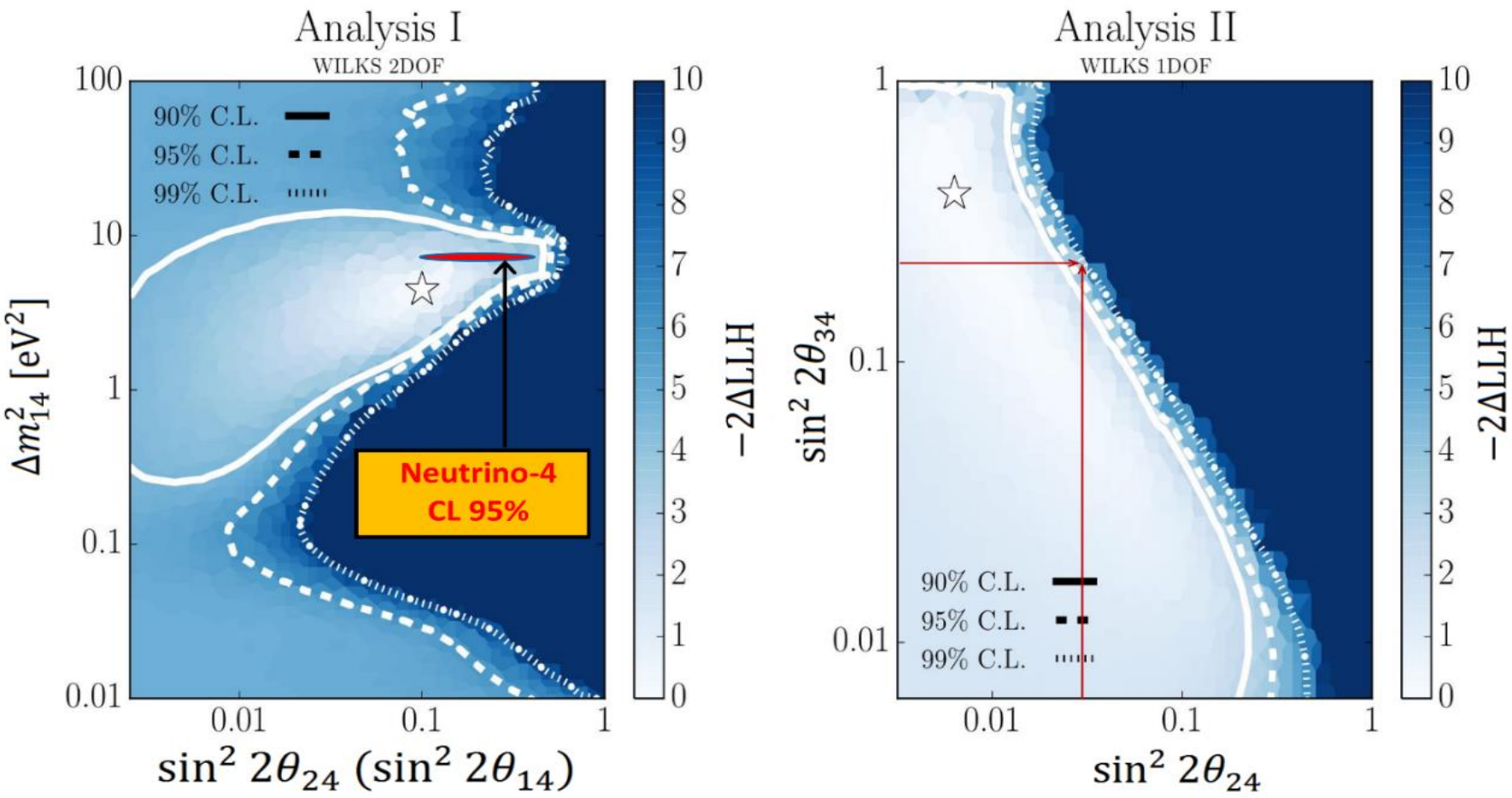

$$\Delta m^2_{14} = 4.47^{+3.53}_{-2.08} eV^2$$

$$sin^2(2\theta_{24}) = 0.10^{+0.10}_{-0.07}$$

$$\sin^2 2\theta_{\mu\mu} = 4\sin^2\theta_{24}\cos^2\theta_{14}(1-\sin^2\theta_{24}\cos^2\theta_{14}) \approx \sin^2 2\theta_{24}$$

COMPARISON OF EXPERIMENT NEUTRINO-4 RESULTS WITH RESULTS OF ACCELERATOR EXPERIMENTS MINIBOONE AND LSND

MiniBooNE Collaboration, A. A. Aguilar-Arevalo et. al., Phys. Rev. Lett. 121 (2018), 221801 [1805.12028]

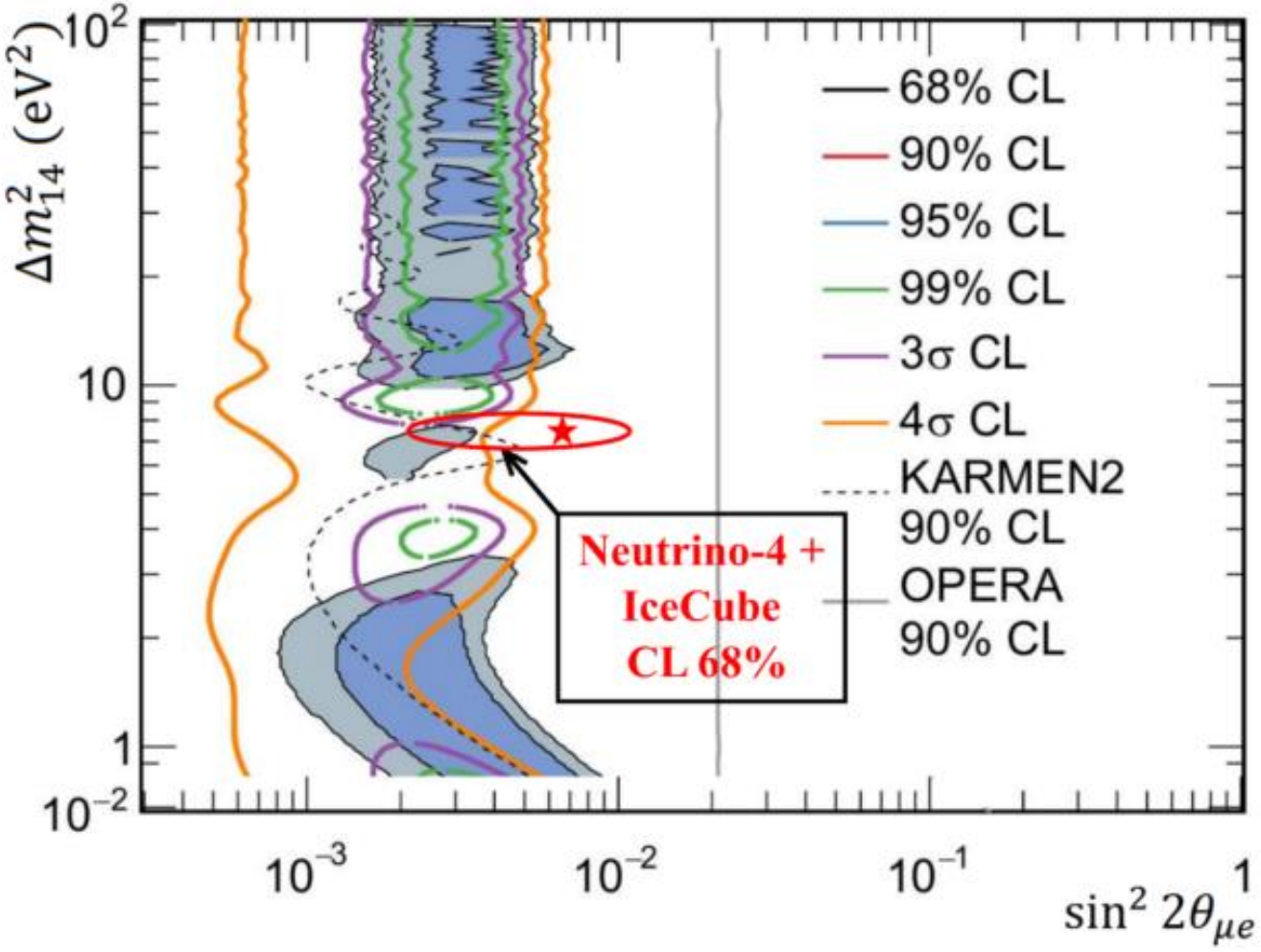

The experiments MiniBooNE and LSND are aimed to search for a second order process of sterile neutrino – the appearance of electron neutrino in the muon neutrino flux ($\nu_\mu \rightarrow \nu_e$) through an intermediate sterile neutrino.

A comparison of $\sin^2 2\theta_{\mu e}$ obtained in MiniBooNE and LSND and $\sin^2 2\theta_{14}$ obtained in Neutrino-4 can be performed using results of the IceCube experiment:

$$\sin^2 2\theta_{24} \approx 0.03 \div 0.2$$

Values of $\sin^2 2\theta_{\mu e}$ and $\sin^2 2\theta_{24}$, $\sin^2 2\theta_{14}$ are related by the expression:

$$\sin^2 2\theta_{\mu e} \approx \frac{1}{4}\sin^2 2\theta_{14} \sin^2 2\theta_{24}$$

Pontecorvo–Maki–Nakagawa–Sakata matrix

PMNS matrix for 3 + 1 model

$$\begin{bmatrix}\nu_e\\ \nu_\mu\\ \nu_\tau\\ \nu_s\end{bmatrix} = \begin{bmatrix}U_{e1} & U_{e2} & U_{e3} & U_{e4}\\ U_{\mu1} & U_{\mu2} & U_{\mu3} & U_{\mu4}\\ U_{\tau1} & U_{\tau2} & U_{\tau3} & U_{\tau4}\\ U_{s1} & U_{s2} & U_{s3} & U_{s4}\end{bmatrix}\begin{bmatrix}\nu_1\\ \nu_2\\ \nu_3\\ \nu_4\end{bmatrix}$$

$$|U_{e4}|^2 = \sin^2(\theta_{14})$$
$$|U_{\mu4}|^2 = \sin^2(\theta_{24}) \cdot \cos^2(\theta_{14})$$
$$|U_{\tau4}|^2 = \sin^2(\theta_{34}) \cdot \cos^2(\theta_{24}) \cdot \cos^2(\theta_{14})$$

$$U_{PMNS}^{(3+1)} = \begin{pmatrix} 0.824^{+0.007}_{-0.008} & 0.547^{+0.011}_{-0.011} & 0.147^{+0.003}_{-0.003} & 0.224^{+0.025}_{-0.025} \\ 0.409^{+0.036}_{-0.060} & 0.634^{+0.022}_{-0.065} & 0.657^{+0.044}_{-0.014} & 0.160^{+0.08}_{-0.05} \\ 0.392^{+0.025}_{-0.048} & 0.547^{+0.056}_{-0.028} & 0.740^{+0.012}_{-0.048} & < 0.229 \\ < 0.24 & < 0.30 & < 0.26 & > 0.93 \end{pmatrix}$$

$$\begin{bmatrix} m_e^2 \\ m_\mu^2 \\ m_\tau^2 \\ m_s^2 \end{bmatrix} = \begin{vmatrix} U_{e,1}^2 & U_{e,2}^2 & U_{e,3}^2 & U_{e,4}^2 \\ U_{\mu,1}^2 & U_{\mu,2}^2 & U_{\mu,3}^2 & U_{\mu,4}^2 \\ U_{\tau,1}^2 & U_{\tau,2}^2 & U_{\tau,3}^2 & U_{\tau,4}^2 \\ U_{s,1}^2 & U_{s,2}^2 & U_{s,3}^2 & U_{s,4}^2 \end{vmatrix} \begin{bmatrix} m_1^2 \\ m_2^2 \\ m_3^2 \\ m_4^2 \end{bmatrix}$$

$$\begin{bmatrix} m_e^2 \\ m_\mu^2 \\ m_\tau^2 \\ m_s^2 \end{bmatrix} = \begin{bmatrix} U_{e,1}^2 m_1^2 + U_{e,2}^2 m_2^2 + U_{e,3}^2 m_3^2 + U_{e,4}^2 m_4^2 \\ U_{\mu,1}^2 m_1^2 + U_{\mu,2}^2 m_2^2 + U_{\mu,3}^2 m_3^2 + U_{\mu,4}^2 m_4^2 \\ U_{\tau,1}^2 m_1^2 + U_{\tau,2}^2 m_2^2 + U_{\tau,3}^2 m_3^2 + U_{\tau,4}^2 m_4^2 \\ U_{s,1}^2 m_1^2 + U_{s,2}^2 m_2^2 + U_{s,3}^2 m_3^2 + U_{s,4}^2 m_4^2 \end{bmatrix}$$

$$m_1^2, m_2^2, m_3^2 \ll m_4^2$$

$$\begin{bmatrix} m_e^2 \\ m_\mu^2 \\ m_\tau^2 \\ m_s^2 \end{bmatrix} \Rightarrow \begin{bmatrix} U_{e,4}^2 m_4^2 \\ U_{\mu,4}^2 m_4^2 \\ U_{\tau,4}^2 m_4^2 \\ U_{s,4}^2 m_4^2 \end{bmatrix}$$

Neutrino mass

3 **complementary** methods to measure:

Method	Observable	curr. [eV]	near/far [eV]	pro	con
Kurie	$\sqrt{\sum \lvert U_{ei}\rvert^2 m_i^2}$	2.3	0.2/0.1	model-indep.; theo. clean	final?; weakest
Cosmo.	$\sum m_i$	0.7	0.3/0.05	best; NH/IH	systemat.; model-dep.
$0\nu\beta\beta$	$\lvert \sum U_{ei}^2 m_i \rvert$	0.3	0.1/0.05	fundament.; NH/IH	model-dep.; theo. dirty

$$m_1^2, m_2^2, m_3^2 \ll m_4^2$$

MAX-PLANCK-INSTITUT FÜR KERNPHYSIK

WERNER RODEJOHANN

COMPARISON WITH EXPERIMENT KATRIN ON MEASUREMENT OF NEUTRINO MASS

$$m_{\nu_e}^{eff} = \sqrt{\sum m_i^2 |U_{ei}|^2}$$

$$\sin^2 2\theta_{14} = 4|U_{14}|^2(1 - |U_{14}|^2)$$

$$|U_{14}^2| \approx \frac{1}{4}\sin^2 2\theta_{14}$$

$$\Delta m_{14}^2 \approx m_4^2, \ldots |U_{14}^2| \ll 1$$

$$\boxed{m_4 = (2.68 \pm 0.13)\text{eV}}$$

$$\sin^2 2\theta_{14} \approx 0.19 \pm 0.04 (4.6\sigma)$$

$$\boxed{m_{\nu_e}^{eff} = (0.58 \pm 0.09)\text{eV}}$$

$$m_{\nu_e}^{eff} \leq 1.1 \text{ eV (CL 90\%)}$$

Limitations on the sum of mass of active neutrinos $\Sigma m\nu = m1+m2+m3$ from cosmology are in the range 0.54÷ 0.11eV

$$m_1^2, m_2^2, m_3^2 \ll m_4^2$$

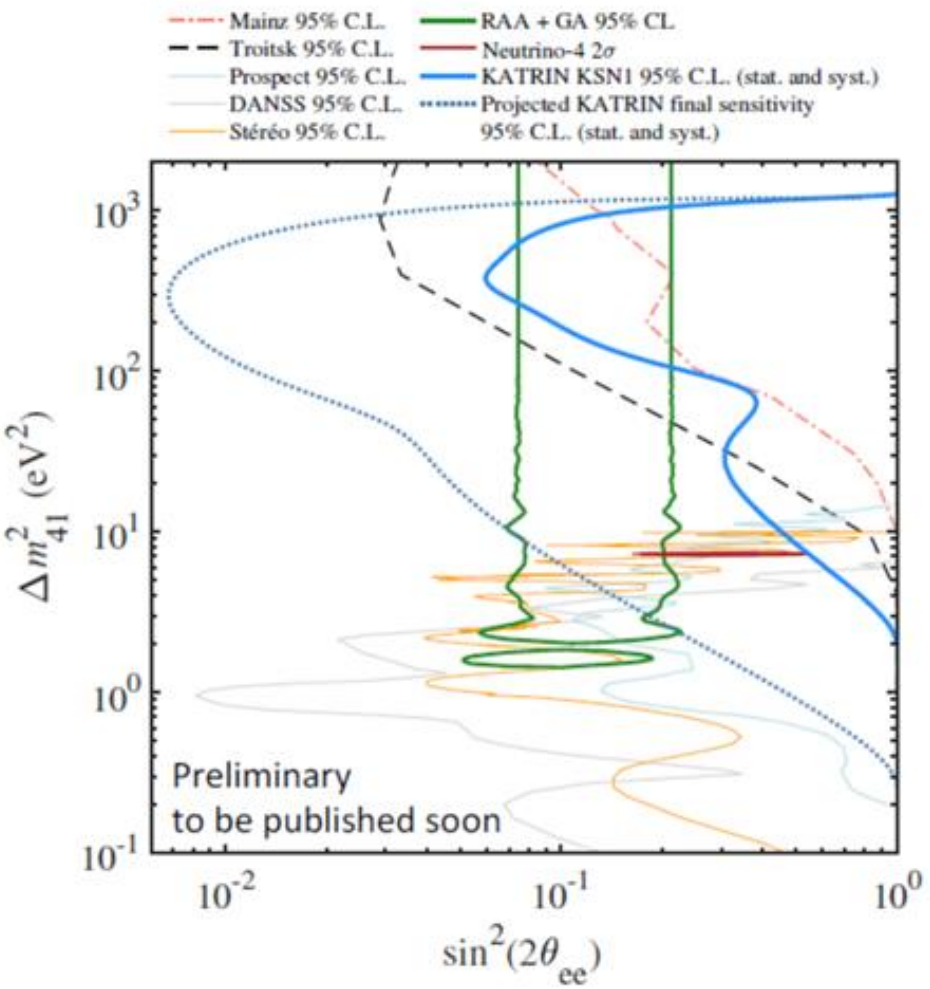

In the same way we can use data about $\sin^2(2\theta_{24}) = 0.10^{+0.10}_{-0.07}$ obtained in the IceCube experiment to estimate muon neutrino mass:

$$m_{\nu_\mu}^{eff} = (0.42 \pm 0.24)\text{eV}$$

Finally, considering upper limit of $\sin^2 2\theta_{34} \leq 0.21$ we can calculate upper limit of tau neutrino mass

$$m_{\nu_\tau}^{eff} \leq 0.65\text{eV}$$

$$\Delta m^2_{14} = 7.25 \pm 0.13_{st} \pm 1.08_{syst} = 7.25 \pm 1.09$$

$$\sin^2 2\theta = 0.26 \pm 0.08_{stat} \pm 0.05_{syst} = 0.26 \pm 0.09(2.8\sigma)$$

$$\sin^2 2\theta_{14} \approx 0.19 \pm 0.04(4.6\sigma)$$

$$m_4 = (2.68 \pm 0.13)\text{eV}$$

$$m^{\text{eff}}_{\nu_e} = (0.58 \pm 0.09)\text{eV}$$

$$m^{\text{eff}}_{\nu_\mu} = (0.42 \pm 0.24)\text{eV}$$

$$m^{\text{eff}}_{\nu_\tau} \leq 0.65\text{eV}$$

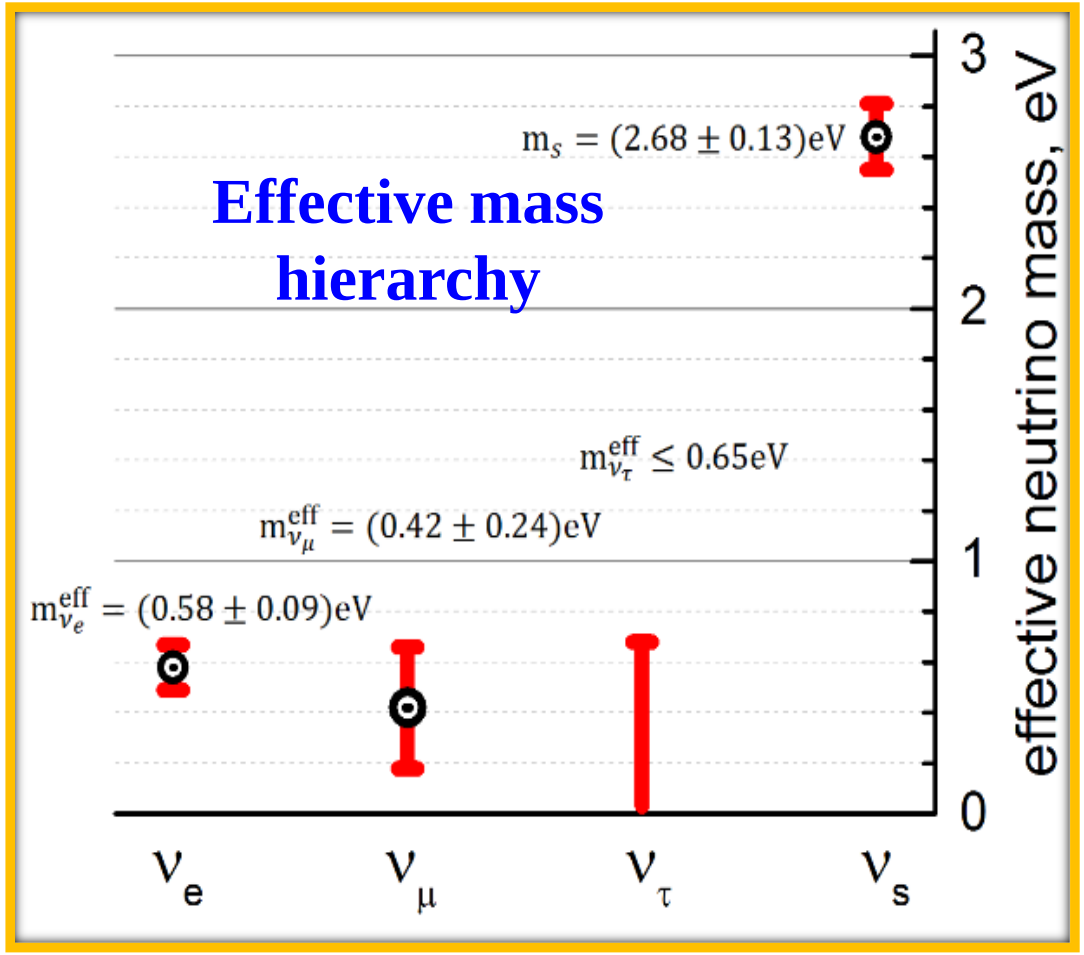

Limitations on the sum of mass of active neutrinos $\Sigma m\nu = m1 + m2 + m3$ from cosmology are in the range 0.54÷ 0.11eV

If we consider the constraints on the sum of squares obtained from cosmology m1 + m2 + m3 < 0.54, and take mi = < 0.54 /3, then the values of effective masses will be:

$$m_{\nu_e}^{\text{eff}} = 0.63, m_{\nu_\mu}^{\text{eff}} = 0.47, m_{\nu_\tau}^{\text{eff}} < 0.64 \text{ eV}$$

If we consider the constraints on the sum of squares obtained from cosmology m1 + m2 + m3 < 0.11, and take mi = 0.11/3, then the values of effective masses will be:

$$m_{\nu_e}^{\text{eff}} = 0.60, m_{\nu_\mu}^{\text{eff}} = 0.43, m_{\nu_\tau}^{\text{eff}} < 0.61 \text{ eV}$$

If we consider the constraints on the sum of squares obtained from cosmology m1 + m2 + m3 =0 effective masses will be:

$$m_{\nu_e}^{\text{eff}} = 0.58, m_{\nu_\mu}^{\text{eff}} = 0.42, m_{\nu_\tau}^{\text{eff}} < 0.65 \text{ eV}$$

59

Comparison with neutrino mass constraints from experiments for neutrino less double beta-decay search

This expression for the model 3 + 1 and with $m1,m2,m3 \ll m4$ assumption can be simplified:

$$m(0\nu\beta\beta) = \sum_{i=1}^{4} |U_{ei}|^2 m_i$$

The numerical for this with Neutrino-4 and other experiments average result is shown below.

$m(0\nu\beta\beta) = (0.13 \pm 0.03)\text{eV}$
our estimation

$m\beta\beta < [0.80 - 0.182]\text{eV}$
experiments

The best restrictions on the Majorana mass were obtained in the GERDA experiment .
In these experiments, the half-life of the isotope is measured, which depends on the Majorana mass as follows:

$$1/T_{1/2}^{0\nu} = g_A^4 G^{0\nu} |M^{0\nu}|^2 \frac{\langle m_{\beta\beta} \rangle^2}{m_e^2}$$

The upper limit for the lower limit - the upper limit for the Majorana mass:

Lower limit for $T_{1/2}/0\nu > 1.8 \times 10^{26}$ years (90% CL)

Upper limit for $m\beta\beta < [80 - 182]\text{meV}$

Pontecorvo–Maki–Nakagawa–Sakata matrix

PMNS matrix for 3 + 1 model

$$\begin{bmatrix}\nu_e\\ \nu_\mu\\ \nu_\tau\\ \nu_s\end{bmatrix} = \begin{bmatrix}U_{e1} & U_{e2} & U_{e3} & U_{e4}\\ U_{\mu1} & U_{\mu2} & U_{\mu3} & U_{\mu4}\\ U_{\tau1} & U_{\tau2} & U_{\tau3} & U_{\tau4}\\ U_{s1} & U_{s2} & U_{s3} & U_{s4}\end{bmatrix}\begin{bmatrix}\nu_1\\ \nu_2\\ \nu_3\\ \nu_4\end{bmatrix}$$

$$|U_{e4}|^2 = \sin^2(\theta_{14})$$
$$|U_{\mu4}|^2 = \sin^2(\theta_{24})\cdot\cos^2(\theta_{14})$$
$$|U_{\tau4}|^2 = \sin^2(\theta_{34})\cdot\cos^2(\theta_{24})\cdot\cos^2(\theta_{14})$$

$$U_{PMNS}^{(3+1)} = \begin{pmatrix} 0.824^{+0.007}_{-0.008} & 0.547^{+0.011}_{-0.011} & 0.147^{+0.003}_{-0.003} & 0.224^{+0.025}_{-0.025} \\ 0.409^{+0.036}_{-0.060} & 0.634^{+0.022}_{-0.065} & 0.657^{+0.044}_{-0.014} & 0.160^{+0.08}_{-0.05} \\ 0.392^{+0.025}_{-0.048} & 0.547^{+0.056}_{-0.028} & 0.740^{+0.012}_{-0.048} & < 0.229 \\ < 0.24 & < 0.30 & < 0.26 & > 0.93 \end{pmatrix}$$

Neutrino flavors mixing scheme including sterile neutrino for normal and inverted mass hierarchy.

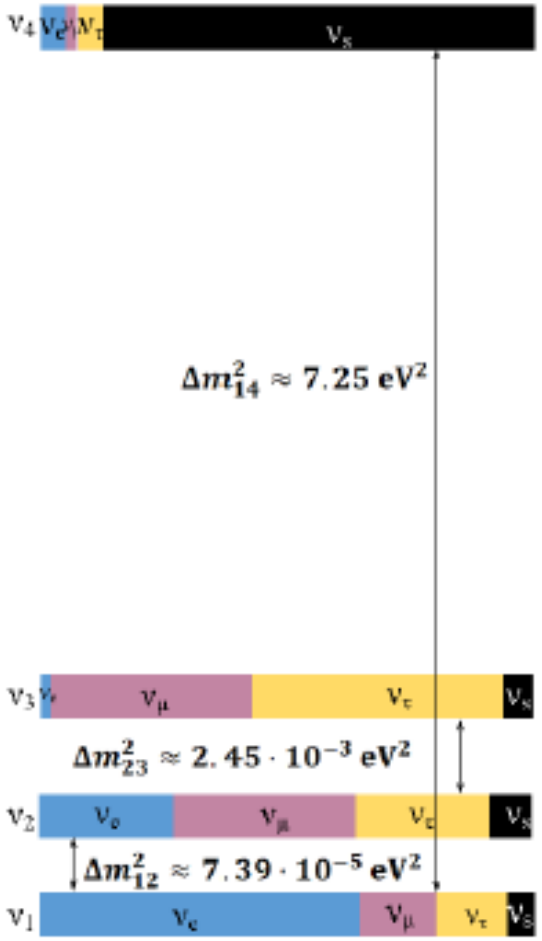

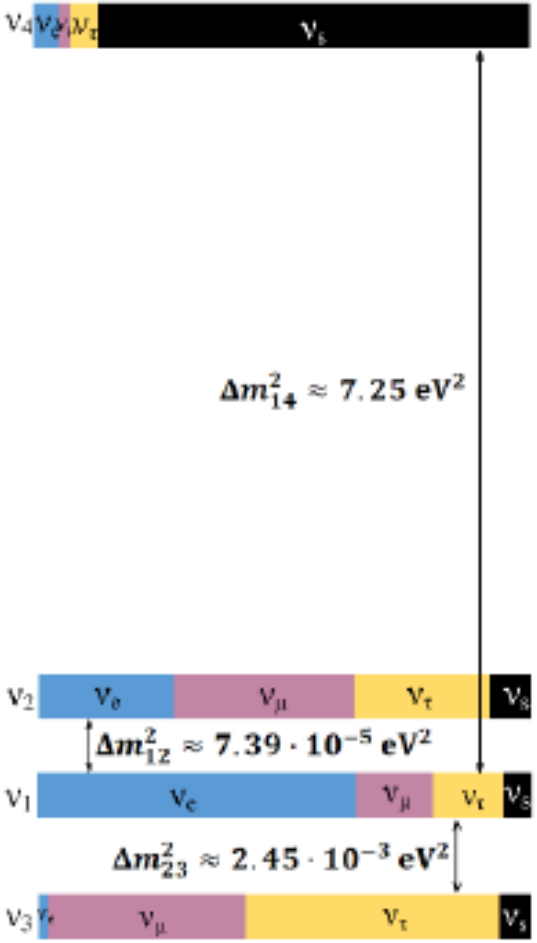

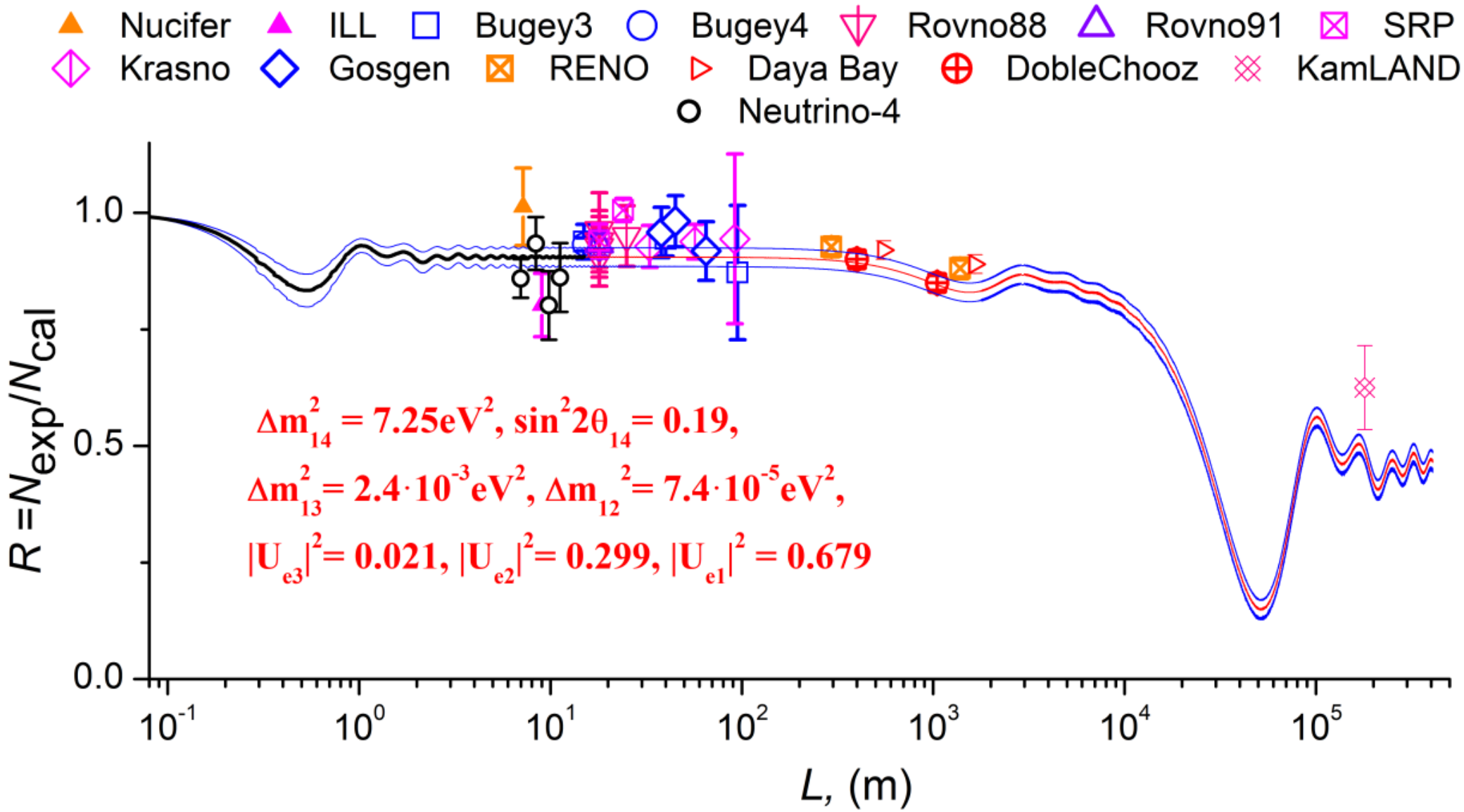
Nucifer
ILL
Bugey3
Bugey4
Rovno88
Rovno91
SRP
Krasno
Gosgen
RENO
Daya Bay
DobleChooz
KamLAND
Neutrino-4
1.0
0.5
0.0
R = N_exp/N_cal
Δm²14 = 7.25eV², sin²2θ14 = 0.19,
Δm²13 = 2.4·10⁻³eV², Δm12² = 7.4·10⁻⁵eV²,
|Ue3|² = 0.021, |Ue2|² = 0.299, |Ue1|² = 0.679
10⁻¹
10⁰
10¹
10²
10³
10⁴
10⁵
L, (m)
Model 3+1 with Δm²14 = 7.25eV², sin²2θ14 = 0.19
Model 3+1 with Δm²14 = 7.25eV², sin²2θ14 = 0.19 ± 0.04

Cosmology – the role of sterile neutrinos during the formation of Universe and the rate of its expansion

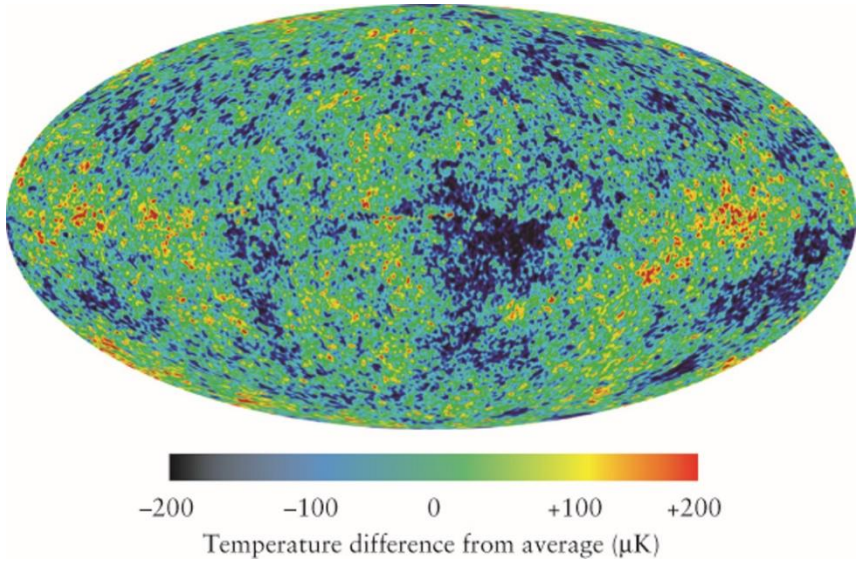

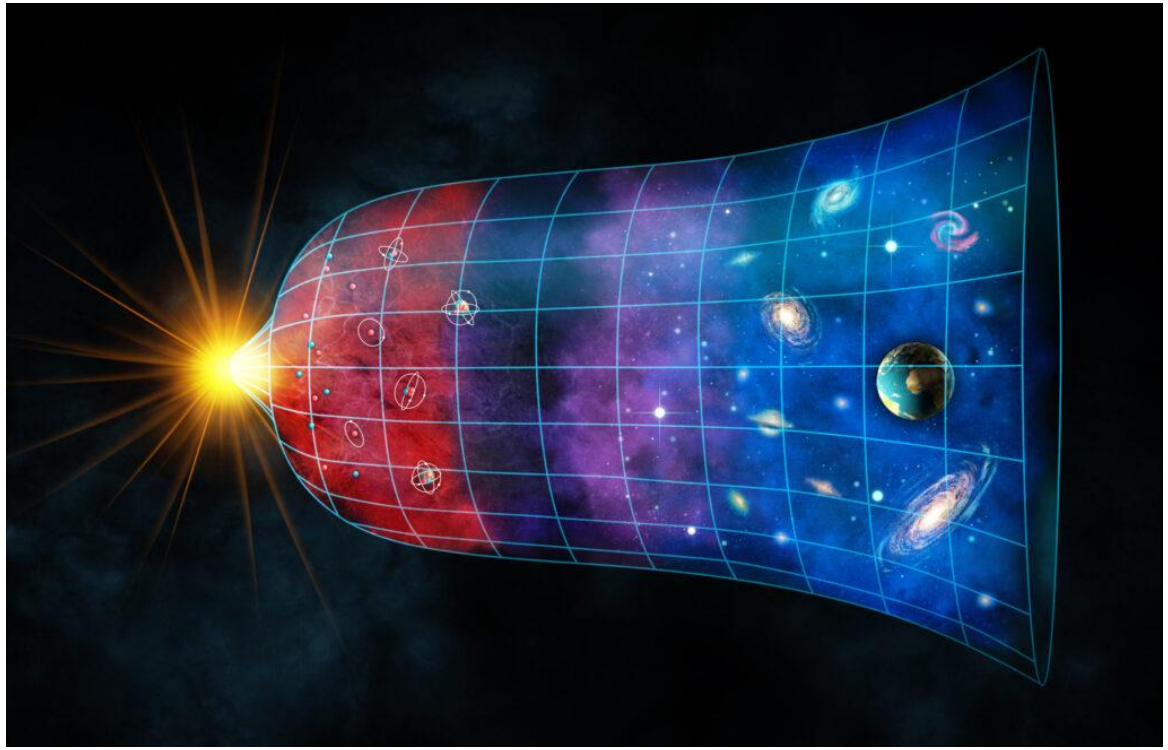

Стерильные нейтрино и их роль в физике частиц и космологии

Д.С. Горбунов

УСПЕХИ ФИЗИЧЕСКИХ НАУК

Том 184, № 5

Такие нейтрино термализуются в первичной плазме, затем отщепляются от неё, но остаются в расширяющейся Вселенной. Как дополнительный ультрарелятивистский компонент (радиация) они дают вклад в полную плотность энергии Вселенной и могут увеличить темп расширения Вселенной в эпоху первичного нуклеосинтеза, тем самым изменив его предсказания.

Тёмная энергия 75% → **Стерильное нейтрино 2.5 эВ**

Тёмная материя 20% → **Активные нейтрино 0.54 эВ**

Thank you for attention

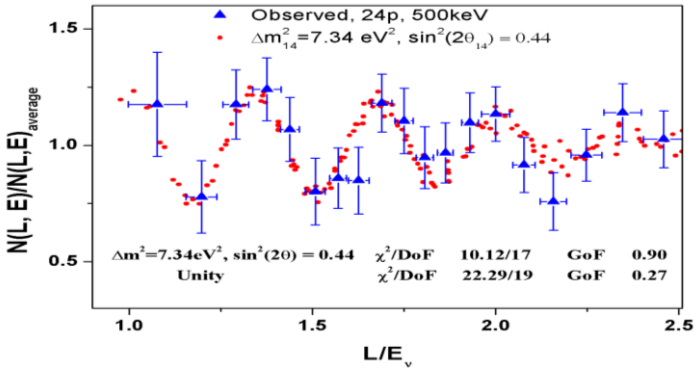

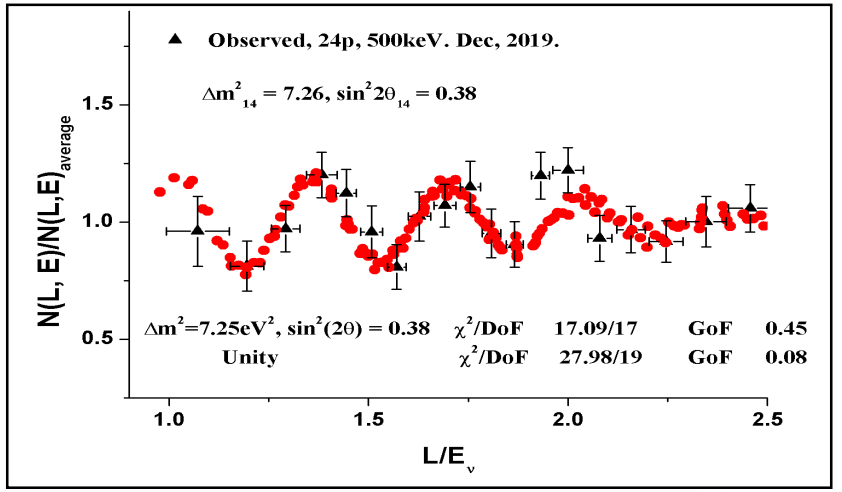

Best regards from Gatchina

Best regards from Dimitrovgrad

The method of coherent addition of results of measurements allows us to directly observe the effect of oscillations

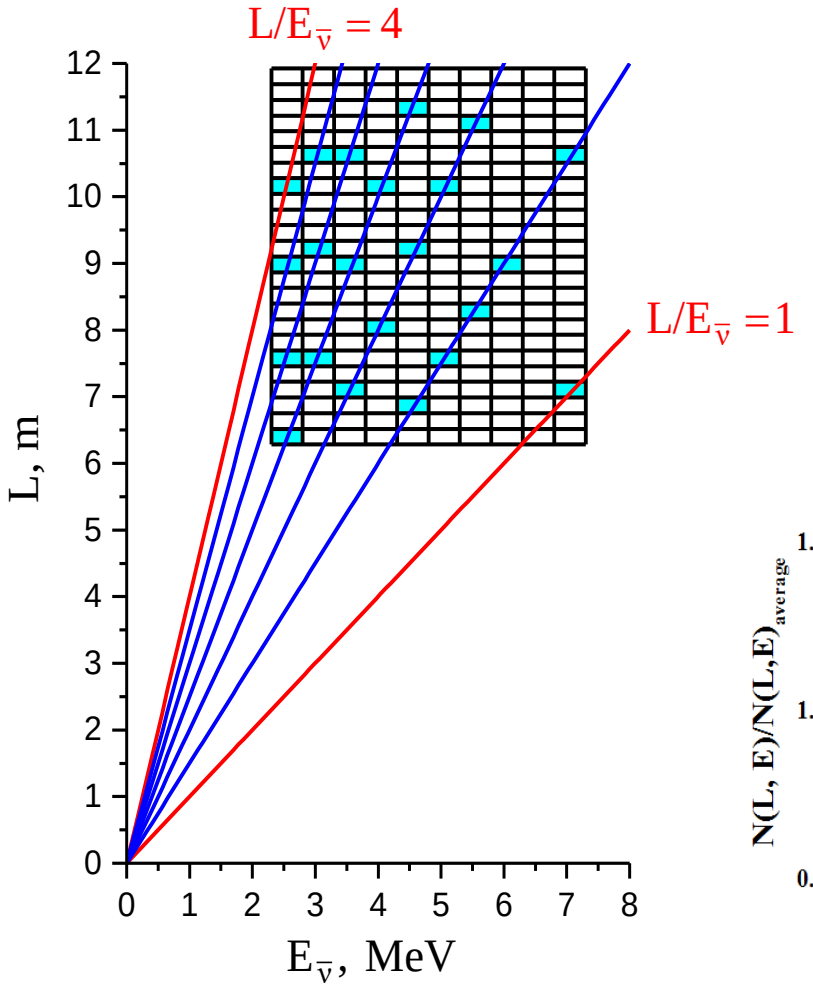

$$R_{i,k}^{\exp} = \frac{N(E_i^{\nu}, L_k)L_k^2}{K^{-1}\sum_k^K N(E_i^{\nu}, L_k)L_k^2} =$$

$$= \frac{[1-\sin^2 2\theta_{14}\sin^2(1.27\Delta m_{14}^2 L_k / E_i^{\nu})]}{K^{-1}\sum_k^K [1-\sin^2 2\theta_{14}\sin^2(1.27\Delta m_{14}^2 L_k / E_i^{\nu})]} = R_{i,k}^{th} \quad (2)$$

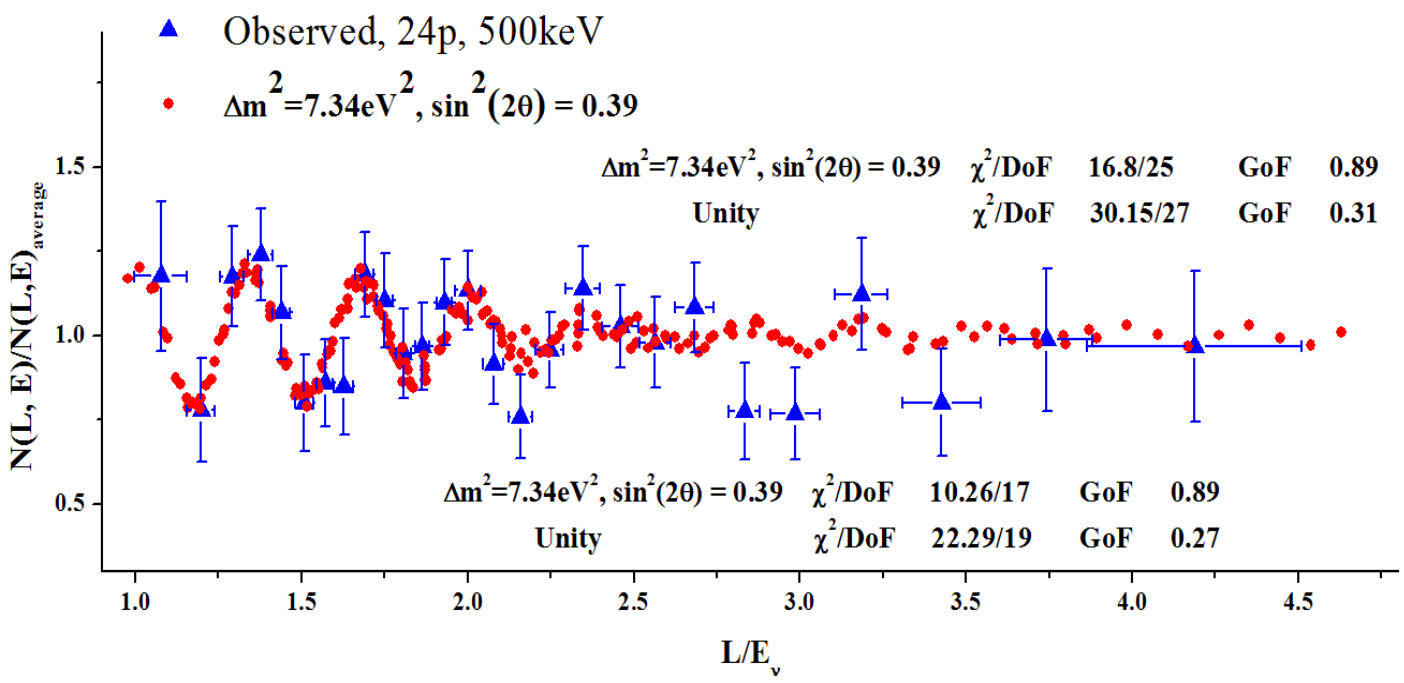

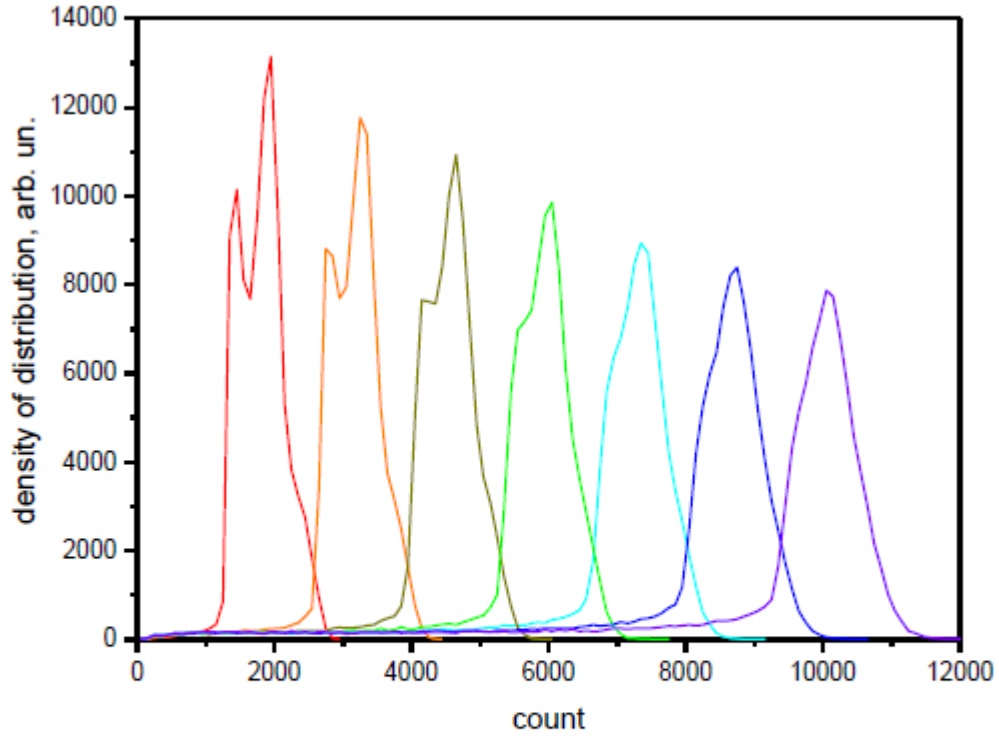

FIG. 25. Distribution of counts of PMT in one section induced by positrons with energies from 1 to 7 MeV with annihilation process (2 gamma-quanta with energies 511keV).

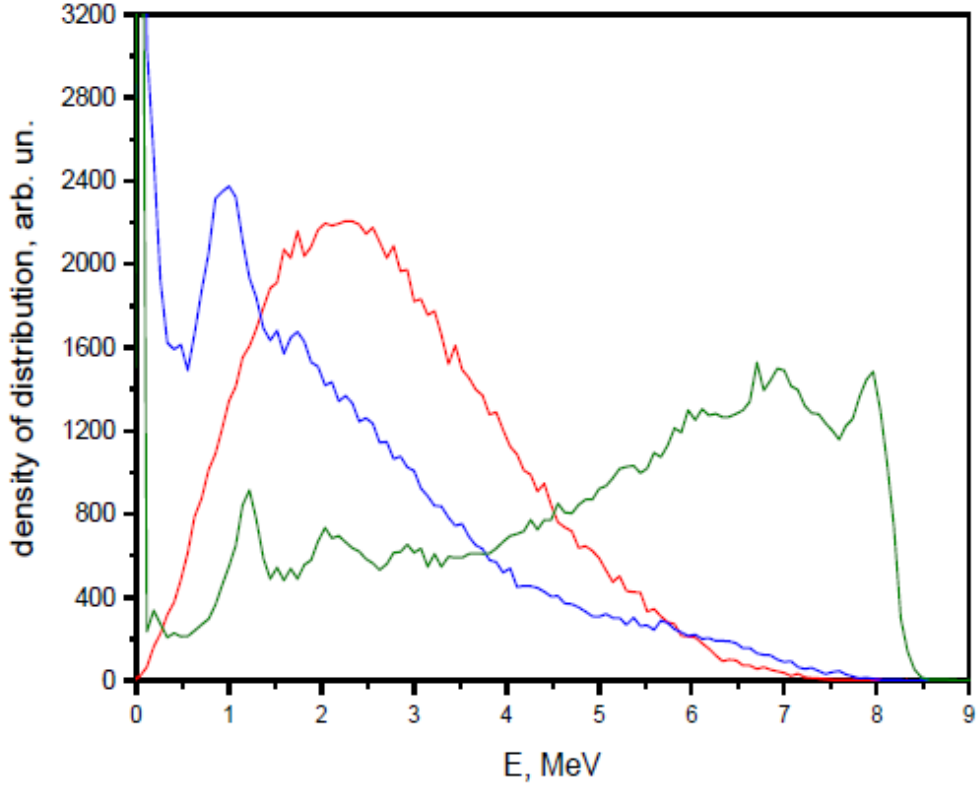

FIG. 26. Signals of positon (positron and 2 gamma-quanta) event - red curve, signals of neutron event – blue curve (only PMT of section where the IBD process took place is used), green curve – signals of PMTs from all sections.

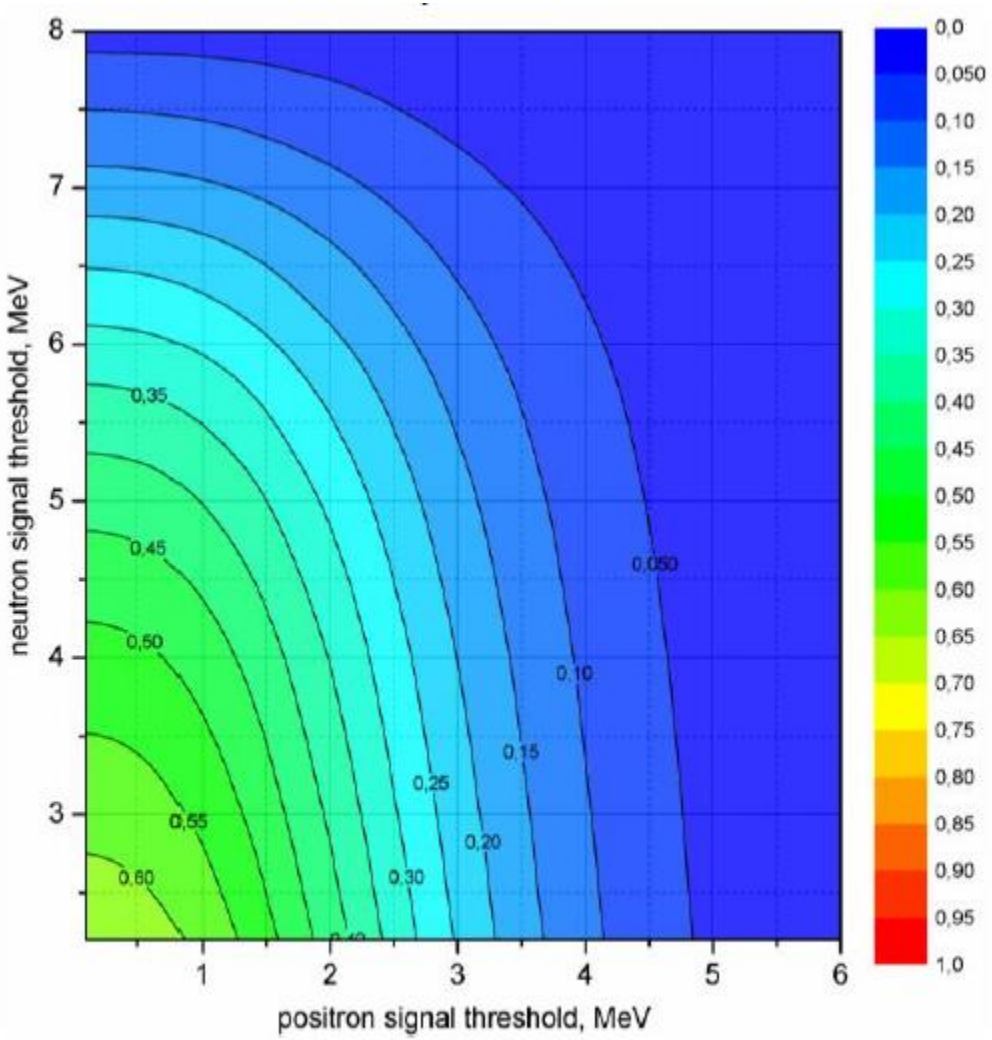

FIG. 27. Efficiency of the detector as function of limits of positron and neutron signals with counts of all PMTs.

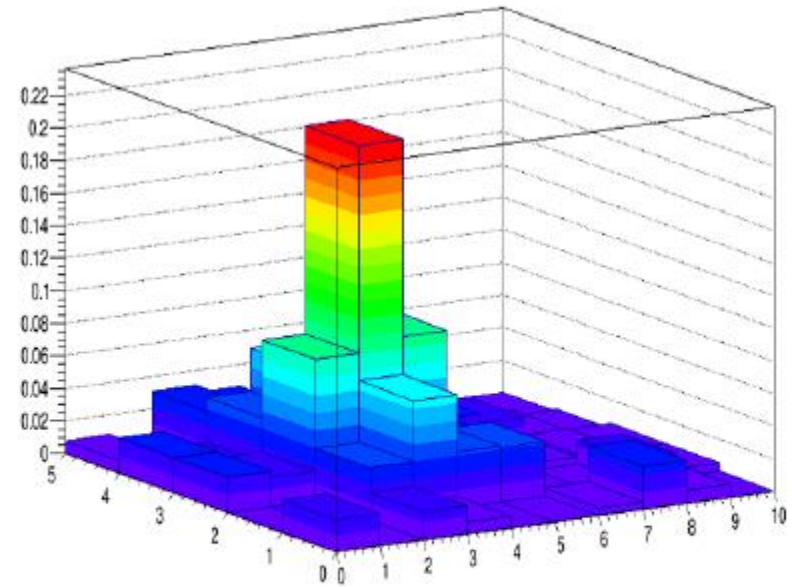

FIG. 30. Experimental distribution of delayed signals over the section (3, 3), in which a reaction of the inverse beta decay occurred.

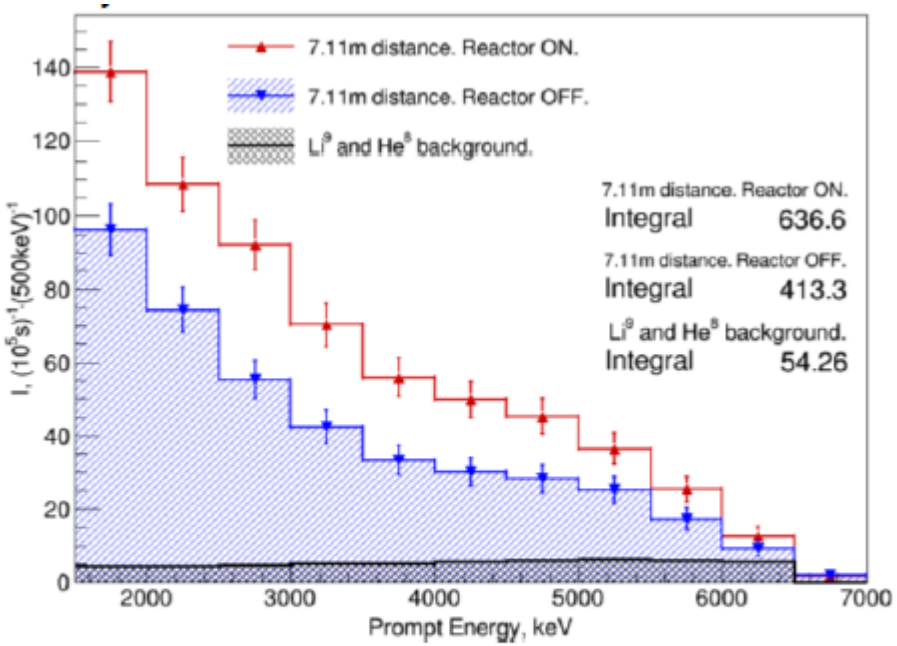

FIG. 28. Example of the spectrum of prompt signals obtained within one month of statistics. The signal (ON – OFF) has made 223 events per day. Relation effect/background (ON-OFF)/OFF = 0.54.

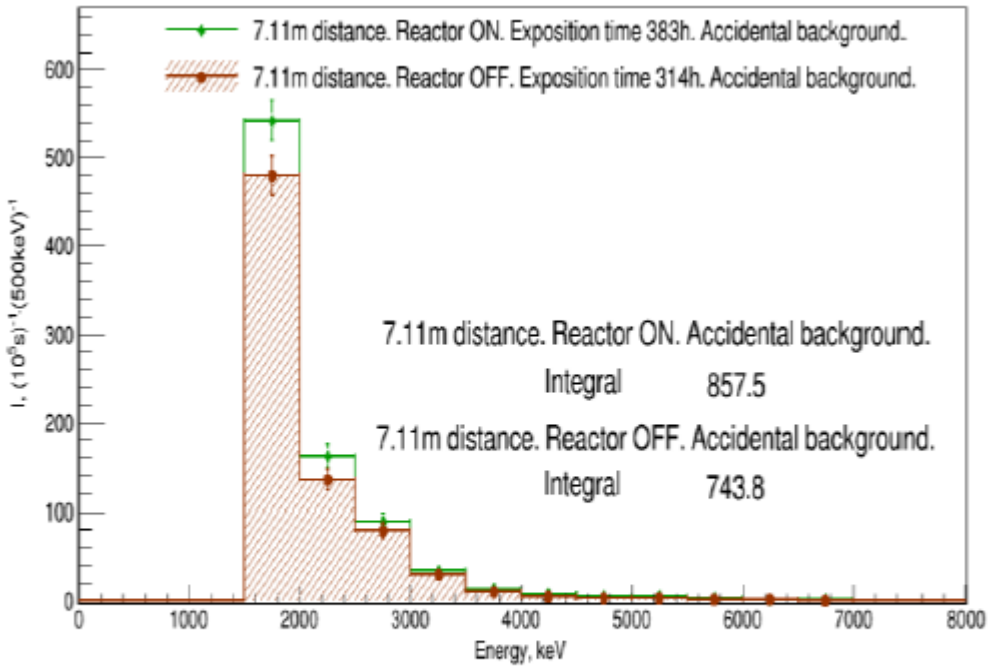

FIG. 29. Dependence of the of accidental coincidence background on the reactor mode and limit of delayed signal.

$$A^{-1}_{11} =$$

$$\left(-U^2_{\mu,2}\,U^2_{s,4}\,U^2_{\tau,3} + U^2_{\mu,2}\,U^2_{s,3}\,U^2_{\tau,4} + U^2_{s,2}\,U^2_{\mu,4}\,U^2_{\tau,3} - U^2_{s,3}\,U^2_{\tau,2}\,U^2_{\mu,4} + U^2_{s,4}\,U^2_{\tau,2}\,U^2_{\mu,3} - U^2_{s,2}\,U^2_{\mu,3}\,U^2_{\tau,4} \right) \Big/ \left(-U^2_{e,1}\,U^2_{\mu,2}\,U^2_{s,4}\,U^2_{\tau,3} + U^2_{s,3}\,U^2_{e,1}\,U^2_{\mu,2}\,U^2_{\tau,4} + U^2_{e,1}\,U^2_{s,2}\,U^2_{\mu,4}\,U^2_{\tau,3} - U^2_{e,1}\,U^2_{s,3}\,U^2_{\tau,2}\,U^2_{\mu,4} + U^2_{e,1}\,U^2_{s,4}\,U^2_{\tau,2}\,U^2_{\mu,3} - U^2_{e,1}\,U^2_{s,2}\,U^2_{\mu,3}\,U^2_{\tau,4} - U^2_{\mu,2}\,U^2_{s,3}\,U^2_{\tau,1}\,U^2_{e,4} - U^2_{\mu,2}\,U^2_{s,1}\,U^2_{e,3}\,U^2_{\tau,4} + U^2_{\mu,2}\,U^2_{s,4}\,U^2_{\tau,1}\,U^2_{e,3} + U^2_{\mu,2}\,U^2_{s,1}\,U^2_{e,4}\,U^2_{\tau,3} + U^2_{s,4}\,U^2_{\tau,3}\,U^2_{\mu,1}\,U^2_{e,2} - U^2_{s,4}\,U^2_{\tau,2}\,U^2_{\mu,1}\,U^2_{e,3} - U^2_{s,4}\,U^2_{\tau,1}\,U^2_{e,2}\,U^2_{\mu,3} - U^2_{s,1}\,U^2_{e,4}\,U^2_{\tau,2}\,U^2_{\mu,3} - U^2_{s,2}\,U^2_{\mu,4}\,U^2_{\tau,1}\,U^2_{e,3} - U^2_{s,2}\,U^2_{\mu,1}\,U^2_{e,4}\,U^2_{\tau,3} - U^2_{s,1}\,U^2_{e,2}\,U^2_{\mu,4}\,U^2_{\tau,3} - U^2_{s,3}\,U^2_{\mu,1}\,U^2_{e,2}\,U^2_{\tau,4} + U^2_{s,3}\,U^2_{\tau,2}\,U^2_{\mu,1}\,U^2_{e,4} + U^2_{s,3}\,U^2_{\tau,1}\,U^2_{e,2}\,U^2_{\mu,4} + U^2_{s,1}\,U^2_{e,3}\,U^2_{\tau,2}\,U^2_{\mu,4} + U^2_{s,2}\,U^2_{\mu,3}\,U^2_{\tau,1}\,U^2_{e,4} + U^2_{s,2}\,U^2_{\mu,1}\,U^2_{e,3}\,U^2_{\tau,4} + U^2_{s,1}\,U^2_{e,2}\,U^2_{\mu,3}\,U^2_{\tau,4} \right)$$

$$\begin{bmatrix} m_e^2 \\ m_\mu^2 \\ m_\tau^2 \\ m_s^2 \end{bmatrix} = \begin{bmatrix} U_{e,1}^2 m_1^2 + U_{e,2}^2 m_2^2 + U_{e,3}^2 m_3^2 + U_{e,4}^2 m_4^2 \\ U_{\mu,1}^2 m_1^2 + U_{\mu,2}^2 m_2^2 + U_{\mu,3}^2 m_3^2 + U_{\mu,4}^2 m_4^2 \\ U_{\tau,1}^2 m_1^2 + U_{\tau,2}^2 m_2^2 + U_{\tau,3}^2 m_3^2 + U_{\tau,4}^2 m_4^2 \\ U_{s,1}^2 m_1^2 + U_{s,2}^2 m_2^2 + U_{s,3}^2 m_3^2 + U_{s,4}^2 m_4^2 \end{bmatrix}$$

$$\begin{bmatrix} m_1^2 \\ m_2^2 \\ m_3^2 \\ m_4^2 \end{bmatrix} = \begin{bmatrix} 1.69\, m_e^2 - 2.87\, m_\mu^2 + 2.22\, m_\tau^2 - 0.18\, m_s^2 \\ -0.47\, m_e^2 + 6.79\, m_\mu^2 - 5.35\, m_\tau^2 + 0.16\, m_s^2 \\ -0.21\, m_e^2 - 2.88\, m_\mu^2 + 4.12\, m_\tau^2 - 0.15\, m_s^2 \\ -0.05\, m_e^2 - 0.29\, m_\mu^2 + 0.09\, m_\tau^2 + 1.16\, m_s^2 \end{bmatrix}$$

$$\begin{bmatrix} m_1^2 \\ m_2^2 \\ m_3^2 \\ m_4^2 \end{bmatrix} \begin{array}{|c|} \hline 0 \\ \hline 0 \\ \hline 0 \\ \hline \end{array} \; 7.2$$

$$\begin{bmatrix} m_e^2 \\ m_\mu^2 \\ m_\tau^2 \\ m_s^2 \end{bmatrix} \; 0.34 \;\; 0.17 \;\; 0.42 \;\; 6.21$$

$$\begin{bmatrix} m_1^2 \\ m_2^2 \\ m_3^2 \\ m_4^2 \end{bmatrix} \; -0.10 \;\; -0.23 \;\; 0.24 \;\; 7.2$$